DEVELOPMENT OF STRONTIUM HEXAFERRITE MAGNETS FROM CELESTITE ORE AND BLUE DUST

A
Thesis

Submitted for the award of the degree of

DOCTOR OF PHILOSOPHY

By
Rajani Kant Tiwary
Regn. No. - 9021551

School of Physics & Materials Science
Thapar University
Patiala- 147 004, India
April/July-2008

CERTIFICATE

This is to certify that the thesis entitled **"Development of Strontium Hexaferrite Magnets from Celestite Ore and Blue Dust"** which is being submitted by **Mr. Rajani Kant Tiwary** in fulfilment of the requirements for the award of the degree of Doctor of Philosophy in the School of Physics and Materials Science, Thapar University, Patiala is a record of candidate's own work carried out by him under our supervision and guidance from February 2003 to January 2008. The matter presented in this thesis has not been submitted in part or full for the award of any degree in any other University or Institute.

Date: 07 - 04 - 2008

Place: Patiala

Dr. D.P.Pandey
Professor & Head
School of Physics & Materials Science
Thapar University
Patiala- 147 004
India

Dr. S.P.Narayan
Scientist F (Deputy Director)
Advance Materials and
Process Research Institute
(Regional Research Laboratory)
Bhopal- 462 026
India

I

ACKNOWLEDEMENTS

It is a matter of extreme honour and privilege for me to offer my grateful acknowledgement to my supervisors **Prof. O. P. Pandey** and **Dr. S. P. Narayan** for providing me a chance to work under their guidance and supervision, assisting with all kinds of support and inspiration, wide counsel, excellent guidance, constant encouragement, sincere criticisms and valuable suggestions which they offered throughout this investigation and preparation of the thesis.

I am profound obliged to **Prof. K. K. Raina**, Deputy Director, Thapar University, Patiala for his continuous encouragement and needful help during various stages of the work.

I am very thankful to **Prof. N. K. Verma**, Dean, Students Affairs, Thapar University, Patiala for his whole hearted support and blessings.

The continuous encouragement by **Dr. Kulvir Singh**, Assistant Professor, **Dr. Manoj Sharma**, Assistant Professor, School of Physics and Materials Science, Thapar University, Patiala is gratefully acknowledged.

Words are inadequate in expressing my sincere thanks to **Dr. Puneet Sharma** for his support at every moment.

I am thankful to **Mr. P. K. Singh, Mr. Ravi Srivastava, Mr. Vishal, Mr. Akshya, Ms. Kamal Preet, Mr. Manoj Sharma, Mr. Sanjeev and Mr. S. Verma** for their incomparable help.

And above all, I pay my regards to my **Parents** and **The Almighty** for their love and blessings.

(Rajani Kant Tiwary)

CONTENTS

List of Figures

Chapter 1

Chapter 2

Chapter 5

List of Tables

Chapter 4

Chapter 5

List of Publications

(a) International Journals

1. R.K.Tiwary, S.P.Narayan and O.P.Pandey, "Conversion of Indian celestite to strontium carbonate", International Journal of Mining and Mineral Engineering, Nov. 2007 (Accepted).
2. R.K.Tiwary, S.P.Narayan and O.P.Pandey, "Preparation of strontium hexaferrite magnets from celestite and blue dust by mechanochemical route" International Journal of Mining and Mineral Engineering, Jan.2008 (Accepted).
3. R.K.Tiwary, S.P.Narayan and O.P.Pandey, "A comparative study of magnetic properties of strontium hexaferrite prepared by pure chemicals and its natural ores" International Journal of Mining and Mineral Engineering, 2007 (communicated).

(b) National Journals

1. R.K.Tiwary, S.P.Narayan and O.P.Pandey, "Preparation of strontium oxide from celestite: A Review" Material Science, Vol-3, Issue-4, 2007, pp-201-211.
2. R.K.Tiwary, S.P.Narayan and O.P.Pandey, "Structural and magnetic properties of strontium hexaferrite derived from natural ores" Transaction of the Indian Ceramic Society, (communicated).

(c) National Conferences

1. R.K.Tiwary, R.K.Sidhu, S.P.Narayan, Puneet Sharma and O.P.Pandey "Preparation of strontium hexaferrite from strontium sulphate and iron oxide" Proceedings of National Conference on Materials and Related Technologies, Feb.19-20, 2003, pp 128-138.

2. R.K.Tiwary, S.P.Narayan, and O.P.Pandey " Preparation of strontium hexaferrite sintered magnets from celestite and iron oxide" Proceedings of National Conference on Advances in Condensed Matter Physics, Feb. 11-12. 2005, pp 118-123.

(d) International Conferences

1. O.P.Pandey, R.K.Tiwary and S.P.Narayan, " Preparation of strontium hexaferrite sintered magnets from celestite and blue dust" Proceedings of Interational Conference on Clay and Refractory Materials, Nov.22-24, 2005, pp 122-128.

PREFACE

Among the class of permanent magnets, M-type ferrites are by far the most important permanent magnetic materials. The M-type ferrites or hexaferrites are characterized by compound having general formula $MFe_{12}O_{19}$ (M = Sr, Ba, Pb) with hexagonal magnetoplumbite or M- structure. Their hard magnetic nature is due to large magnetocrystalline anisotropy with hexagonal *c* axis as the preferred direction. The most characteristic feature that underlines the great economic success of M- type ferrite magnets is the low price per unit of available magnetic energy. This is particularly due to the relatively low cost and wide availability of the raw materials. Compared with the alnico magnets, M-type ferrites have high coercivity (H_c) and a moderate remanence (B_r) resulting in moderate energy product $(BH)_{max}$. Strontium ferrite has higher magnetocrystalline anisotropy compared to barium or lead ferrite.

Commercially, strontium ferrite magnets are available in the sintered (Isotropic/ Anisotropic) and plastic bonded form. Apart from chemical composition, the magnetic properties of sintered strontium ferrite depend upon on the processing technique and microstructure. The most important microstructural features are high degree of grain alignment, high density and small grain size. These characteristics are dependent on powder processing, sintering temperature, sintering additives and powder alignment in the magnetic field.

The present study focuses on preparation of sintered strontium hexaferrite ($SrFe_{12}O_{19}$) magnets from natural ores celestite and blue dust and from pure strontium carbonate and iron oxide. The magnets were made by conventional calcination method. Synthesis of strontium hexaferrite by mechanoalloying was also carried out.

Chapter 1 describes the natural occurrence, properties of iron ore fines, blue dust, and celestite (strontium sulphate). The process to prepare strontium oxide from celestite using different procedure is discussed in this chapter. The history, different preparation procedures, physical properties, market trends and applications of strontium hexaferrite is discussed in this chapter.

Comparison of magnetic properties, price ratio, market share of other permanent magnets such as Alnico, $SmCO_5$ is also mentioned in this chapter.

In chapter 2 celestite upgradation by acid leaching to remove the acid soluble impurities is given. Descriptions of different processes for the conversion of Indian celestite to strontium carbonate are outlined. The comparison of black ash and direct decomposition method for conversion of celestite in terms of percentage yield, purity and by-product is given in this chapter. In the black ash method different types of coal is used for reduction of celestite to strontium sulphide. Different variables like quality of reducing agents, temperature and time affecting reduction of celestite is outlined. In the direct conversion method optimization of various parameters like molar ratio ($Na_2CO_3/SrSO_4$) temperature time, temperature etc. influencing conversion of celestite to strontium carbonate is given in this chapter.

Chapter 3 describes physical and chemical beneficiation of blue dust. Under physical upgradation method magnetic separation and froth floatation process are mentioned. The preparation of high purity iron oxide from chemical upgradation of blue dust is given. The comparison of both process in terms of process easiness, product purity and its limitations is given.

Chapter 4 deals with preparation of strontium hexaferrite from celestite and blue dust by mechanochemical alloying method. The development and brief account of research work carried out by other groups by adopting mechanoalloying route is discussed.
The results of magnetic properties obtained in this investigation are compared with results obtained by other researchers. The phases obtained after different duration of ball milling is given. The microstructural evaluation of the final product is also discussed.

In chapter 5 preparation of strontium hexaferrite ($SrFe_{12}O_{19}$) from the natural ore celestite and blue dust (processed) is given. The mole ratio (Fe_2O_3/SrO) was taken 5.0, 5.3, 5.6 and 5.9. The calcination temperature was varied between 1100^0C to 1175^0C. Sintering temperature for each calcined sample was kept between 1200^0C to 1260^0C. The effect of different mole ratio, calcination temperature; sintering temperature on the magnetic property is discussed in this chapter. The strontium hexaferrite was also prepared from pure chemicals at different mole

ratios. Comparative study of magnetic properties of the samples obtained from two different methods i.e. from processed ore and pure chemicals is carried out. X-ray diffraction analysis of different mole ratios at different calcination temperatures has been given for both types of samples. The SEM microstructure of both kinds of ferrite samples has been analyzed in this chapter. The change in lattice parameter with mole ratio and calcination temperature is reported in the chapter.

Chapter 6 summarizes the results of various experiments pertaining to this study. At the end, the suggestion for future work in this area is given.

Chapter 1

Introduction

Overview

This chapter describes the history, occurrence of different kinds of strontium ores, iron ores. Different methods for conversion of celestite to strontium oxide are described. Blue dust and different grade of iron ores, its chemical composition with its application is mentioned in the chapter. The basic concepts of permanent magnet materials particularly M-type strontium hexaferrite is discussed in this chapter. Account of various preparation methods of strontium hexaferrite is described. The magnetic properties, their relations with other variables have been given in details. The properties of strontium hexaferrite, its comparison with other permanent magnets and its applications in different areas are also discussed in this chapter. At the end outline of present work is presented.

1.1 Blue dust

Iron is one of the most common element on earth which consists of about 5% of the total earth crust. The primary form of iron ores are Magnetite (Fe_3O_4) and Hematite (Fe_2O_3). The important ore of iron is Hematite which is the main source of primary iron for the world's iron and steel industries. Iron ore is mined in about 50 countries worldwide. In India it is mined in Jharkhand, Chatishgarh, Orrisa, Karnataka, Goa etc.

The deposits of iron ore of India are partly soft and friable in nature which contain a significant amount of fine particles of -100 mesh size. The fine particles associated with the ore mines is known as Blue dust. India is endowed with vast reserves of iron ores. Blue dust is present with almost all hematite deposits in India. Due to its fineness it blocks passage of ascending gas inside blast furnace. Thus it does not find much of the value added application in iron and steel industries. Many of the mines just dispose off in tailing dumps. However, due to its high purity and suitability for powder metallurgical process, it may be beneficially utilized for the preparation of ferrites. The blue dust contains more than 95% iron oxide. The high iron content in grade of iron ore fines with silica open up the scope of effectively utilizing it to prepare hard ferrites, which will have great economic impact [1, 2].

Table 1.1 Typical chemical composition of different types of iron ores [3**]**

Types of ore	Chemical composition (wt %)			
	Fe	Al_2O_3	SiO_2	Loss on ignition
Hard ore	65.15	2.34	1.22	2.14
Shaly flaky	62.60	3.42	3.28	2.16
Friable flaky	65.20	2.10	1.78	2.06
Soft ore	60.50	3.90	2.10	6.33
Soft ore mixed	61.10	4.47	2.04	5.56
High alumina soft ore	55.90	7.14	0.90	11.08
Blue dust	66.00	1.57	1.45	1.92

Iron ore is generally classified into three grades based on iron content i.e. high grade, medium grade and low grade. The high grade iron ore contains more than 65% iron, medium grade (62-65) % iron and low grade below 62% iron.

It is evident from the table 1.1 that among all types of iron ores, blue dust is the purest form, since it contains highest amount of Fe (66%) whereas silica, alumina remains in the lowest amount i.e. 1.57 % and 1.45% respectively.

The blue dust is subjected to physical beneficiation which consists of the operations like magnetic separation and froth floatation to reduce the silica and alumina content cost effectively. Also, there is chemical upgradation process through which Fe_2O_3 of high purity can be prepared.

1.2 Celestite

Strontium was first detected in the mineral strontianite ($SrCO_3$) found in lead mine at the place Strontian, located on the shores of Loch Sunart, Argyllshire, and Scortland. In 1793 Thomas Hoop, Professor of chemistry, Edinburgh University conducted a series of experiments and showed that it contained a "hitherto unknown kind of earth". He called the mineral strontianite and the new compound was named after the names of mine "Strontia". During 1807-1808 Sir Humphy Davy managed to isolate the unknown metal strontium from strontianite [12].

Strontium is a silvery white material. It amounts to 0.04% of the Earth's crust and ranks 15^{th} among elements in abundance. The surface of strontium metal is covered with a thin layer of oxide to prevent oxidation. Strontium occurs in nature as strontianite ($SrCO_3$) and celestite ($SrSO_4$). The two natural minerals of strontium known as celestite and strontianite contain strontium in sufficient quantity to make its recovery practical. Out of the two, celestite occurs much more frequently in sedimentary deposits of sufficient size to make the mining more practicable. Celestite ores are obtained by open cast and underground mining. Many important deposits cannot be mined because of unacceptably high level of barium deposit along with specific trace elements [13].

Strontianite would be the more useful of the two common minerals because strontium is used most commonly in the carbonate form but only few deposits have been found to be suitable for mining. Only one strontianite mine in China is believed to operate in the world [4]. Due to the expected demand of additional strontium carbonate new facilities for the production of strontium

carbonate was set up. The production of celestite was increased significantly from 1995 onwards [5]. Celestite is abundantly available in most part of world and generally occurs in sedimentary rocks such as bedded deposits of gypsum and barite.

Between 1870 and 1920 strontianite was the principle starting material for the production of strontium compound. Now it has been completely replaced by celestite due to its wide spread availabilities. Strontium compound like strontium carbonate¸ strontium oxide, strontium nitrate, strontium hydroxide etc. are produced from celestite [14].
In India celestite is found in Trichirrapalli district and nearby areas of Tamil Nadu State. It occurs in coarse fibers and columnar crystals. The Indian celestite has a light buff colour but after breaking it is white, pale blue or pale yellow colour. The main area of celestite mineralization in Tamil Nadu (India) is located at a depth of 0.62 to 0.91meters. Indian celestite is of medium grade quality [6].

A great proportion of the world production is dedicated to the production of strontium chemicals particularly strontium carbonate, nitrate and hydroxide. The most important among these chemicals is strontium carbonate which is used in the fabrication of cathode ray tubes for colour monitors and ceramic ferrites [7, 8].

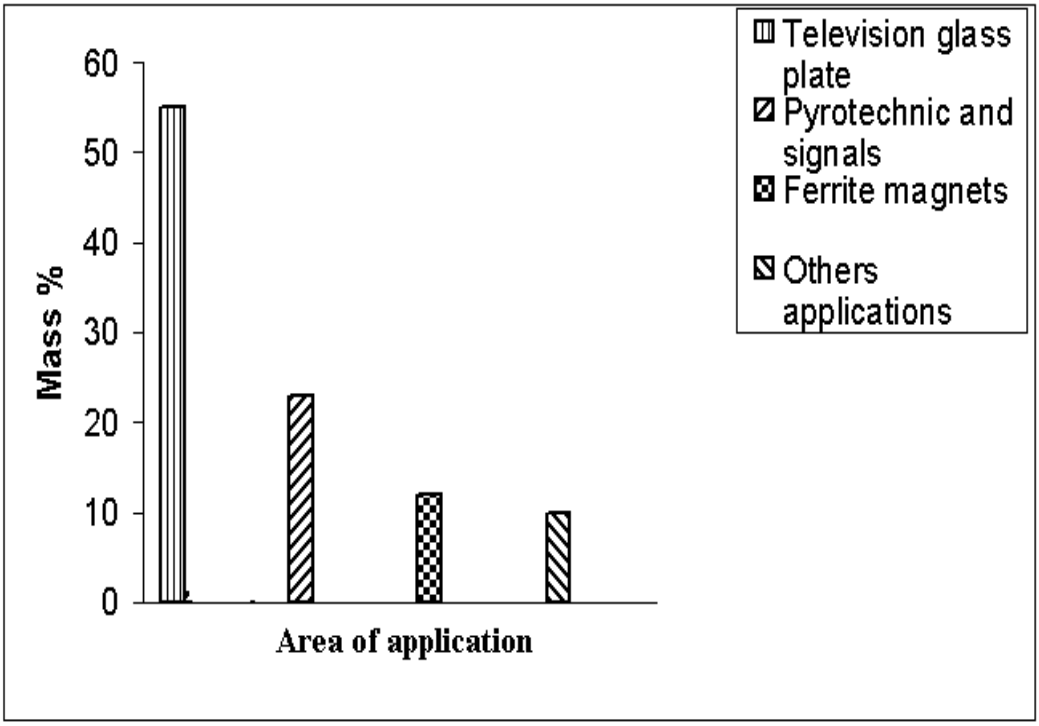

Fig. 1.1 Application of strontium compounds in various applications [9]

Fig. 1.1 shows the application of strontium compound in the different areas. The major uses are in television industries, pyrotechnics and ferrite industries respectively. It is obvious from the fig. 1.1 that more than 50% consumption is in the television picture tube industries. The pyrotechnic applications mark second major uses. Around 10 to 20% of strontium compound is used by the ferrite industries.

Table 1.2 Physical property of celestite

Formula	Density g/cm^3	Solubility g/100ml at20^0C	Melting point ^0C	Crystal structure	Appearance
$SrSO_4$	3.9	0.0113	1580	Orthorhombic	Yellow to faint blue

1.3 Crystallography of Celestite [10]

Crystal System: Orthorhombic

Class (H-M): *mmm(2/m 2/m 2/m)*- Dipyramidal

Space group: *Pnma($P2_1ln2_1lm2_1la$)*

Cell Parameter: a= 8.359 Å, b= 5.352 Å, c= 6.866 Å

Ratio : a: b: c = 1.562: 1:1.2383

Unit Cell Volume: V =307.17 $Å^3$ (derived from unit cell)

Fig. 1.2 shows the celestite production worldwide during year 2001 to 2006. Spain leads in the production of celestite in this period followed by China. The major producers of celestite are Mexico and Spain but largest exporter is Spain.

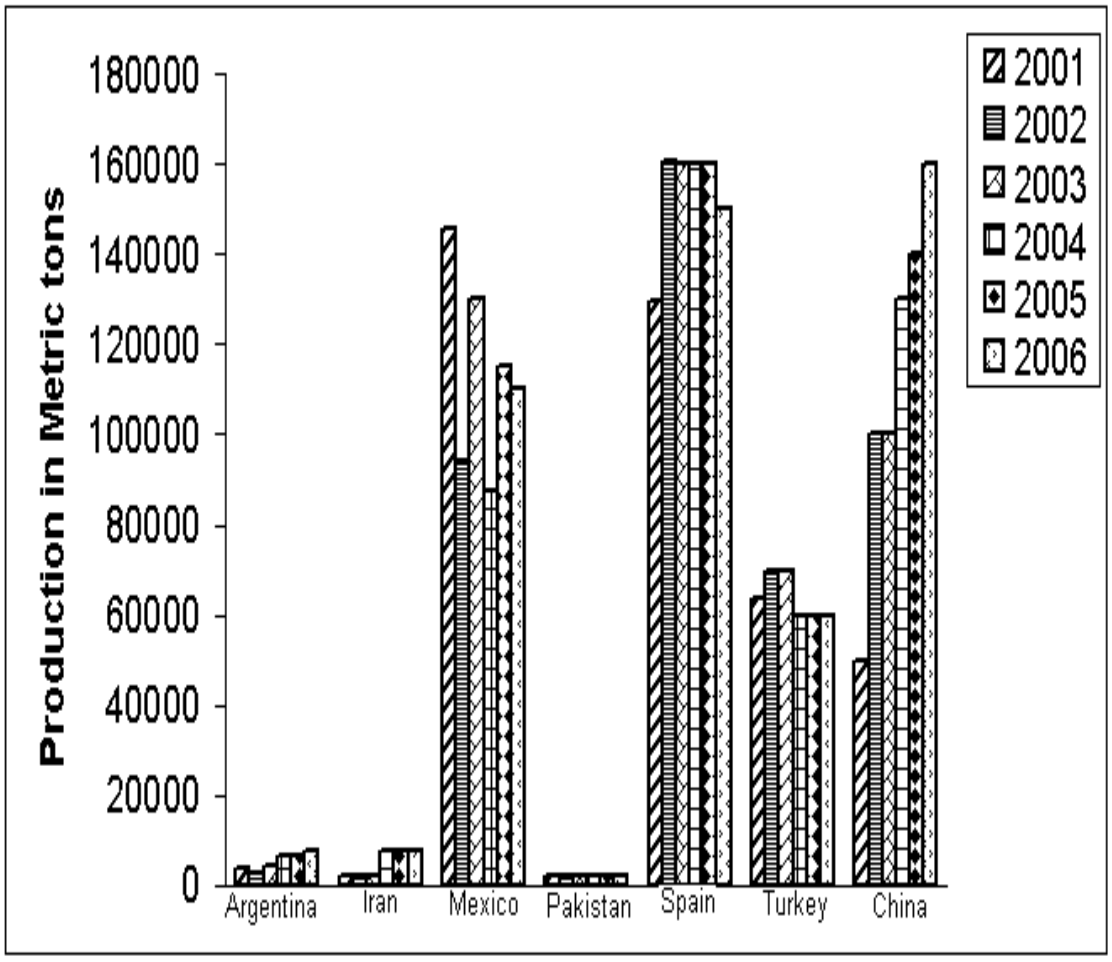

Fig. 1.2 Worldwide production of celestite (Mt) (year 2001-2006) [11]

1.4 Application of Strontium oxide

Presently strontium oxide is used in frit form below 1100^0C. Above this temperature it can be used as a glaze flux. Strontium oxide has been used as substitute for lead oxide in glazes as it has no toxicity as compared to lead. Strontium oxide develops vivid colors similarly to lead. Strontium oxide when added in small amount improves the high viscous high fire zirconium glazes. The compound SrO exhibits different colour response to copper and cobalt. SrO is slightly more powerful fluxing compound due to its lower expansion. Even though SrO has very high melting temperature it is effective in combination with other fluxes at lower temperature and this gives good example of mixed oxide effect. It also finds application in glass, optic and ceramic industries. It is emerging as a promising material for electronic materials and in the

production of lightweight structured component for aerospace. In electrochemical application such as fuel cells, it is also being used in glass to have sealing property. SrO is used for the extraction of strontium metal from electrolysis of its fused salt. The major use of strontium carbonate as strontium oxide is in production of television picture tube glass. Strontium carbonate is an effective X-ray barrier because strontium has a large atomic radius and its presence is required in the relatively high voltage television sets used in USA and Japan [15]. Strontium carbonate when added to special glasses, glass frits and ceramic glazes, increases the firing range, lowers acid solubility and reduces pin holing phenomenon. Strontium oxide is used to prepare strontium hydroxide, which is used as the source material for the production of strontium peroxide. Permanent ceramic magnets (as strontium ferrite) are another end use for strontium compound. These magnets are used extensively in small direct current motors for automobiles windshield wipers, loudspeakers, magnetically attached decorative items, toys and other electronic equipment. Strontium compound is used to remove lead impurities during the electrolytic production of zinc [16-19].

Due to porous nature of strontium oxide it is also used as thermal insulators, automotive catalytic converters, chemical catalysts, heat exchangers [20]. Recently Tsunetake Seki used strontium oxide as catalyst for the Tishchenco reaction of furfural and reported that SrO exhibits high reactivities for the Tishchenco reaction of furfural [21]. The basic physical properties of SrO is shown in table 1.3.

Table 1.3 Physical Property of Strontium Oxide

Formula	Density g/cm^3	Solubility g/100ml at 20^0C	Melting point ^0C	Boiling Point ^0C	Crystal structure	Appearance
SrO	5.7	3.8	2530	3000	Cubic	White crystalline solid

1.5 Preparation of SrO from celestite

The present work reviews the work of different scientists for the preparation of strontium oxide from celestite by different processes. Celestite being natural ore of strontium is treated to obtain strontium oxide. Strontium oxide is prepared by heating strontium carbonate obtained from

celestite with carbon (charcoal) in a resistance-heating furnace at high temperature (1400^{o}C). The conversion consists of multi step preparation. The final product characterization with respect to different analytical tools (physical & chemical) is necessary to get the product of desired level of purity. Many processes have been developed to remove the undesired impurities generally associated with the celestite ore by a number of researchers. The preparation of SrO by different methods, its advantage over other processes and utilization of by products are described. The drawback associated with all these processes are for existence of different level of impurities. For the removal of lot of chemicals, energy etc. are required that makes the product costly. Different processes adopted in industries to convert celestite to strontium carbonate are described below:

1.5.1 Black ash method

In the year 1972 Pedak *et al.* [23] conducted experiments to reduce celestite in hydrogen and also in a mixture of hydrogen and carbon monoxide atmosphere. This process has main disadvantage that consumption of large amount of gaseous reductants occurs. Gritis *et al.* in the year 1985 [24] replaced the gaseous reducing material through solid reducing agent. He performed the experiments with carbon as solid reductant. The experiment was done by using celestite and carbon (stoichiometic amount) in a rotary kiln at a temperature of 600^{0}C to 700^{0}C at the loading zone and 1200^{0}C to 1300^{0}C at discharging zone. This process has also the disadvantage of consumption of higher electrical energy since it requires higher temperature. Plewa in the year 1989 studied the reaction kinetics of strontium sulphate with carbon monoxide [25]. Till this date there was no data available regarding kinetics of the reduction reaction of celestite with carbon. In this experiment it was found that water insoluble SrO also forms in considerable amount, which hampers the formation of water soluble SrS. To overcome above mentioned drawbacks Sonawane *et al.* in the year 2000 **[**26**]** showed that conversion temperature of celestite into strontium carbonate can be reduced by activated charcoal in presence of some catalyst. Carbon impregnated with various catalysts such as K_2CO_3, Na_2CO_3, $K_2Cr_2O_7$, $Na_2Cr_2O_7$ and lime were investigated. The molar ratio of active charcoal with respect to celestite was fixed between 1 to 2.5. He found a substantial decrease in conversion temperature from 1200 to 875^{0}C. The temperature of the conversion reaction was kept 800^{0}C to 875^{0}C with a variation of time period from 5 to 90 minutes. Most of the experiments were conducted in inert atmosphere by

maintaining a slow flow of nitrogen gas. The particle size of the celestite and active charcoal was kept less than 105 µm in this experiment. The results indicate that conversion efficiency is better at the mole ratio (charcoal/celestite) 2.5. The extent of conversion increases with temperature from 800^0C to 875^0C, but there was not much of an increase at 1000^0C. The kinetic study showed that there is definite enhancement in the celestite reduction rate when active charcoal with 2% of a catalyst which was further confirmed by K_{cat}/K_{nocat} values at three common temperature 825^0C, 850^0C and 875^0C. This study indicates that lot of time and energy can be saved as the reaction takes place at lower temperature as compared to without catalyst [26]. The formed SrS is then converted to strontium carbonate either by sodium carbonate or ammonium carbonate. The strontium oxide is then prepared from the produced strontium carbonate by heating with carbon at 1400^0C [5, 14].

Wen Chen in the year 2000 **[**27**]** studied the reduction of celestite into strontium carbonate prepared by precipitation from strontium sulphide by Black ash method. The appropriate amount of celestite ore from Lanping was collected for this experiment. The celestite contains approximately $SrSO_4$ 75%, BaO 0.88%, CaO 1.88%, Al_2O_3 0.46%, MgO 0.6%. Three grades of coals like brown coal, bituminous coal and coke powder were used as reducing agents in this experiment. The appropriate quantity of celestite with coal was mixed properly and heated at 1000^0C for three hours. Brown coal was reported as the best reductant. To remove Ba as $BaSO_4$, six to ten times excess of sulphuric acid was added for longer duration of reaction time. The results show that around 92% of Ba^{+2} was eliminated from $SrCl_2$ solution after 12 hours of reaction time. To remove calcium, magnesium and ferric ions the pH of the solution was increased to 12 in order to hydrolyze the above ions completely. The strontium carbonate was precipitated by ammonium carbonate with 2 moles/l at a pH 9-11 at 60^0C. The strontium carbonate produced by above process can be used for the preparation of strontium oxide as mentioned earlier. Fig. 1.3 shows the schematic flow sheet for the production of strontium oxide from celestite.

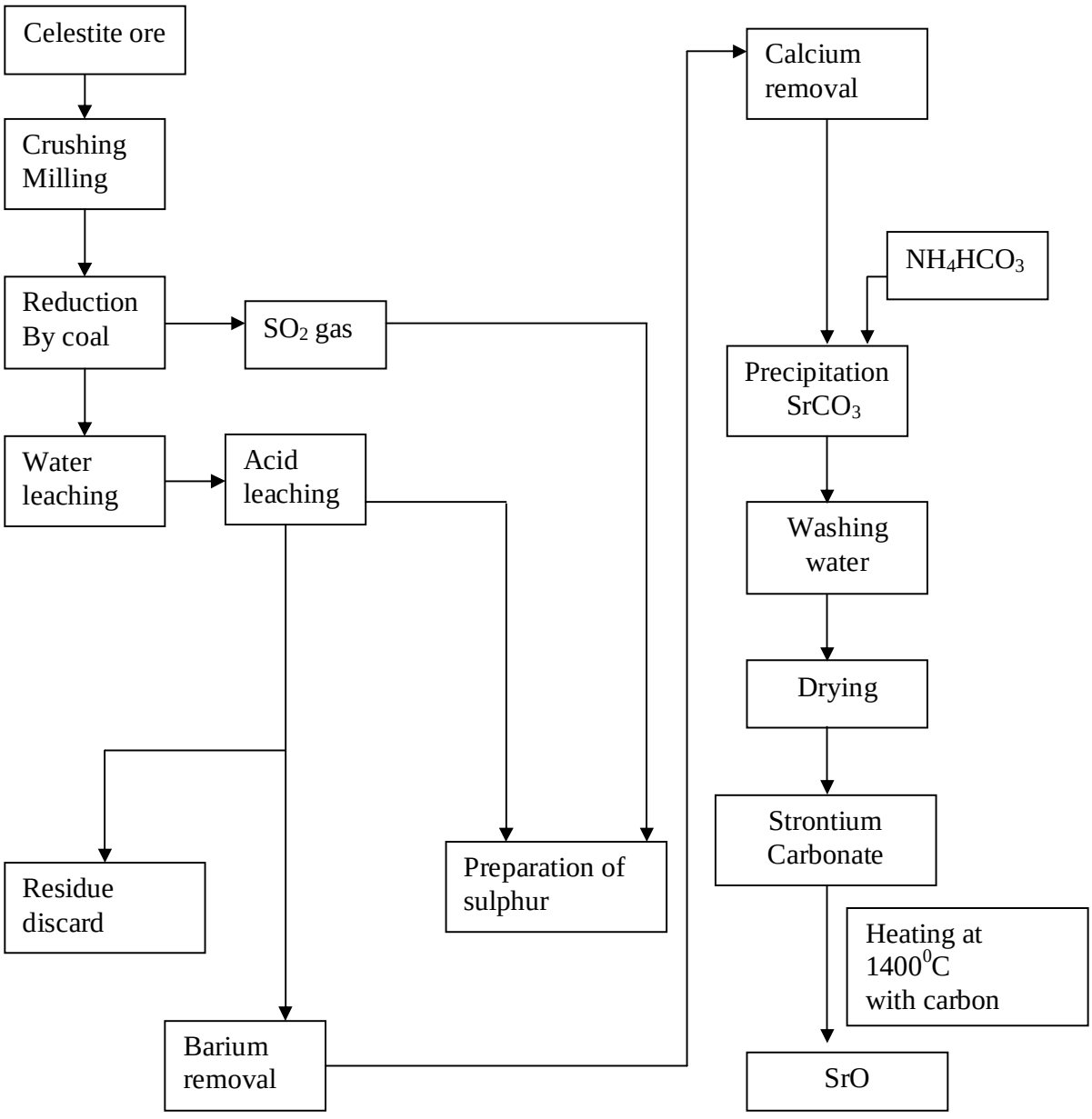

Fig.1.3 Schematic flow sheet of production of strontium oxide from celestite by black ash method [27]

1.5.2 Direct decomposition method

In the year 1983 Patent [No. - 4,421,729] [28] describes the process to prepare strontium carbonate from celestite. In this process strontium carbonate was prepared by the reaction of strontium nitrate with CO_2 in aqueous medium. This process has two-stage reaction. The first reaction consists of strontium carbonate precipitation by carbonization with CO_2 in an aqueous solution of strontium nitrate. The second reaction includes neutralization of aqueous nitric acid formed during first reaction. The neutralization is done by addition of lime. The desired range of Ca/Sr molar ratio is maintained by adding sufficient amount of lime and nitric acid. The controlled mole ratio of Ca/Sr and lower reaction temperature favours the strontium carbonate precipitation and stops the formation of calcium carbonate. The pH of the solution medium is maintained below 6 more preferably between 4.5 to 6 by adjusting the rate of addition of lime. The lime may be added in the form of CaO or Ca $(OH)_2$ and the lime slurry should contain minimum 5-30% CaO. The obtained strontium carbonate after filtration was washed to remove any soluble strontium and calcium nitrate. The washed strontium carbonate is dried in oven. The purity of the strontium carbonate reported in this patent is around 90%. To purify further strontium carbonate may be dissolved in hydrochloric acid to form strontium chloride in soluble condition. The strontium chloride may be precipitated with sodium carbonate/ammonium carbonate solution to give pure strontium carbonate. The dried strontium carbonate may be calcined in an electric furnace at a temperature of 1400^0C for specific time depending on the amount of sample taken for the preparation of strontium oxide.

Another U.S Patent [No.-4,666,688] filed in 1987 [29] claims a novel method for the preparation of strontium carbonate from low and medium grade celestite ore. The process consists of leaching of celestite with mineral acids like HCl, HNO_3 etc. to remove impurities such as Ca, Mg, Ba and Fe. After that the residue containing strontium sulphate is treated with ammonium carbonate solution to precipitate insoluble strontium carbonate. A double decomposition method was employed for getting strontium carbonate of high purity. The difference with earlier processes and this process is the use of ammonium carbonate in place of sodium carbonate. This patent claims that low to medium grade celestite containing up to 80% of strontium sulphate may be converted to strontium carbonate having high purity. The

fine celestite is treated with 10 to 12 % hydrochloric acid. This treatment removes most of the extraneous impurities such as calcium, magnesium, barium and other carbonates by converting them into soluble chloride, which remains in the solution leaving strontium sulphate as insoluble residue. The washed strontium sulphate is treated with ammonium carbonate solution added in slight excess to the stoichiometic value of strontium sulphate present in the celestite ore at a temperature 60-80^{0}C. This treatment converts strontium sulphate into strontium carbonate. The excess ammonium carbonate solution and the ammonium sulphate is separated from the residue through filtration or by other separation techniques. The strontium carbonate produced in this process is washed with water. This strontium carbonate also contains impurities like silicates, clays and residual iron along with barium compound. In order to extract the strontium carbonate from this residue it is treated with hydrochloric acid (18% by volume) once again. As a result the strontium carbonate dissolves and remains in soluble form as strontium chloride. The solution is filtered to remove the insoluble residue. If the acid solution is contaminated with any impurities like iron or barium, the pH of the solution is raised to 9. The iron hydrolyses and remains insoluble and it may be separated by filtration. In order to remove barium the filtered solution is neutralized with dilute hydrochloric acid. This solution is treated with potassium dichromate to convert the barium into insoluble barium chromate, which can be separated by filtration. The strontium chloride solution free from iron and barium is treated with aqueous solution of ammonium carbonate until precipitation of strontium carbonate occurs. The insoluble carbonate produced is filtered from the solution and washed with water. The produced strontium carbonate in this process acquires a purity of more than 99% [29]. The strontium oxide can be prepared from the strontium carbonate by heating with carbon at 1400^{0}C. The strontium oxide produced from this strontium carbonate will essentially of high purity i.e. 99% or more.

In the year 1996 Costillejos E. *et al.* [31] has conducted experiments for conversion of celestite into strontium carbonate by double decomposition method in aqueous media. The study includes effect of different variables like stirring speed, particle size and concentration of Na_2CO_3 on the reaction rate. In this experiment celestite powder was allowed to react with sodium carbonate in different molar ratio i.e. 1.0, 1.1, 1.2, 1.5 at different temperatures ranging from`25^{0}C to 75^{0}C for different time. Effect of particle size of celestite on its

conversion shows that with reduced particle size from 275 μm to 58 μm the rate of conversion of celestite was increased. In this study different processing parameter were optimized to get larger amount of strontium carbonate from celestite. Strontium oxide may be obtained by calcination of strontium carbonate with carbon obtained from this process at elevated temperature (1400^{o}C). The flow diagram of the process is shown in fig 1.4.

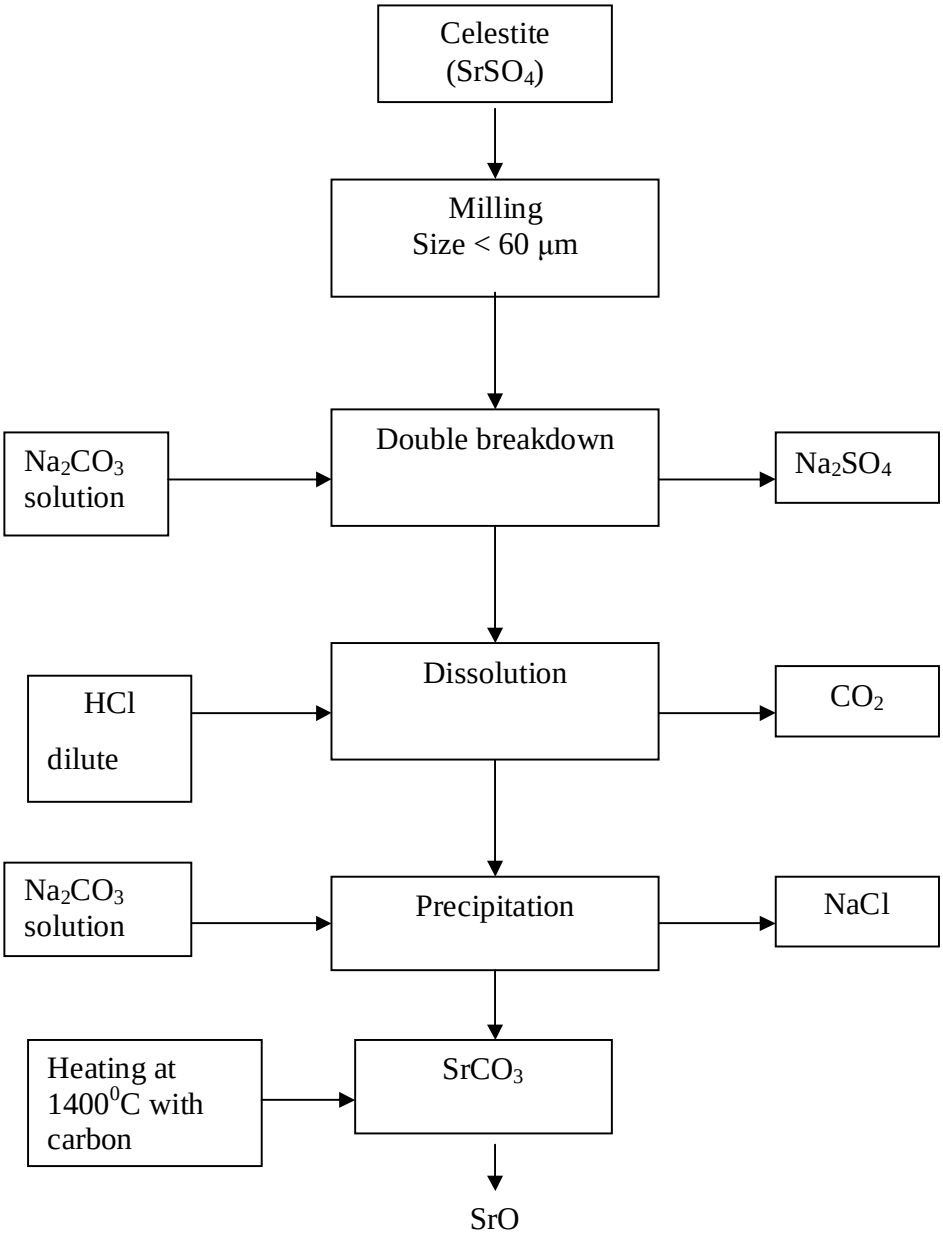

Fig.1.4 Schematic flow diagram of direct double decomposition process for preparation of strontium oxide from celestite [31]

In year 2000 an U.S Patent [No.-6,159,436] [30] has reported in which air/vapor-lift loop reactor is employed to carry out this reaction. This project was examined for carbonate rich celestite ore for the celestite conversion. The acid wash stage is carried out in a mechanically or pneumatically agitated tank with hydrochloric acid. The celestite particle size below 70 μm was used for acid leaching. If pneumatically agitation in airlift loop reactor is used, pulps containing up to 60% solids by weight can be easily handled. Under this condition dissolution of carboneous and ferrous gangue, mainly calcite, dolomite, magnetite, and iron oxide along with hydroxide is completed in short period of time. After the acid wash the upgraded concentrate is separated from the solution by sedimentation or by other separation technique. The liquor is transferred to an evaporator for recovering a calcium chloride rich solid. The strontium sulphate enriched concentrate is washed with fresh water before being fed to air/vapour-lift loop reactor for conversion to strontium carbonate using a sodium carbonate aqueous medium. Thus, an almost complete conversion of the strontium sulphate is achieved according to patent claim [30].

In the year 2004 in another experiment Surerez-Orduna *et al.* [32] made another experiment for the conversion of celestite mineral to strontianite under hydrothermal condition. In this experiment a single crystal of celestite was investigated under alkaline hydrothermal condition. Single crystal of mineral celestite was taken from Coahulia, Mexico and was cut parallel to the cleavage (001) direction with 10 mm width and 3mm thickness. A celestite crystal around 5 gram was placed at the bottom of a Teflon lined stainless steel vessel with inner volume of 27 ml and then the Na_2CO_3 solution was added to get three different CO_3^{-2}/ SO_4^{-2} ratios (1, 5 and 10) with 17 ml of deionized water. The conventional hydrothermal treatments were conducted at a temperature (150-250^{0}C) by heating the vessel at a rate of 10^{0}C per minute. The reaction vessel was held at each temperature for several duration (1-96 hrs.). The cooling stage was maintained by using an electric fan. After the hydrothermal treatment, the reaction products were washed with deionized water in ultrasonic equipment. SrO may be prepared from the strontium carbonate obtained as mentioned above.

In the year 2004 Hacer Dogan *et al.*[33] studied the effect of acid leaching of Turkish celestite for the conversion of celestite into strontium carbonate. Double decomposition method was employed for conversion of celestite. Different mineral acids like HCl, HNO_3 and H_2SO_4 were

used for acid leaching of celestite. Organic acid such as acetic, oxalic, citric, tartaric and di-glycolic acid was also tried but their price and effectiveness were not as reasonable as inorganic acids. The decrease in calcium percentage was around 0.5% with acid leaching of celestite. Nitric acid, ammonium nitrate and potassium per chlorate were used as oxidizing agent to increase the decomposition of iron. Ammonium fluoride was also used to decompose the silicate material and iron bonded to it. The iron content was reduced to around 0.20 g/l with addition of NH_4F. Nitric acid of 3.5% concentration was found to be sufficient for removal of iron. This experiment showed that particle size of celestite is very important for the total completion of the reaction. The smaller the particle size of celestite, the lower iron content was obtained under the same condition. The strontium carbonate produced from leached celestite ore contained iron below 0.10 g/l and calcium below 0.2%.

The strontium carbonate found in this process may be used for the production of SrO by calcination method using carbon as reductant at high temperature as mentioned earlier.

Murat Erdumoglu *et al.* in the year 2006 **[**34**]** carried out the experiment on the leaching of celestite with sodium sulphide at 20^0C to prepare strontium disulphide. The acid leaching of strontium disulphide by dilute HCl were conducted to form strontium chloride. Any residue remaining in the strontium chloride solution was filtered and removed. The liquid containing strontium chloride was allowed to react with sodium carbonate solution for the precipitation of strontium carbonate. In this study the reaction kinetics with respect to different parameters like particle size of celestite, concentration of Na_2S, stirring speed was studied. The results showed that the rate of conversion of celestite to strontium disulphide depends on concentration of sodium suphide [13]. The celestite in this experiment was upgraded to 99.8% strontium sulphate. Therefore strontium carbonate produced by this method will be of high purity. The strontium oxide of very high purity may be prepared from this strontium carbonate by similar way as described above. The flow sheet diagram of this process is given in fig. 1.5.

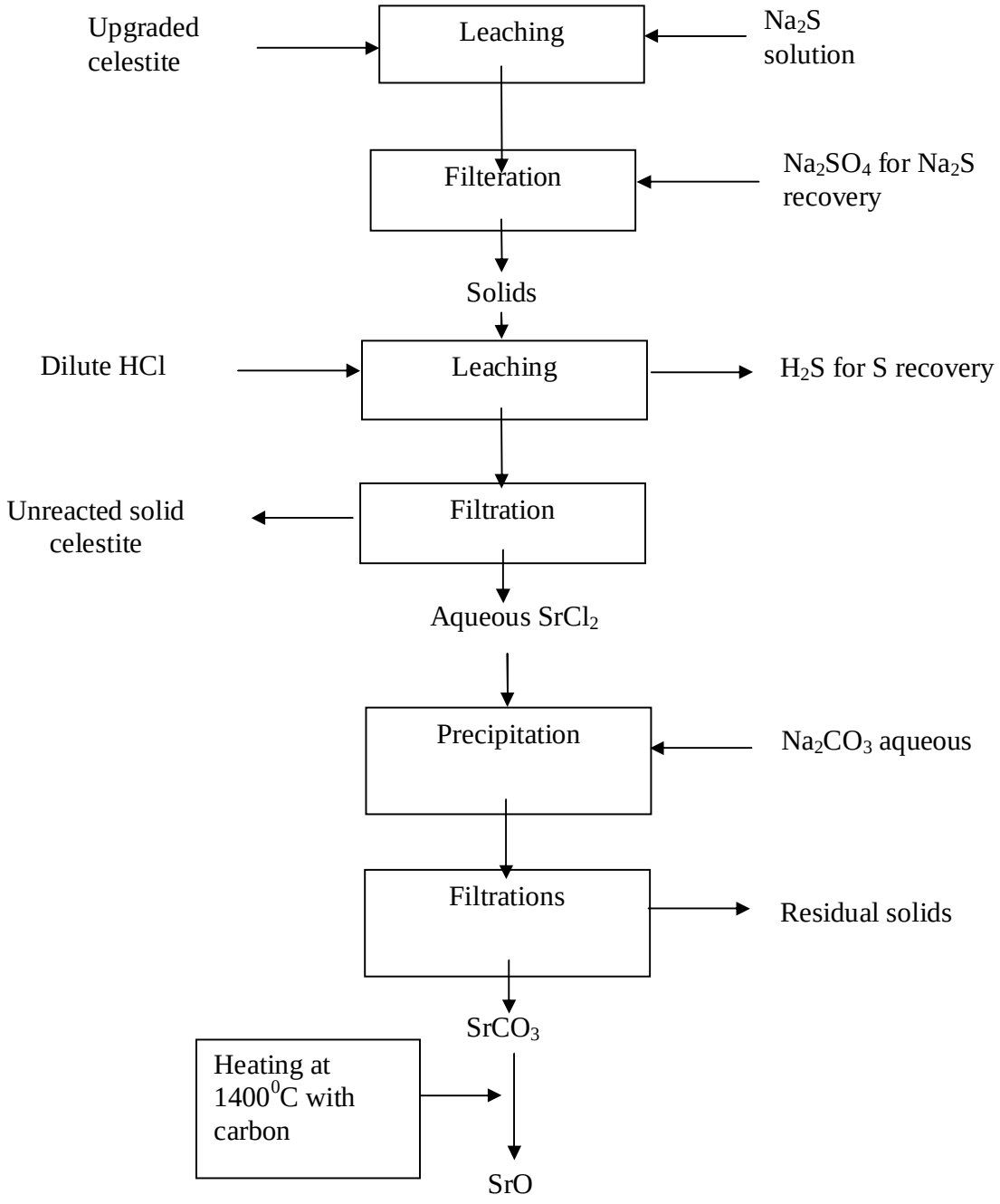

Fig 1.5 Schematic process flow diagram for preparation SrO from celestite [34]

1.5.3 Conversion of celestite to SrS by microwave heating

Most recently in the year 2007 conversion of celestite to SrS by microwave heating was reported by Abdullah Obut[35]. He used charcoal as a reducing agent and heating was done in commercial microwave oven. In this experiment celestite was taken from Turkey having purity more than 98% and particle size less than 200 micron. The laboratory grade charcoal was used. In each experiment appropriate quantity of celestite with stoichiometic, 50% and 100% excess charcoal has been taken and mixed properly. The mixture was heated in a lightly covered porcelain crucible, which is placed inside a commercial microwave oven. The oven was operated at 900W and at a frequency of 2450 MHz for a time of 2, 4, 7 and 10 minutes. The temperature of the mixture immediately increases by the application of microwave energy due to the strong interaction between microwave and charcoal. The temperature of celestite with stoichiometic carbon reaches 354^0C whereas the mixture containing 50% and 100% excess charcoal reaches 880^0C in equivalent time. There is no considerable loss in weight until 550^0C.The loss values increases steeply after 800^0C indicating starting of the reaction. The weight loss value practically stops after 1100^0C showing the completion of the reaction. The temperature of stoichiometic mass reaches 800^0C after 7 minutes of microwave heating and after 10 minutes heating its temperature reaches 1160^0C. The mixture of 50% and 100% charcoal-celestite exceeds 1200^0C. For 50% and 100% excess charcoal–celestite mixture the weight loss values are almost in range with theoretical values indicating complete conversion of celestite to strontium sulphide. The experiment concludes that conversion of celestite to SrS having conversion ratio more than 97% can be achieved through microwave heating [36-38]. The strontium sulphide obtained by this method may be used for the preparation of strontium carbonate, which can be further used for the synthesis of strontium oxide by above-mentioned process.

1.5.4 Conversion of celestite to strontium oxide by mechanochemical method

In the year 2007 Abdullah Obut *et al.* [39] made an attempt for the conversion of strontium carbonate from celestite by mechanochemical method. In this experiment (+600μm) Turkish

celestite containing 96.12% $SrSO_4$, 2.61%$CaSO_4$, 0.6 %$BaSO_4$, and 0.45% Fe_2O_3 has been employed for this experiment using reagent grade sodium carbonate. The planetary type ball mill with 500rpm, ball/sample weight ratio: 20, numbers of balls 50, diameter of balls 10 mm has been used to carry out the mechanochemical reaction. The general flow sheet of the work is given in fig.1.6. The result shows that 74.23% of celestite is dissolved in distilled water only after 10 minutes of milling. The dissolved sulphate and dissolution percentage of initial celestite and milled solids increases from 91.52% to 93% in 20 minutes. After 40 minutes of milling 98% celestite was dissolved. The dissolved sulphate is converted to strontium carbonate. The result also indicates that the increase in dissolution values of sulphate for 20 and 40 minutes is not as significant as the values between 10 to 20 minutes mixing. The effect of amount of sodium carbonate on the preparation of strontium carbonate was also investigated in this experiment and it was found that 10 minutes milling is preferred to 20 minute milling in relation to reduce tungsten carbide ball milling chamber wear. The result also showed that 1:1.2 mole ratio (strontium sulphate/sodium carbonate) and 20 minutes activation time is sufficient for 90% of conversion celestite into strontium carbonate. The whole experiment concludes that the reaction between celestite and strontium carbonate in aqueous medium is diffusion controlled because of the formation of solid strontium carbonate layer over the celestite particle whereas in wet high energy milling gives increased rate of conversion of celestite due to creation of fresh reactive surfaces as a result of continuous mixing and size reduction. The strontium oxide may be prepared by heating the strontium carbonate powder with carbon at 1400^0C. The flow diagram is given in fig. 1.6.

Recently in the year 2007 Tanaka Knniaki [40] has prepared strontium oxide thin films as an electron injection layer for organic EL De reactive ionization assisted deposition method.

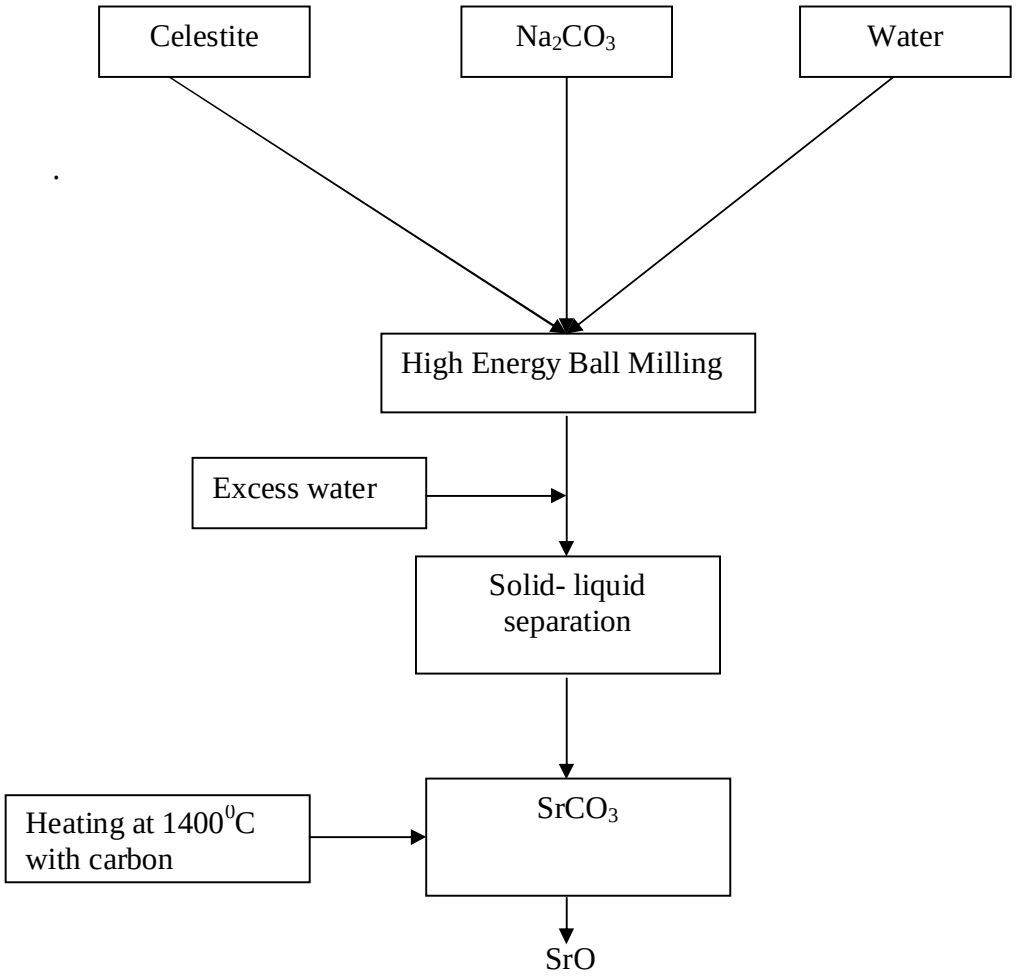

Fig. 1.6 Schematic process flow sheet for the preparation of strontium oxide from celestite by mechanochemical method [39]

1.6 Permanent Magnets and their Characteristics

Magnetic materials can be divided into two group soft and hard materials. The soft materials are one that is magnetized and demagnetized easily. The hard magnetic materials are those which are difficult to magnetize and demagnetize. The distinguished features of the soft materials are its high permeability and the flux multiplying power that makes it suitable for its application in

machines and devices. On the other hand for hard materials the primary requirement is high coercivity. Because the high coercivity will resist the magnetization action of its own. The basic difference of two types of permanent magnets is best described on the basis of hysteresis loops. The soft magnetic materials exhibit a narrow hysteresis loop whereas the hard magnetic materials show a broad hysteresis loop. In the narrow hysteresis loop magnetization follows the variation of the applied field without significant loss. The broad hysteresis loop shows the magnetic energy that can be stored in the materials.

When a magnetic field *H* is applied to ferromagnetic materials it develops a flux density *B* due to orientation of magnetic domains. The relation between *B* and *H* can be represented by the following equation.

$$B = \mu_0 (H + M) = \mu_0 H + J$$

Where *M* is the magnetization and μ_0 is the permeability of free space equals to $4\pi \times 10^{-7}$(Tm/A). The value of $\mu_0 M$ represents the magnetic polarization and is often exhibited by *J*. *B* vs. *H* and *B* vs. *J* curve of ferromagnetic materials which has been given in figure 1.7 [41]

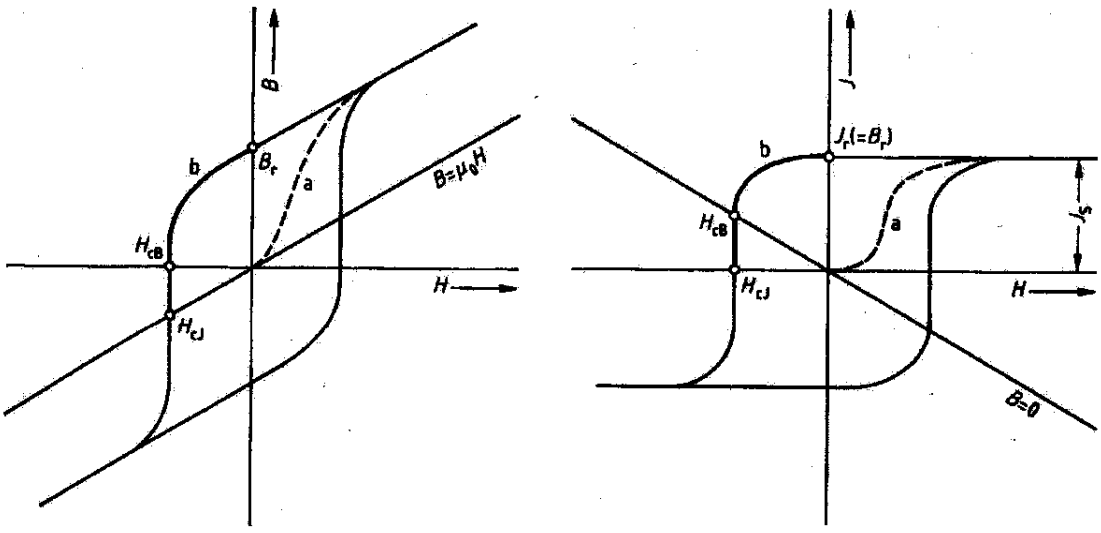

(a) (b)

Fig. 1.7 B Vs H and J_s Vs H curves of Ferromagnetic Materials showing important characteristics (a) Virgin curve (b) Hysteresis loop

The basic parameters that describes a permanent magnet are B_r remanent induction, the coercive force H_c and the energy product $(BH)_{max.}$

The remanent induction *Br* is the flux density existing without magnetic field. Since a magnet is always subjected to its own field it can only be determined in closed circuits.
The coercive force H_c is measure of the external field needed to demagnetize the material completely. The term intrinsic coercivity H_{ci} is the field necessary to reduce J_s, upper limit of remanence to zero. The upper limit of the coercivity is determined by H_A which is given below:

$$H_A = 2K_1 / J_s$$

Where J_s and K_1 are the saturation magnetism and anisotropy constant respectively which determine the value of magnetocrystalline anisotropy. The value of K_1 is positive for uniaxial anisotropy and negative for planar anisotropy. It also determines the work done per unit volume to rotate the magnetic polarization from easy direction to hard direction. The value of H_A is generally determined by measuring the magnetizing curve with field applied parallel and perpendicular to easy magnetizing direction. H_A is also defined as the intersection point of the two magnetization curves. In another way H_A can also be defined as the field required obtaining saturation in hard direction of magnetization.

The primary magnetic properties of the material are affected by the extrinsic parameters such as phase chemistry and microstructure. The intrinsic coercivity H_{ci} may be represented as

$$H_{ci} = cH_A - N_{eff} * M_s / \mu_0$$

Where *c* and N_{eff} are the constant which depends upon grain structure and grain boundary [2, 3]. The microstructure parameter *c* depends on the alignment of the particle, its shape and size of the defect regions where nucleation or pinning of the domain wall takes place. The parameter N_{eff} is the effective demagnetizing factor. The value of *c* for an ideal magnet should be equal to 1. But the actual magnets have lower *c* values because of imperfect grain boundary defects [42, 43].

The largest possible product of B and H values along the demagnetization curve is called the energy product $(BH)_{max}$. This measures the quality of a permanent magnet. The relation with B_r is given below.

$$(BH)_{max} = B_r^{\,2} / 4\mu_0$$

To obtain the high energy product value in a material the shape of hysteresis loop should be square and the value of B_r should be close to the saturation polarization Js and coercivity should be minimum $B_r/2\mu_0$. The unit of energy product in CGS system is Mega Gauss-Orested (MGOe) and Kilojoules per meter cube (kJ/m^3). The value of 1 MGOe equals to 7.96 kJ/m^3.

Curie temperature is the fundamental characteristic of magnetic materials which is denoted as T_c. It is the temperature above which the long range alignment of the atomic dipoles due to exchange energy is totally destroyed and the material gets demagnetized. Therefore, it is desirable to have higher Curie temperature for the permanent magnet materials.

The other important parameters of permanent magnets are α and β which are called the temperature coefficient for the reversible change in B_r and H_c respectively. These coefficients show the change in the respective magnetic properties with the change in temperature and expressed as the percentage change per unit temperature.

1.7 Common Hard Magnetic Materials – A comparison

Among the permanent magnetic materials the important materials are alnico, hard ferrite, samarium cobalt and neodymium-iron-boron. Each of these materials exhibits different set of properties. By comparison with production cost we find the hard ferrites most suitable. A comparison of commercial permanent magnets in terms of magnetic properties, temperature coefficient of remenence and coercivity, temperature behavior, availability of raw materials with their relative cost is given in table 1.4 [44].

Table 1.4 Comparison of commercial permanent magnet materials [44]

Parameter	Ferrite	Alnico	$SmCO_5$	Nd-Fe-B
B_r (mT)	370	700-1200	890	1100
H_{ci}(kA/m)	255	50 – 150	1200	> 1000
$(BH)_{max}$(kJ/m^3)	30	60-80	150	350
T_c (K)	750	860	933	585
α (% K^{-1})	-0.20	-0.02	-0.05	-0.13
β(% K^{-1})	+0.40	-0.03	-0.03	-0.60
Max. operating temperature(K)	523	773	523	373
Raw material source	Very good	Poor	Poor	Good
Density(kg/m^3)	4650	7300	8300	7400
Price ratio per unit magnetic energy	1	7.5	23	7

By comparing the cost of different materials in the above table 1.4 it is found that ferrites are most economical. The comparison shows that rare earth based magnets have better magnetic properties as compared to ferrite. The characteristics diamagnetic curves of these are shown in figure 1.8 [45]. It is obvious that alnicos possess a high remanence but low coercivity whereas the ferrites are characterized by low remanence and moderate coercivity.

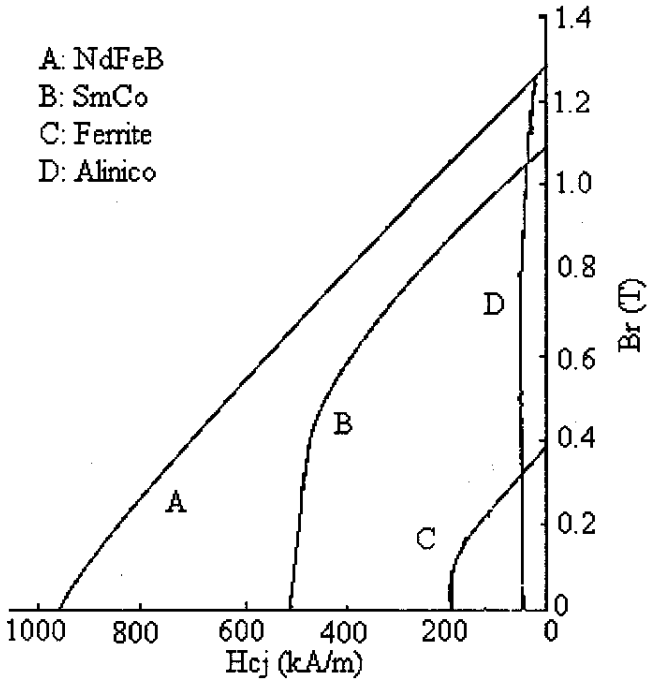

Fig.1.8 Demagnetization curve

1.8 Hexagonal Ferrites

The ferrite is generally used to describe a class of magnetic oxide compound, which contains iron oxide as a principal component. The most ancient ferrite ever known is Magnetite, Fe_3O_4 also called loadstone. Ferrites can be classified according to crystal structure cubic vs. hexagonal ferrite or magnetic behavior i.e. soft vs. hard ferrite. Soft ferrites are easy to magnetize and demagnetize. Hard ferrites are hard to magnetize and demagnetize. Hard ferrites have a hexagonal structure and can be classified as following types. The types and formula are given below.

Types	**Chemical Formula**	
M-	$RFe_{12}O_{19}$	R = Ba, Sr, Pb
W-	$R\ Me_2\ Fe_{16}$	Me = Fe^{+2}, Ni^{+2}, Mn^{+2} etc.
X -	$R\ Me\ Fe_{28}$	
Y-	$R_2Me_2Fe_{12}O_{22}$	
Z -	$R_3Me_2Fe_{12}O_{41}$	

W-, X-, Y-, Z- types are not important economically because of their relatively difficult processing. The chemical composition of various hexagonal compounds is shown in figure 1.9 as part of ternary phase diagram for BAO-MeO-Fe_2O_3 system. Me represents a divalent ion among the first transition elements, Zn, Mg or a combination of ions whose valency is two. S denotes a cubic spinel $MeO.Fe_2O_3$.

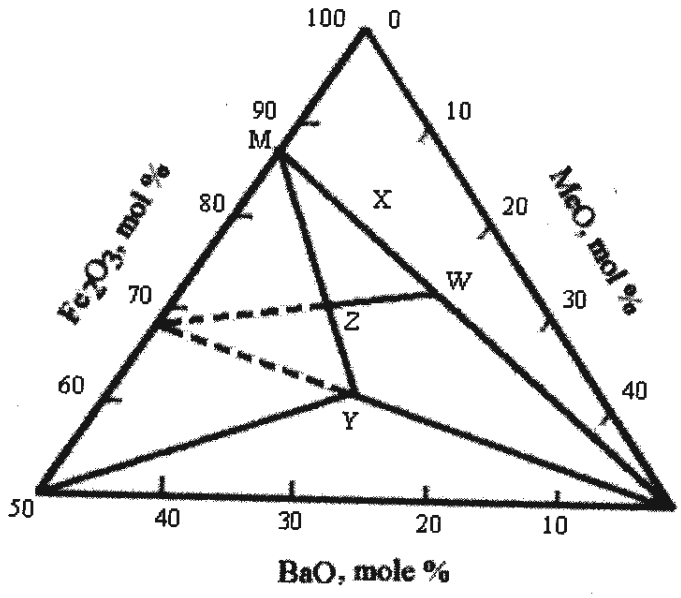

Fig. 1.9 Composition diagram for hexagonal ferrites

1.9 M-Type Ferrites

M-type ferrite has a formula $SrO.6Fe_2O_3$ (SrM), $BaO6Fe_2O_3$ (BaM) and $PbO.6Fe_2O_3$ (PbM). These are the most important ferrites and isostructure with the mineral magnetoplumbite which has the chemical formula $Pb_2Fe_{15}Mn_7(AlTi)O_{38}$ [46]. The M-type ferrites are generally used as permanent magnetic materials because they have higher coercivity. They are preferred over alnicos due to lower material and processing cost and superior coercivity. Sr-Ferrite and Ba-Ferrite are the two main materials in the M-type ferrite family. These ferrites have moderate magnetic properties and price per unit of available magnetic energy is lowest.

1.10 Historical Development of M-type Ferrite

The magnetite (Fe_3O_4) which is also known as loadstone is the earliest everknown magnet and was used for navigational purpose. At the end of the last century the plain carbon steel with 1.5% carbon were developed as the principal magnet alloy till about 1910. Afterwards steel containing some chromium and tungsten were developed. However, the value of coercivity could not increase more than 6 kA/m. The most significant work appeared in the year 1917, when Japanese introduced Honda Steel which contains 36% of cobalt exhibiting coercivity value of 20kA/m. The low coercivity in all these martensitic magnetic steels is due to the difficulties in domain boundary movement, resulting from the combined effect of non magnetic inclusions, lattice defects or voids. The major drawback of these materials was instability of permanent magnetic properties due to the aging and demagnetization influence of vibration, mechanical effects and weak magnetic fields [47].

In the year 1932 the discovery of precipitation hardened Al-Ni-Fe alloys took place. In the year 1940 the Al-Ni-Co (alnico) was developed [41]. Alnicos are the alloy of Al, Ni, Co and Fe having minor additive of other elements. It was the first magnets to be designated as permanent, because of their resistance to stray magnetic fields, mechanical shocks and elevated temperatures. The main difficulties with the processing of alnico were the heat treatment of the alloy which is controlled in such a way as to precipitate rod shaped Co-Fe particles in a Al-Ni-Fe matrix. These materials showed an energy product value of 60-70 kJ/m^3. However, they largely suffered from the scarcity and irregular supply of the cobalt affecting its production adversely. In

the mean time the discovery of barium and strontium ferrite appeared as a welcome relief [48]. Their constituents were much economical as compared to less abundant and expensive element such as nickel and cobalt. These ferrites are hexagonal oxides and are characterized by low remanence and reasonable coercivity. Typical energy product for hard ferrite is 30 kJ/m^3. The hard ferrites were the first magnetic material with the remarkable uniaxial magnetocrystalline anisotropy, resulting in very high intrinsic coercivity.

The basic discovery that magnetoplumbite could be used as a permanent magnet was made by Kato and Takei in late 1930s [48]. The real breakthrough took place in 1950s with the development of isotropic barium ferrite as a commercial magnetic material, by Philips Company in Netherland which has nominal composition of $BaO.6Fe_2O_3$ [49]. The first anisotropic barium ferrite magnet was prepared in the year 1952 by compacting the powder in a magnetic field [50, 51]. Barium ferrite is mostly used for magnetic tape recording due to its platelets type of crystallite shape with the preferred axis normal to the wide surface and its low coercivity. Until 1962, all ferrite magnets were of barium ferrite type. Earlier the barium ferrite was the ultimate oxide permanent magnet materials [46]. In the mid 1960s Ba^{++} was replaced by Sr^{++} in all type of applications because of its high intrinsic properties particularly in coercivity.

Sr-ferrite powder has been manufactured by various processing routes e.g. chemical co-precipitation, hydrothermally and sol-gel methods etc. and studies of their magnetic properties have been carried out by various researchers [52- 54]. Recently some work has been done for developing nano size (80 nm) ferrite powders by chemical co-precipitation [52]. From the very beginning the main emphasis has been laid on strontium ferrite sintered magnets through calcination. The B_r and H_c values for ferrites are usually given by the following formula:

$$B_r = f\,(d/dx)\,S.\,J_s$$

Where f is the degree of alignment, d/dx is the relative density, S is the fraction of pure ferrite in the solid and J_s is the saturation magnetization.

$$H_c = aH_A - bJ_s / \mu_s$$

Where 'a' is the coefficient whose value depends on grain size, H_A is anisotropic field; 'b' is coefficient whose values depends on remanence and grain shape.

It is, therefore, possible to tailor B_r and H_c values by changing the saturation magnetization, anisotropic field, grain size and shape. All these parameters can be varied by using various additives such as Al^{+3}, Ga^{+3}, Cr^{+3} in the ferrite magnets.

1.11 Crystal Structure, Magnetic Structure and Phase Diagram of M-type Ferrite

The crystal structure of M-type was determined by Adelskold [55]. Fig. 1.10 shows the unit cell of strontium hexaferrite. The crystal structure consists of two formula units. Its symmetry is characterized by the space group $P6_3/mmc$. In the unit cell, the O^{-2} ions form a hexagonal close packed lattice. Every five oxygen layers, one O^{-2} ion is replaced with Sr due to the similarity of their ionic radii. The structure is build up from smaller unit: a cubic block S, having the spinal structure and a hexagonal block R, containing Sr^{+2} ions. Five oxygen layers make one molecule and two molecules make one unit cell. Each molecule shows 180 degree rotational symmetry around the hexagonal *c*-axis against the lower or upper molecule. The O^{-2} layer containing Sr^{+2} is a mirror plane being perpendicular to the *c*-axis. Fe^{+3} ions occupy interstitial positions at different crystallographic sites i.e. tetrahedral, octahedral and hexahedral sites of oxygen lattice. Table 1.5 shows the crystallographic properties of M- type ferrite.

Table 1.5 Crystallographic properties of M-type ferrite [41].

Parameter		Ferrite(s)		
Lattice Constant (nm)	*a*	BaM	SrM	PbM
		0.5893	0.588	0.588
	c	2.3194	2.307	2.302
Molecular wt.		1112	1062	1181
Density gm/cc		5.28	5.11	5.68

M-type compounds have a typical ferrimagnetic structure. The magnetism of $SrFe_{12}O_{19}$ comes from the ferric iron, each carrying a magnetic moment of $5\mu_B$. These are aligned to give either

parallel or anti parallel ferromagnetic interaction. Ions of the same crystallographic position are aligned parallel which constitute a magnetic sublattice. The interaction between neighboring ions of different sublattices is a result of super exchange by oxygen ion [48]. The theory predicts that the atomic moments are parallel when Fe-O-Fe angle is about 180^0 and antiparallel when this angle is about 90^0[49]. In figure 1.10, S block contains four Fe^{+3} of up spin in octahedral sites and two Fe^{+3} of down spin in tetrahedral site. In R block there exist three Fe^{+3} of up spin in octahedral site, two Fe^{+3} of down spin in octahedral sites and one Fe^{+3} of up spin in trigonal bipyramid site. The exchange scheme of the compound is shown in figure 1.10 [56]. The number of ions, its co-ordination and direction of spin orientation for five iron sub lattice has been given in table 1.6.

The total magnetization at temperature T therefore can be expressed as:

$$\mathbf{J_s(T) = 6\sigma_k(T) - 2\sigma_{f1}(T) - 2\sigma_{f2}(T) + \sigma_b(T) + \sigma_a(T)}$$

Where σ_k, σ_{f1}, σ_{f2}, σ_b, and σ_a represents the magnetization of one Fe^{+3} ion in each sublattice. Because Fe^{+3} has a magnetic moment of $5\mu_B$ at 0 K so the net magnetic moment calculated at 0 K is 20 μ_B for each unit cell.

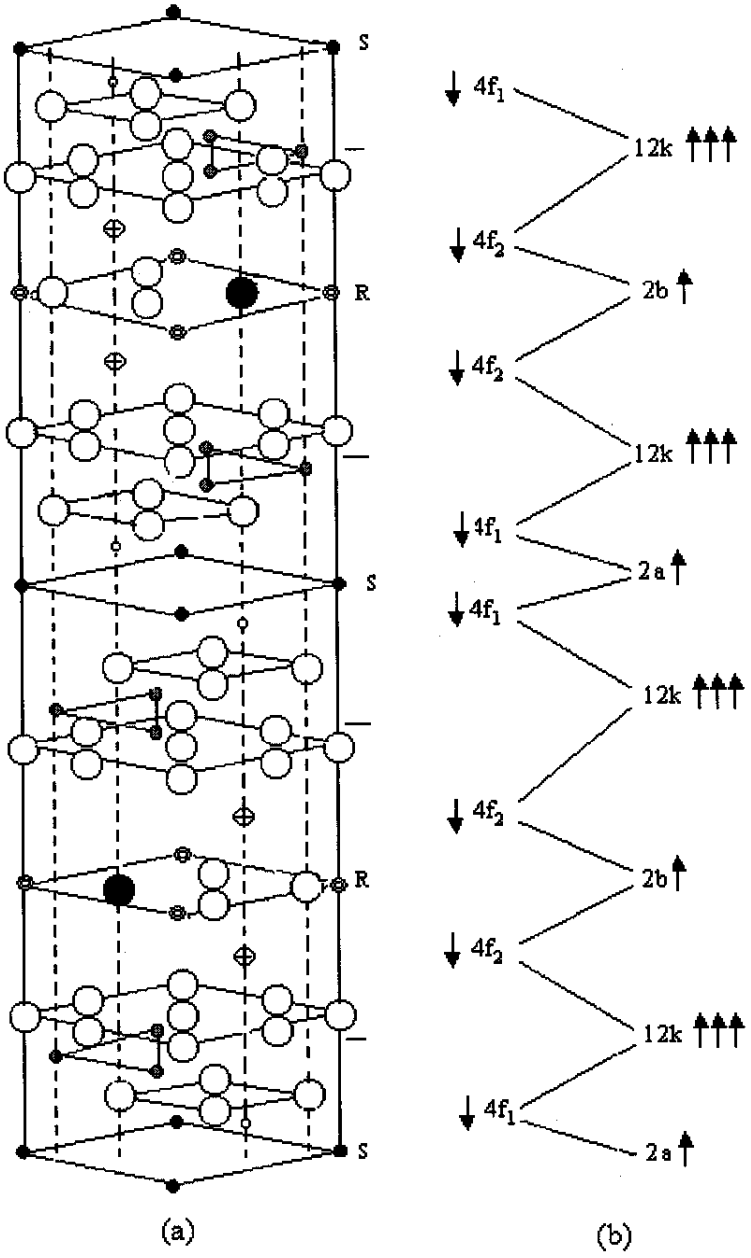

M-type ferrite (a) Crystal structure showing the S and R subunits where ○ is O^{2-}; ● is Sr^{2+}; ▣, ⊕, ●, ○ and ◎ are all Fe^{3+} at $4f_1$, 2b, 12k, $4f_2$ and 2a positions respectively.(b) Magnetic structure where the arrows represent size and spin direction of unpaired electron at various crystallographic positions.

Fig. 1.10 (a) crystal structure and (b) magnetic structure of $SrFe_{12}O_{19}$

Table 1.6 Number of ions, co-ordinate and spin orientation in the five iron sub lattice of $MFe_{12}O_{19}$ (M= Sr, Ba, Pb)

Sub lattice	Co-ordination	Number of ions	Spin
12_k	Octahedral	6	Up
$4f_{iv}$	Tetrahedral	2	Down
$4f_{iv}$	Octahedral	2	Down
2_a	Octahedral	1	Up
2_b	Five fold (Triagonal)	1	Up

Figure 1.11 shows the phase diagram of SrO and Fe_2O_3 system [57]. In the phase diagram the homogeneity range is very narrow and in the eutectic range somewhat enlarged, at most towards the side rich in the SrO. Towards higher temperature range, incongruent melting occurs at 1448^0 C (1 bar O_2) and 1390^0C (air), with the W phase $SrFe_{18}O_{27}$ (= SrO $2FeO.8Fe_2O_3$) is formed [58]. However, in vacuum annealing above 1100^0C, Fe_3O_4 and S_7F_5 phase is formed with the release of oxygen, where S = $2(MeO.Fe_2O_3)$ and F = SrO. $6Fe_2O_3$.

$SrFe_{12}O_{19}$ phase is stable only towards lower temperature range. Towards the Fe_2O_3 richer side the two phase region ($SrFe_{12}O_{19}$ + α Fe_2O_3) are formed. On the SrO richer region, the phase S_7F_5 and S_3F_2 are the neighboring phases both of them being very close to the composition S_4F_3 [59]. The eutectic temperatures of 1210^0C (1 bar O_2) or 1195^0C (air) as well as the eutectic content of 53.5 or 55 mole % are close to one another.

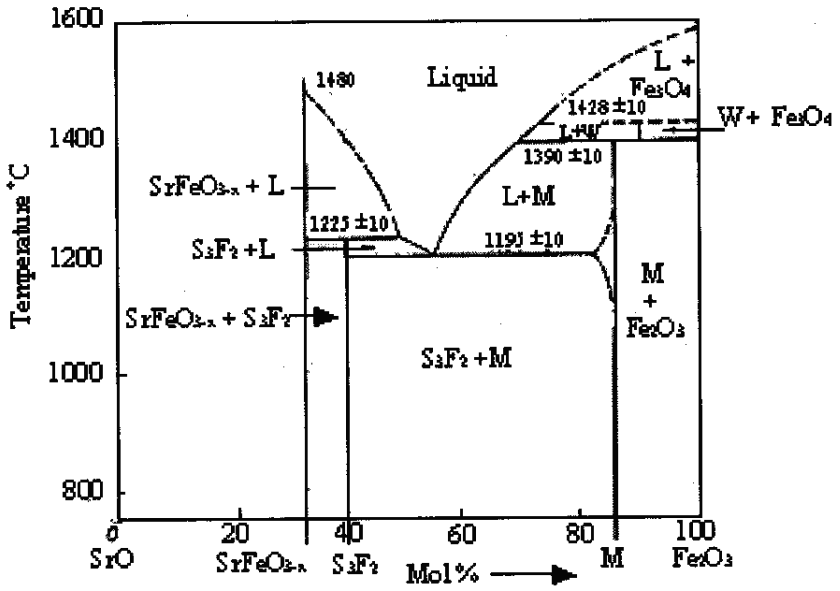

Fig. 1.11 Phase diagram of SrO – Fe_2O_3

1.12 Intrinsic Magnetic Properties of M-Type Ferrite

The intrinsic magnetic properties are subdivided into primary and secondary one. The primary properties such as saturation magnetization *Js* and magnetocrystalline anisotropy constant K_1 are directly related to the magnetic structure. The secondary magnetic properties such as anisotropy field strength H_A and the specific domain wall energy (γ_w) are derived from the primary ones. The secondary magnetic properties characterize the actual magnetic state. These govern the actual magnetic behavior. The primary and secondary magnetic properties characterize the actual magnetic state. These govern the actual magnetic behavior. The primary and secondary magnetic properties are shown in table 1.7. The temperature behavior of the primary magnetic properties is shown in fig. 1.12.

Table 1.7 Primary and secondary magnetic properties of SrM

Primary Properties	
Saturation Magnetization, mT	475
Anisotropic constant, kJ/m^3	360
Curie Temperature, K	750
Secondary Properties	
Specific wall energy, J/m^2	54.2 x 10 $^{-4}$
Anisotropy field H_A, kA/m	1506
Max. coercivity, $(H_c)_{max}$ kA/m	1240

The saturation magnetization, J_s is the maximum magnetic moment per unit volume per gram. It is easily derived from the spin configuration of the sublattices, eight ionic moments and 40 μ_B per unit cell, which corresponds to 668 mT at 0 K.

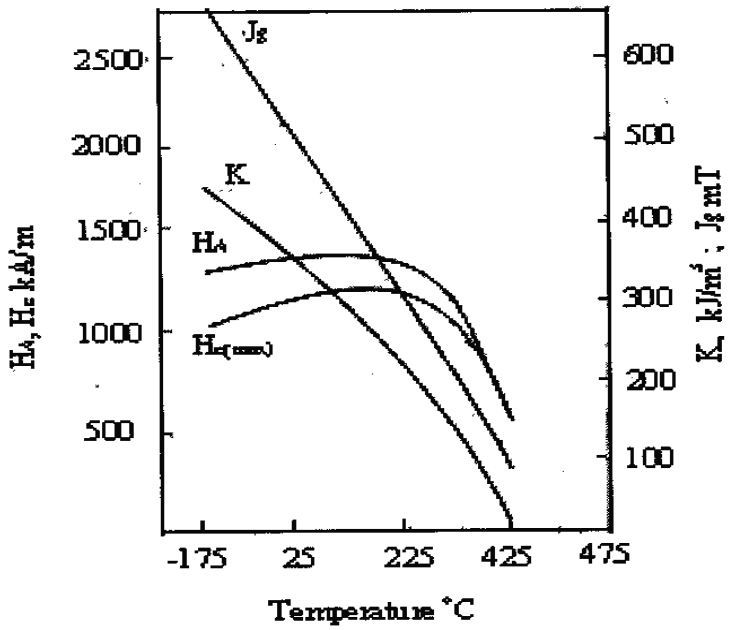

Fig.1.12 Temperature dependence of J_s, K_1, H_A and $H_{c(max)}$ for SrM

The magnetization is strongly bound to the hexagonal c-axis, owing to spin orbit coupling of Fe-ions, in particular on the *2b* sites [60]. When the direction of the spontaneous magnetization in a hexagonal crystal is expressed by polar co-ordinates θ and ϕ with respect to crystal axis, assuming z axis is the hexagonal axis, then the magnetocrystalline anisotropy *E* is given by:

$$E = K_1 \sin^2 \theta + K_2 \sin^4 \theta + K_3 \sin^6 \theta + \text{----------}$$

The energy involved in this process is characterized by the anisotropy constant K_1. The values of higher order constants (K_2, K_3) are almost negligibly small.

The secondary magnetic properties characterize the actual magnetic state. The latter minimizes the three energy involved: the exchange energy E_c, the anisotropy energy E_a, and the magnetostatic energy E_m, which are characterized by the value of exchange energy coefficient *A*, anisotropic constant *K* and saturation magnetization J_s respectively. The secondary magnetic properties for strontium ferrite are given in table 1.7.

The specific wall energy γ_w represents a combination of both E_e and E_a. The critical diameter for single domain behavior, D_c, is the diameter below which the magnetic domains are unfavorable in isolated spherical particle. Although M-ferrite particles are not spherical but magnetostatic interaction between the particles also play a role. D_c remains an important indicator for the grain size needed in high quality magnets. In the absence of domains, magnetization reversal proceeds by rotation. The ratio E_a/E_m determines the rotation magnetism. For M-type ferrites where $E_a/E_m > 0.36$, rotation is completely coherent.

The anisotropic field strength H_A is the maximum internal field strength needed for magnetization reversal by coherent rotation. The maximum coercivity $H_{c(max)}$ corresponds to H_A, but refers to external field. It is the reversal field necessary to coerce the material back to zero induction. It explicitly takes into account of self demagnetization field of the crystal (NJ_s/μ_0) as governed by the self demagnetization factor N. The latter ranges from 0 (for needles) to 1 (for thin plates). For platelet shaped M-type ferrite crystal N ranges 0.6 to 0.9. $H_{c(max)}$ represents an upper limit for the coercivity of unaligned assembly of non interacting crystals and 0.48 $H_{c(max)}$ the same for an isotropic assembly. Real coercivity values are much smaller resulting from the formation of transient domains and magnetostatic interactions.

1.13 Processing of Strontium Ferrite

Strontium ferrite magnets are produced by ceramic process involving powder preparation, shaping, firing and finishing operation. Further, sintered magnets are also subdivided in two classes depending upon the pressing condition. Pressing under the magnetic field gives anisotropic magnets and pressing without magnetic field gives isotropic magnets.

1.13.1 Sintered Strontium Ferrite

The conventional powder metallurgy process is the most common technique for making commercial sintered isotropic and anisotropic ferrite magnets. Isotropic ferrites have uniform magnetic properties in all directions, whereas anisotropic magnets have higher flux density in the orientation direction. The properties of the magnets are largely dependent on the process parameters, which in turns, affect the grain size, shape, volume fraction of phases and their alignment. The schematic process flow diagram for the preparation of sintered strontium hexaferrite magnet is given in figure 1.13.

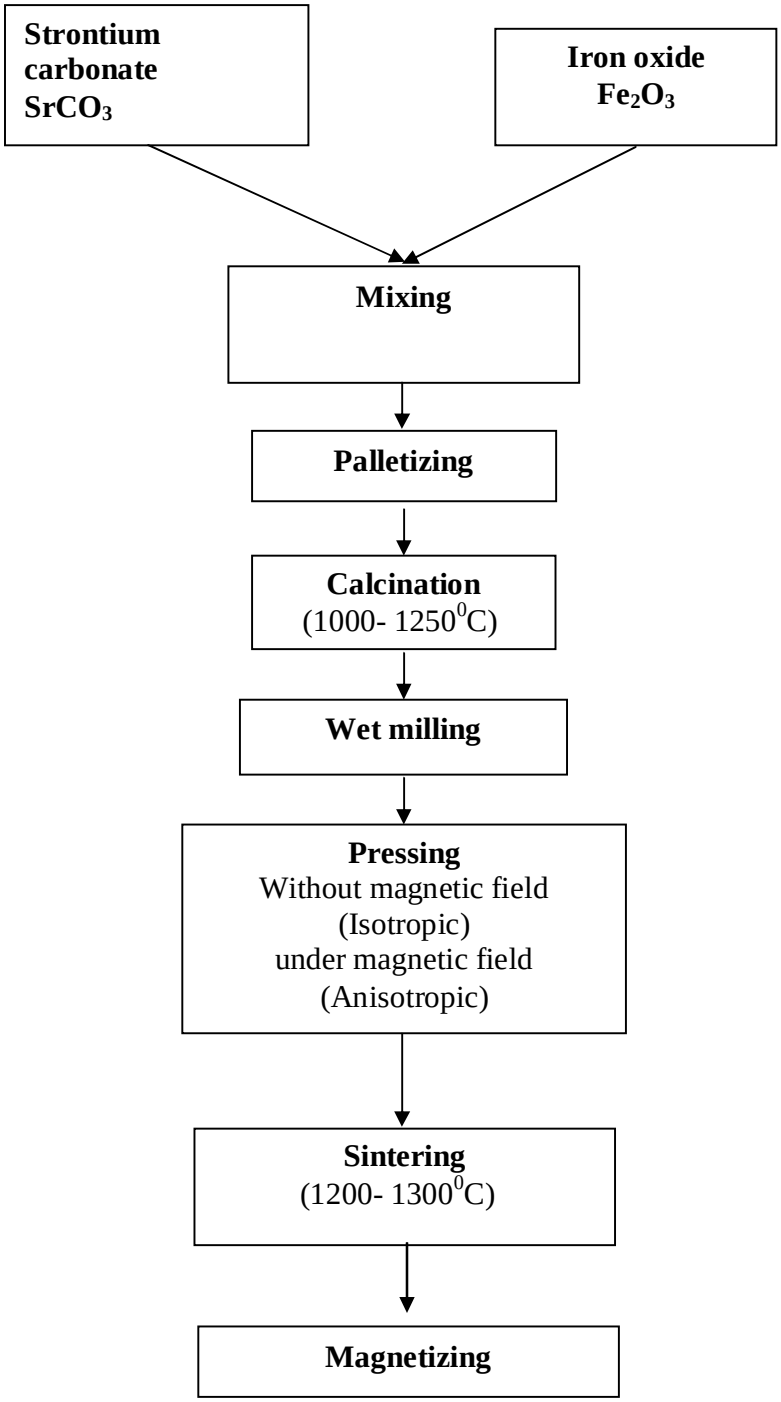

Fig.1.13 Schematic process flow sheet of preparation of strontium ferrite sintered magnets

1.13.2 Raw Materials

Strontium carbonate ($SrCO_3$) and iron oxide (Fe_2O_3) are the major raw materials used for the preparation of $SrFe_{12}O_{19.}$ In addition to these other oxides such as CaO, Al_2O_3, SiO_2, Cr_2O_3 etc are used individually or combined in amounts of about 0.5 to 2.5 % by weight. They serve to control the reaction kinetics, shrinkage and grain growth but sometimes also affect the primary magnetic properties of the hexaferrite phase.

1.13.3 Composition

The mole ratio of Fe_2O_3/SrO is critical parameter for obtaining high remanence and coercivity. As per the chemical formula ($SrFe_{12}O_{19}$) this ratio should be 6.0. However, it is observed that good magnets are never obtained when the Fe_2O_3/SrO ratio is 6.0. This is due to the fact that Fe_2O_3 and $SrCO_3$ used are never 100% pure. Therefore, common impurities shall be accounted while fixing the mole ratio of Fe_2O_3 and SrO. The following condition shall be met for obtaining high B_r and H_c values [61].

$$\mathbf{5.57 - 0.25 \times \log(Cl) - 0.95 \times SiO_2 < Fe_2O_3 / (SrO + BaO) < 5.81 - 0.25 \times \log(Cl) - 0.65 \times SiO_2}$$

The above condition takes into account the common impurities, such as SiO_2, Cl and $BaCO_3$ found in raw materials. If the mole ratio is less than lower limit set by above inequality, then Sr is in excess and lower remenence and $(BH)_{max.}$ If the mole ratio is in excess of upper bound defined by the inequality then excessive liquid phase is formed during sintering, and coercive force is reduced due to abnormal grain growth during calcination. Presence of SiO_2 less than 1% allows calcination at higher temperature without grain growth.

1.13.4 Mixing

Mixing is done to homogenize the raw materials and can take place with a wet process easily. In this process the raw material are mixed in planetary mill using zircon ware-ball set in hexane or acetone medium for 1 to 3 hours depending upon the particle size of the raw materials.

1.13.5 Calcination

Calcination involves heat treating a powder or mixture of powder at a temperature well below its melting point to effect decomposition i.e. to liberate unwanted gases or chemically bound waste, solid waste, solid state reactions and structure transformations to produce the desired compositions and phase product.

Calcination facilitates solid state diffusion of SrO and Fe_2O_3 and converts the raw materials into hexaferrite phase. The total reaction takes place in two steps.

$$\mathbf{SrCO_3 + Fe_2O_3 \longrightarrow SrO.Fe_2O_3 + CO_2}$$

$$\mathbf{SrO.Fe_2O_3 + 5\,Fe_2O_3 \longrightarrow SrO.6Fe_2O_3}$$

$$\mathbf{SrCO_3 + 6Fe_2O_3 \longrightarrow SrO.6Fe_2O_3 + CO_2}$$

The intermediate product, which occurs, is the monoferrite $SrO.Fe_2O_3$. The calcination temperature also plays an important role in the formation of hexaferrite phase. If the calcination temperature is low the grains of uniform $SrFe_{12}O_{19}$ is not formed. Similarly, if the calcination temperature is too high, excessive grain growth occurs and coarse grain of $SrFe_{12}O_{19}$ is formed. An optimum temperature for calcination is decided based on silica content in Fe_2O_3 powder.

1.13.6 Wet Grinding

The calcined mass is generally hard and coarse in size. To fulfill certain magneto-physical requirements it should be grinded to make fine powders. Wet grinding is carried out in ball mills to obtain powder of narrow particle size of the order of domain size 1 μm. There is always grain growth and recrystallization during sintering and so before sintering crystallite size has to be considerably smaller than 1 μm. Average particle size in the range of 0.7 –0.9 μm is recommended for achieving good magnetic properties. Moreover, the standard deviation shall not be very large. The standard deviation in the range of 0.14 to 0.16 has found to be optimum.

1.13.7 Compaction

The powder is compacted wet or dry in the presence or absence of magnetic field. Pressing under magnetic field is done to obtain anisotropic magnet by aligning powder in the direction of magnetic field. For dry compaction polyvinyl alcohol is used which gets evaporated during sintering. It is possible to prepare both isotropic and anisotropic magnets by dry pressing. The direction of the applied magnetic field during pressing may be parallel or perpendicular to the pressing direction. The magnetic properties obtained in perpendicular pressing have been found to be better than parallel field. A magnetic field of 0.5- 1.0 T has been found adequate for magnetic alignment. The remanence is strongly affected by the magnetic pressing and it is given by the following formula:

$$B_r = f\,(d/dx).S.\,J_s$$

Where *f* is the degree of alignment, d/dx the relative density and *S* is the fraction of pure ferrite. The value of *f* is 0.5 for isotropic and 0.9 for anisotropic magnets. The relative density is generally 0.9 and fraction of pure ferrite 0.98. Compaction pressure in the range of 5-15 MPa has been found sufficient in wet pressing and 40-80 MPa for dry pressing.

1.13.8 Sintering

Sintering is carried out to bring about the bonding between the powder particles and effect densification. During sintering the relative density increases from about 55-65% to over 90%. The reduction in linear dimension amounts to 10-12% and radial reduction 13-16%. The reduction in dimension is due to the extensive elimination of pores between the particles, crystal recovery, recrystallization and crystal growth. The driving force behind all this is the decrease in the surface and grain boundary energy and potential energy elastically stored in the lattice. Sintering is carried out in the temperature range 1373- 1573 K. However, care is taken to avoid excessive grain coarsening during sintering since at low temperature coercivity increases with crystal recovery and it falls again as a result of crystal growth when the temperature is set to the value needed for the temperature. Typical sintered magnets have grain size of 1 μm, which is

somewhat bigger than the critical domain size but sufficiently small to avoid domains down to considerable reverse fields.

The rate of sintering process and the properties of the sintered materials are mainly affected by nature and quality of chemicals, particle size, pressing conditions, sintering time, temperature and atmosphere. The rapid heating will allow the ferrite to maintain fine grain size due to the shrinkage occurring prior to any grain growth. As these two processes are inter-related, it is difficult to predict whether fine or coarse grain size is obtained without correct knowledge of kinetics mechanism.

The average grain size can exceed even 50 µm due to secondary grain growth and average grain size can be reduced by increasing the pressure. As the pressure is increased, the density of the ferrite increases and porosity decreases. The ferrites prepared by hot pressing technique require comparatively lower sintering temperature because of the increased elastic stress at inter-particle contacts and this technique provides the driving force for sintering. The duration of sintering time governs the rate of growth in the initial stage of sintering. The mean grain diameter (D) during the final stage of sintering is proportional to n th power of time (t) which is given as [62]

$$D = Kt^{n}$$

Where K is temperature dependent proportionality constant and n is about 1/3.
In crystalline materials and ceramics gases get trapped within the pores, when the pore formation becomes discontinuous and gets compressed. Pore shrinkage causes compression until internal pressure reaches equilibrium. When reducing atmosphere is provided, the lattice vacancies enhance diffusion and would increase sintering rates, thereby enhancing densification. The growth rate of ferrites sintered in different atmosphere is also different.

The particle size distribution is an important factor which affects sintering. The shrinkage produced due to sintering depends on the matter which is transported to the pores from the grain boundaries. Regardless of whether this transport occurs by bulk diffusion, grain boundary diffusion or through a liquid phase concentrated at the grain boundary, the transport distance will be small. This results in high sintering rate for small particle size.

It is very important to control the grain growth of the powders during the initial stage of sintering. Fine powder may cause some of the grains to show spontaneous growth to large sizes during sintering while other grains may remain much smaller. This results in a large grain surrounded by many small grains producing discontinuous grain growth. Keeping the grain boundary mobility low and the pore mobility high, will minimize this haphazard growth. The distribution of particle size also affects the sintering process attributing to the fact that increased heterogeneity of particle size results in discontinuous grain growth.

1.13.9 Final Magnetization

In as-manufactured condition a permanent magnet is either totally non magnetic or only incompletely magnetized. It is usually magnetized after being incorporated into the magnet system. Final magnetization is carried out at a field, which is 2.5-3 times higher than the intrinsic coercivity. Thus, the final magnetization is done at 1.2 –1.5 T.

1.14 Magnetic Properties of Commercial SrM

A large variety of strontium ferrite magnets for its end application is available. Typical magnetic properties of commercially available sintered and bonded SrM magnets are given in table 1.8.

Table 1.8 Typical magnetic properties of SrM magnets

Magnet Type	B_r (T)	H_C(kA/m)	$(BH)_{max}$ (kJ/m^3)
Sintered isotropic	0.20-0.23	136 -152	6.4 –8.4
Sintered anisotropic (High B_r)	0.39-0.43	192- 200	28.8- 34.4
Sintered anisotropic (High H_c)	0.35- 0.40	260 – 292	22.4- 30.4
Bonded flexible (Isotropic)	0.10 - 0.17	76 – 128	2.4 - 5.6
Bonded flexible (Anisotropic)	0.20 - 0.25	140 -176	8.0 - 12.0
Bonded rigid (Isotropic)	0.13 - 0.14	72 – 84	2.8 – 3.2
Bonded rigid (Anisotropic)	0.20 - 0.30	120 -185	7.3 – 16.0

1.15 Applications

Due to its low price ferrite magnets are used for a number of applications ranging from magnetic holding tools to motors and generators. The ferrites have replaced other magnet materials in the existing systems. This is particularly the case with static application where small demagnetizing fields are involved. A typical example is the application of flat ring instead of high metallic centre core magnets in loudspeaker systems. The high H_c has stimulated the development of the new system, especially in the dynamic application where periodically high demagnetizing fields are present. A typical example is the electric motor with its strong armature electric field. New electric motors are being developed which require very high H_{ci} value lying far beyond the range of Al-Ni-Co materials, for example the starter motor ,requiring H_{ci} >320 kA/m.

The main ferrite products are anisotropic segment for motor in car, anisotropic blocks for ore separator. These products together represent about 75% of the total production. It appears that large scale production is concentrated on application requiring relatively large magnets. In this case, the greatest advantage is taken of the low material price. The remainder of the production is distributed over a wide range of applications, involving mostly small magnets, such as shakers, mixers and coffee grinders.

Application of hard ferrite other than permanent magnets is in the field of microwave, magnetic bubbles memories, magnetic tape recording and magneto optics. M-type ferrites are of interest for resonance type microwave devices e.g. isolators, filters and calculators. Below 20 GHz such devices normally employ garnet or spinel ferrite in combination with the bias magnets. At high frequencies the required bias becomes impracticably high (> 570kA/m). M-type ferrite are then preferred because of their large anisotropic field which acts as a built-in bias field and provides a resonance frequency of about 50 GHz in a small tuning field. Apart from these magnets are used in magneto-therapy, purification, magnetic bearing and automatic camera are a few more applications. Some of the common application in gadget used in everyday life is shown in table 1.9.

Table 1.9 Common application ferrite magnets

Gadget	Parts
Cassette recorder	Speaker, synchronous motor, mike etc.
Video cassette recorder	Main wheel motor
TV sets	Speaker, colour adjusting magnet
Air conditioner	Fan motor
Refrigerator	Fan motor, compressor motor, rubber lining
Car	Starter motor, window motor, viper motor
Computers	Disk drive, fan motor, speaker etc.
VCD and DVD	Main wheel motor

1.16 Market Information

The global permanent magnet market is estimated to be $5.0 billion, which is growing at the rate of 12.5%. Ferrite constitutes 56% of the total market. Japan, USA and China are the major producers of the ferrite magnets. While annual growth rate in USA and Japan is not appreciable, the growth rate in China and other south East Asian countries is substantial. After five years of development in terms of quantity, China has become first in the global hard ferrite market.

1.17 Outline of the Present work

Extensive research has been carried out to observe the effect of the various process parameters on the magnetic properties, microstructure and phase present. This has led to development of variety of compositions (dopants) and processing routes of strontium hexaferrite to achieve better magnetic properties. The present work is an attempt to add something more to the existing work by adopting different processing routes and raw materials.

In the present work strontium hexaferrite sintered magnets were prepared using pure chemicals such as strontium carbonate and iron oxide. The influence of mole ratio, calcination temperature, sintering temperature and time on magnetic properties of $SrFe_{12}O_{19}$ is discussed. Apart from this strontium hexaferrite were also prepared from processed celestite and upgraded blue dust. A comparison of magnetic properties of the two magnets prepared from pure chemicals and processed ores has been discussed. Also the synthesis of strontium hexaferrite has been carried out by mechanochemical method using chemically treated celestite and upgraded blue dust. Apart from this the conversion of Indian celestite to strontium carbonate was carried out. Effect of different parameters influencing conversion percentage has been studied. The different types of upgradation processes for upgradation of blue dust have been done in this work.

References

1. Sujoy K. Dutta and Ahindra ghosh, ISIJ International, vol. 33(11), pp 1168-1173.
2. R.Dasgupta, S.K.Bose and S.P.Narayan, "Hard ferrites from Blue dust of Bailadila Iron Ore Mines of Madhya Pradesh" Research and Industry, vol.40, 1995, pp 236-239.
3. A.K. Jouhari, P.S.R. Reddy, B. K. Mahapatra and Vibhuti N. Mishra, "Raw Material Preparations for Metallurgical Industries" Proceedings of the seminar on raw material, 2002, pp 32-35.
4. W. Hong, "Celestite and Strontionate", Industrial Minerals, 1993, pp 55-59.
5 Kirk-Othmer, Encyclopedia of Chemical Technology, Fourth Edition, John Willey & Sons-1997, vol. 10, PP 947-955.
6. www.tidco.com
7. C.I.Mantell "Strontium" in C.A.Hampel, Rare Metal Handbook, 2nd edition, Reinhold Pub. Co, London, 1961, pp 27-31.
8. "Strontium- Supply, Demand and Technology".U.S. Bureau of Mine Information Circular 9213, 1989.
9. A. Joyce Ober, "Strontium" from Mineral Commodities Summaries, U.S Bureau of Mines. 1992, PP 1323-13.
10. U.S. geological survey, Mineral Commodity Summaries, 2007, pp 1-2.
11. A. Joyce Ober, USGS Mineral Yearbook, 2006, pp 1-7.1963, pp 1251.
12. http://elements.vanderkrogt.net/elem/sr.html.
13. Strontium Chemical in Mineral Facts and Problems, U.S. Bureau of Mines Bulletins,1985, vol. 675.
14. Ullmann's Encyclopedia of Industrial Chemistry, fifth edition, VCH-1994, vol-A25, PP 321-327.
15. Strontium Chemical in Industrial Mineral and Rocks (7th edition), Society for Mining, Metallurgy and Exploration Inc., 2006.
16. W.G., Lidman, "Master Alloys Improve Aluminum Casting Properties",Foundry Management and Technology, Vol. 112(8), 1984, pp 46-47.
17. T. H., Haberberger, "Ferrite Application Ever Changing and Expanding Ceramic Industry Magazine, 1971, vol. 115, pp 29-32.
18. R.G. Wager, "Glass as a CRT Fabrication Material glass" 1986, vol. 63, pp 191-192.
19. Metals Handbook, 9th edition, vol.2, American society of Metals, Metal Park, OH. 1979.

20. H.Szelagowski, I. Arvanitidis and S. Seetharaman, “Effective Conductivity of Porous Strontium Oxide and Strontium Carbonate Samples”, Journal of Applied Physics, 1999, vol.85, pp 193-198.
21. Tsunetake Seki, Kazumasa akatsu and Hideshi Hattori, “Calcium Oxide and Strontium Oxide as Environmental Benign and Highly Efficient Heterogeneous Catalyst for the Tishchenko Reaction of Furfural, Chem. Commun, 2001, pp 1000-1001.
22. U.S. Beauro of mines- A report, 1959.
23. E. Pedak, M. Allsalu and M. Kanter: Zh.Prikl. Khim (Leningrad), 1972 vol., 45(12), pp 2619-23 (in Russian).
24. E.B.Gitis, P.I.Stigunov, S.K.Solynaik, L.F. Vasileva, F.D. Pushkanov Y.N. Zinchencho and V.I. Krasinyakov: Otkritiya Izobret, 1985, vol. 46 pg. 1.
25. J. Plewa, J. Steindor and J. Nowakowski, Thermochem acta, 1989, vol. 138(1), p 55.
26. R.S.Sonawane, B.B.kale, S.K.Apte and M.K. Dongare. “Effect of a Catalyst on the Kinetics of Reduction of Celestite ($SrSO_4$) by Reactive Charcoal”. Metallurgical and Material Transaction, 2000. Vol. 31B, pp 35-41.
27. Wen Chen and Yun Zhu, “Preparation of Strontium Carbonate from Celestite” Mineral Processing and Extractive Metallurgy, 1998, vol. 109, pp 65-68.
28. U.S Patent No-4421729, 1983.
29. U.S Patent No-4666688, 1987.
30. U.S Patent No-6159 436. 2000.
31. A.H. Castillejos E, F.P de la Cruz del B. A.Uribis, “The Direct Conversion of Celestite to Strontium Carbonate in Sodium Carbonate Aqueous Media”. Hydrometallurgy, 1996, vol.40, pp 207-222.
32. R. Suarez-Orduna, J.C Rendon-Angeles, J Lopez-Cuevas and K Yanagisawa “The Conversion of Mineral Celestite to Strontianite under Alkaline Hydrothermal Condition”, Journal of Physics Condensed Matter, (16), 2004, pp 1331-1334.
33. Hacer Dogan, Murat Koral, Sidika Kocakusak “Acid Leaching of Turkish Celestite Concentration” Hydrometallurgy, 2004, vol.71, pp 379-383.
34. M.Erdemoglu, M. Canbazoglu and H. Yalcin, “Carbothermic Reduction of high-grade Celestite Ore to Manufacture Strontium Carbonate”Trans. Inst. Min. Metal Sec C- Mineral Processing Extractive Metal, 1998, vol. 109, pp. 65-68.

35. Abdullah Obut, “Direct Conversion of Celestite to SrS by Microwave Heating” Materials Engineering, 2007 (Article in Press).
36. J.M., Osepchuk, “A History of Microwave Heating Application”, IEEE, Transaction on Microwave Theory and Techniques, 1984, vol. 32 (9), pp 1200-1224.
37. K.J. Rao Vaidyanathan, B. Ganguli, M. Ramakrishnan, P.A. 1999 “Synthesis of Inorganic Solids using Microwave”.Chemistry of Materials, vol. 11, pp 882-885.
38. D.E Clark, D.C Folz, J.K. West, “Processing Materials with Microwave Energy”, Material Science and Energy, 2000, vol. A287, pp 153-158.
39. Abdullah Obut, Peter Ballaj, Ismail Girgin “Direct Mechanochemical Conversion of Celestite to $SrCO_3$”. Mineral Engineering vol.19, 2006, pp 1185-1190.
40. K.A. Kobe, N.J. Deiglameier. “Conversion from Strontium Sulphate by Metathesis with Alkali Carbonates Solution”,Ind. and Eng.chemistry, 1946, vol. 40, pp 1988-1990.
41. W. Ervens and H. Wilmesmier, in “Magnetic Material” Ullmann’s Enclyclopedia of Industrial Chemistry, Eds. B. Elvers, S. Hawkins, G.Shulz, VCH Verlag GmbH, D. Wernheim, Germany, Fifth edition, vol. A16, 1990, pp 1-51.
42. K.H.J. Buschow, F.H. Ferjen and K.D. Kort, Rare Earth Permanent Magnet,”J. Magnetism and Magnetic Materials”, vol. 140, 1995, pp 9-12.
43. S. Hirosawa, A. Hanaki, H. Tomizawa and A.Hamamur, Physica B, vol. 164, 1990, pp 117-123.
44. F.X.N.M Kools and D. Stoppels, Kirk-Othmer Enclyclopedia of Chem Tech., Fourth edition, vol.10, 1993, pp 381-413.
45. J. Wernic, Kirk-Othmer Encyclopedia of Chem. Tech., Fourth edition, vol. 15, 1995, pp. 723-769.
46. H. Kojima, Ferromagnetic Materials, Edited by E. P.Wohlfarth, vol.3, 1982, chapter 5.
47. M.A. Bohlman, F.G. Jones and F.E. Luborsky, Metals Handbook, Ninth edition, vol. 3, 1980, pp 615- 639.
48. Y. Kato and T. Takei, U.S.Patents 1,976,230 and 1,997,193; 1937.
49. J.J. Went, G.W. Rathenau, E.W. Gorter and G.W. Van Oosterhout,”Ferroxdure, A class of new permanent magnetic materials” Philips Techn. Rev., vol.3, 1980, pp 194-197.
50. E.W. Gorter, G.W. Rathenau and A.L.Stuyts, U.S.Patent 2, 762,777, 1956.
51. A.L. Stuyts, G.H.Weber and G.W. Rathenau,“Ferroxdure II and III, Anisotropic Permanent Magnet Materials”, Philips Technical Review, vol. 16, 1954, pp 141-148.

52. C.W.Chang, M. S. Tzeng and S.J. Wang and Y.C.Yu, IEEE Transaction of Magnetics, vol.26, 1990, pp 832-835.
53. Lin, Z.W. Shoh, T.S. Chin, M.L. Wang and Y.C.Yu, IEEE Transaction of Magnetics, vol.26, 1990, pp 15-17.
54. A. Ataie, I.R.Harris, C.B.Ponton, "Magnetic Prpperties of Hydrothermally synthesized strontium Hexaferrite as a function of synthesis conditions", Journal of Material Science, vol.30(6), 1995, pp 1429- 1433.
55. F. Kools, Science of Sintering, vol. 17, 1985, pp 1-12.
56. E.W.Gorter, Proceeding IEEE, vol. 104B, 1957, pp 2255-2257.
57. Y.Goto and K. Takahashi, Journal of Japanese Society Powder Metallurgy, vol. 17, 1971, pp 193-197.
58. A Kockel and F. Habery," The Formation of Strontium Hexaferrite $SrFe_{12}O_{19}$ from pure Iron Oxide and Strontium Carboinate",IEEE Transaction Magnetism, vol. MAG-12(6), 1976, pp-983-985.
59. F.Kamamaru, M.Shimada and M.Koizumi,"Crystallogarphic properties of and Moessbauer Effects in Sr_4FesOa", Journal of Physical Chemical solids, vol. 33, 1972, pp 1169-1171.
60. F.K.Lotgering, P.R. Locher and R.P. van Stapele, Journal of Physical Chemical Society, vol. 41, 1980, pp 481-484.
61. P.I. Slick, Ferromagnetic Materials, North-Holland Publishing Company, 1980.
62. E.A. Schawabe and D.A. Campbell, Journal of Applied Physics, vol. 34,

Chapter 2

Conversion of Indian celestite to strontium carbonate

Overview

Celestite is an ore of strontium sulphate which is primary source of strontium carbonate. This chapter deals with different processes to convert Indian celestite to strontium carbonate. The purification of celestite by chemical treatment is discussed. The black ash and direct conversion methods for conversion of celestite into strontium carbonate are described. The effect of different reducing agents, mole ratios, temperature on conversion percentage of strontium sulphide and strontium carbonate is described for different time intervals. The comparison of processes in terms of process easiness, economy, and percentage yield has been discussed. Phase characterization of raw materials and product materials using XRD is described. The morphological characteristics of celestite and the derived product strontium carbonate was carried out using SEM.

2.1 Introduction

The mineral Celestite existing in different places across the world is main source for the production of $SrCO_3$, which contains 65 to 90 percent of strontium sulphate [1, 2]. In India it is found in Trichirrapalli district of Tamilnadu state. This is medium grade celestite as it contains large amount of impurities like Fe, Ba etc. Many other strontium chemicals like strontium nitrate, strontium chloride, strontium hydroxide and strontium oxide is being manufactured from celestite [3-7]. The major consumption of strontium carbonate is in glasses for colour television picture tubes to block X-ray transmission and improvement of glass appearance. The next major application of $SrCO_3$ of ferrite grade is in ceramic industries to produce ferrites of different grades for electrical and electronic appliances. Apart from this strontium carbonate is also used in purification of zinc electrolyte (to remove lead impurities) and as ceramic paints [1]. It is also used in farm chemicals, medicine and as tanning material [3].

The Beneficiation, purification of strontium carbonate from the natural ore celestite finds great difficulties to obtain required level of purity in the final product. Black ash and direct conversion are the two methods by which conversion of celestite to strontium carbonate is being carried out [4, 5]. A group of researchers have attempted to study the thermodynamic and kinetic parameters of the direct reduction and black ash processes [6, 8]. Apart from this scientists have conducted experiments on conversion of celestite to strontium carbonate using different techniques [9-12]. Hydrogen and mixture of H_2 and CO was used at high temperature for the reduction of celestite by Pedak *et al.* [13]. The major disadvantage of this process is consumption of large amount of gases and evolution of highly pollutant compound like H_2S, which is not eco- friendly. Gits *et al.* [14], Lepsin *et al.* [15] and Erdemoghi *et al.* [4] have also studied the thermo chemical reaction with a stoichiometic amount of carbon at a temperature 1200-1300^{0}C. The loading zone temperature of rotary kiln was 600-700^{0}C and discharge zone temperature was 1200^{0}C to 1300^{0}C. This process has many disadvantages such as high electrical energy requirements, sintering of reactants and product etc. To overcome such type of problems experiments have been carried out with easily available reductants like coke, bituminous coal, and activated charcoal [5, 6]. There is no data available for the comparative study of direct reduction process and black ash process through simultaneous experiments with respect to percentage yield, application etc. of Indian celestite. The present study aims to prepare strontium carbonate of

ferrite grade, which consists of many purification steps. These include black ash method and direct reduction method for the comparative study of conversion of celestite to $SrCO_3$ with respect to process cost, process simplicity, by product application etc. The basic aim of the project is to prepare strontium hexaferrite sintered magnets using celestite ore. In this chapter experiments performed for conversion of Indian celestite to strontium carbonate by different processes is reported.

2.2 Experimental procedure

The celestite ore obtained from Trichirapalli deposit of Tamil Nadu (India) was supplied by M/s J.M. Mines & Minerals, 37, Williams Road Cantonment, Tamil Nadu (India). The ore was ground to fine powder in a mortar pestle. The powder was sieved. The fraction less than 45 µm was collected for the experimental work. The chemical analysis of celestite was carried out to know its chemical composition. For different trace element analysis flame type (AAS) atomic absorption spectrometer flame type (Model GBC-932AA, Australia) was used.

2.2.1 Chemical treatment of celestite ore

100 gm celestite powder (<45µm) was taken in 2 liter borosilicate glass beaker. About 500 ml of 1:1 HCl, 20 ml conc HNO_3 and small amount of NH_4F was added in this fine powder mass. All acids and other chemicals were of Laboratory Reagent. grade purity. The beaker containing acid and celestite was heated on a hot plate at a temperature of 60^oC with constant stirring for 36 hours. The acid portion was decanted and fresh HCl (1:1) was added followed by small amount of HNO_3 addition to repeat this process. Acid treated celestite was filtered and washed many times with distilled water till the pH of residue on the filter paper attains neutral value. The filter paper with residue was dried in an oven at 110^0C for 2 hours. By addition of HCl, HNO_3, the strontium carbonate present with celestite along with Fe, Ca, dissolves and remains in the dissolved condition in the liquid. NH_4F has been added to dissociate any silicate materials present in celestite. By chemical treatment process celestite upgradation is performed and acid soluble impurities like Fe, Ca, etc. reduce significantly. The chemical composition of celestite before and after acid treatment is given in table 2.1 and 2.2.

Table 2.1 Chemical analysis of celestite ore before and after acid treatment

Composition	Before Acid leaching	After acid leaching
$SrSO_4$	91.60	96.66
$SrCO_3$	1.30	<0.02
$BaSO_4$	0.90	0.87
Fe_2O_3	4.01	0.60
SiO_2	0.10	0.10
Al_2O_3	0.21	0.15
CaO	0.36	0.01

Table 2.2 AAS results for other trace elements before and after acid treatment

Element	Mg	Pb	Zn	Ni	Cu	Na	K
Process							
(i) Before leaching	0.12	0.24	0.01	0.006	0.29	0.24	0.026
(ii) After leaching	0.012	0.021	0.01	0.005	0.002	0.002	0.021

2.2.2 Synthesis by Black Ash Method

In this process celestite obtained after acid treatment is reduced by carbon, at higher temperature. Three different sources of carbon viz. activated charcoal, bituminous coal and coke has been used as reducing agent. Chemical composition of these coals are given in table 2.3. The particle size of all three carbons was less than 100 micron.

Table 2.3 Chemical composition (wt. %) of different coals

Coal	Fix carbon	Ash	Volatile material	Moisture
Active Charcoal	97.00	1.70	0.50	0.70
Coke	82.86	12.26	0.20	3.85
Bituminous coal	62.26	25.62	6.32	8.62

The reaction involved in this reduction reaction can be written as:

$$\mathbf{SrSO_4 + 4\ CO \rightarrow SrS + 4\ CO_2 \ldots\ldots..(I)}$$

$$\mathbf{CO_2 + C \rightarrow 2CO \ldots\ldots\ldots\ldots.(II)}$$

$$\mathbf{SrSO_4 + CO \rightarrow SrO + SO_2 + CO_2 \ldots\ldots..(III)}$$

The carbon monoxide generated in this process diffuses and reacts with celestite which is not in contact with carbon. The excess carbon used in the process will give rise to formation of CO which will help in gas solid diffusion reaction. To start this experiment treated celestite powder (< 45 μm) has been taken and mixed with charcoal (heated at 110^{o}C for 24 hours before mixing). These experiments were done with different amount of charcoal, which varies with 10%, 20%, 30%, 50% and 60% in excess amount (weight ratio) of celestite taken. For example for 100gms celestite 110 gm of charcoal was taken and similarly the amount of charcoal was varied. This mixture was kept in silica crucible and covered with silica cover lid. Thick ceramic paste was applied around the cover. The system was heated in a muffle furnace at 1000^{o}C for 100 minutes. The experiment setup is shown in fig. 2.1. This experiment was conducted with different grades of coal at same temperature with variation in reducing time. The reduced SrS was leached with water. A little amount of HCl was added to dissolve non-soluble SrS. An excess amount of H_2SO_4 (6-10 times more then theoretical amount) was added to remove Ba as $BaSO_4$ and for it a long reaction time period was employed (8 hours) [5].

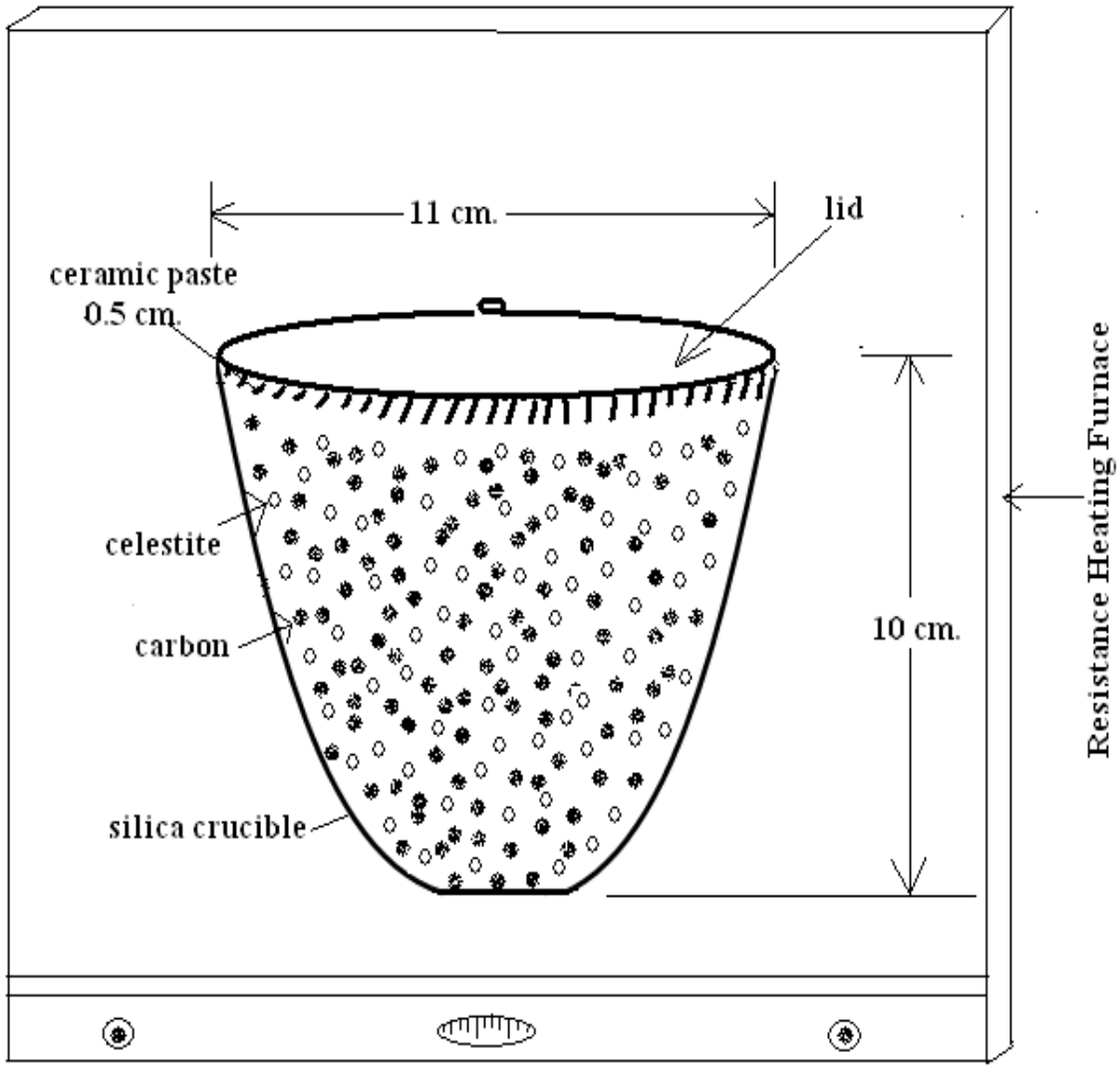

Fig.2.1 Experimental setup for reduction of celestite to strontium sulphide

The leached solution was filtered through the qualitative filter paper. This facilitates the removal of silicate and other insoluble constituents. The dissolved portion has been used for the precipitation of strontium carbonate. A 10% solution of sodium carbonate was added to the dissolved acidic strontium solution with constant stirring at 50^{o}C for precipitation of strontium carbonate. The precipitated strontium carbonate was filtered through qualitative filter paper and washed with distilled water many times until the residue on the filter becomes neutral which was tested with pH paper.

2.2.3 Direct conversion of celestite to strontium carbonate

In another effort celestite after leaching treatment was treated with Na_2CO_3 solution. The reaction involved in this process can be written as:

$$\mathbf{SrSO_4 + Na_2\,CO_3 \rightarrow SrCO_3 + Na_2SO_4 \ldots\ldots\ldots\ldots (IN)}$$

For this purpose 100 gm powder (<45μm) of treated celestite and sodium carbonate was taken in mole ratio of (Na_2CO_3 / $SrSO_4$) 1.0, 1.1, 1.2, 1.5. The sodium carbonate in required quantity was dissolved in 1 liter solution. The celestite powder was added slowly to the carbonate solution under the constant stirring at a temperature ranging from 25^0C to 75^0C at an interval of 10^0C with time variation from 30 minutes to 330 minutes at an interval of 30 minutes. The beaker containing solution was cooled and the converted $SrCO_3$ was filtered through the filter paper. The sodium sulphate produced in this reaction remains in the dissolved form. The residue on the filter paper was washed many times with distilled water until the residue becomes neutral.

The filtered and dried mass was again taken in 2 liter borosilicate beaker and dissolved in (1:1) HCl at a temperature of 40^0C for 1 hour. After cooling the liquid the mass was filtered through filter paper. In this way any silicate material and un-dissolved impurities was collected on filter paper leaving Sr as $SrCl_2$ in the solution. It was observed that Na_2CO_3 /$SrSO_4$ of molar ratio 1.5 give better yield. of strontium carbonate. $SrCO_3$ obtained from 1.5 molar ratios (Na_2CO_3/$SrSO_4$) was again added to sodium carbonate solution with constant stirring to precipitate strontium carbonate. The $SrCO_3$ obtained was analyzed by wet chemical analysis.

The study of phase analysis for the raw material celestite and the product SrS, $SrCO_3$ formed during reduction of celestite was conducted by XRD (Model Rigaku D-Max IIIC) and particle morphology was analyzed by scanning electron microscope (Model JEOL 840A).

2.3 Results and discussion

2.3.1 Black ash method

Celestite ore consists of $SrSO_4$ as major constituent as can be seen from X-ray diffraction pattern (fig.2.2). The reduction of celestite was done with different grades of coal. In all the experiments

excess amount of charcoal by weight percentage was taken. The celestite to charcoal ratio was varied as 1:1.2, 1:1.3, 1:1.4 and 1:1.6. Figure 2.3 shows the effect of excess activated charcoal content on reduction of celestite with variation in reducing time at 1000^0C. The reducing effect decreases considerably when the activated charcoal is less than 40% excess of the celestite mass. The reducing effect of activated charcoal with 60% excess mass was better. The conversion process is completed after 60 minutes of reduction time after that it becomes virtually constant. As the percentage of excess charcoal with respect to celestite mass increases the conversion percentage also increased.

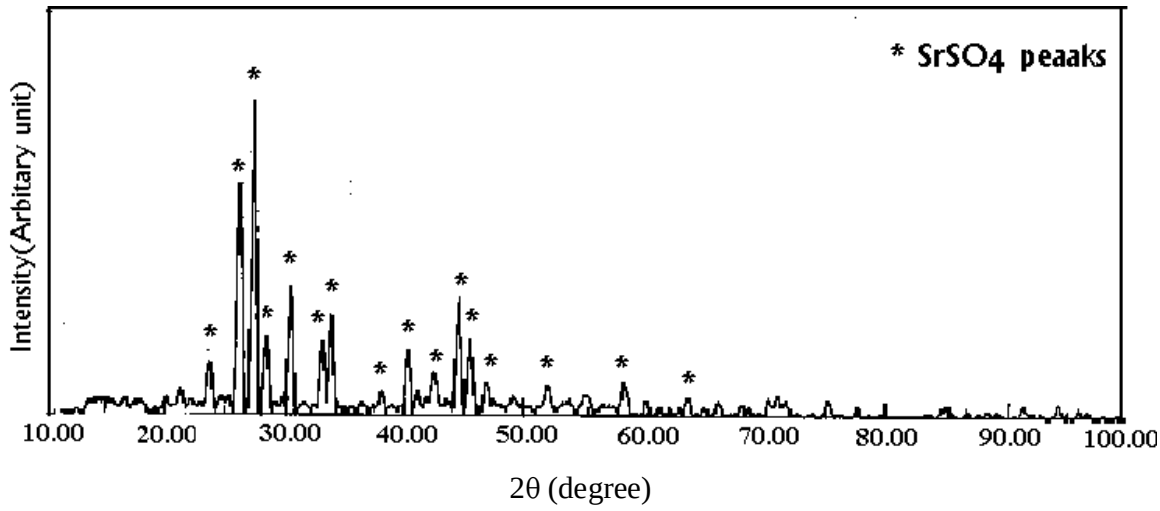

Fig. 2.2 Typical X-ray diffractogram of celestite showing the peaks of $SrSO_4$.

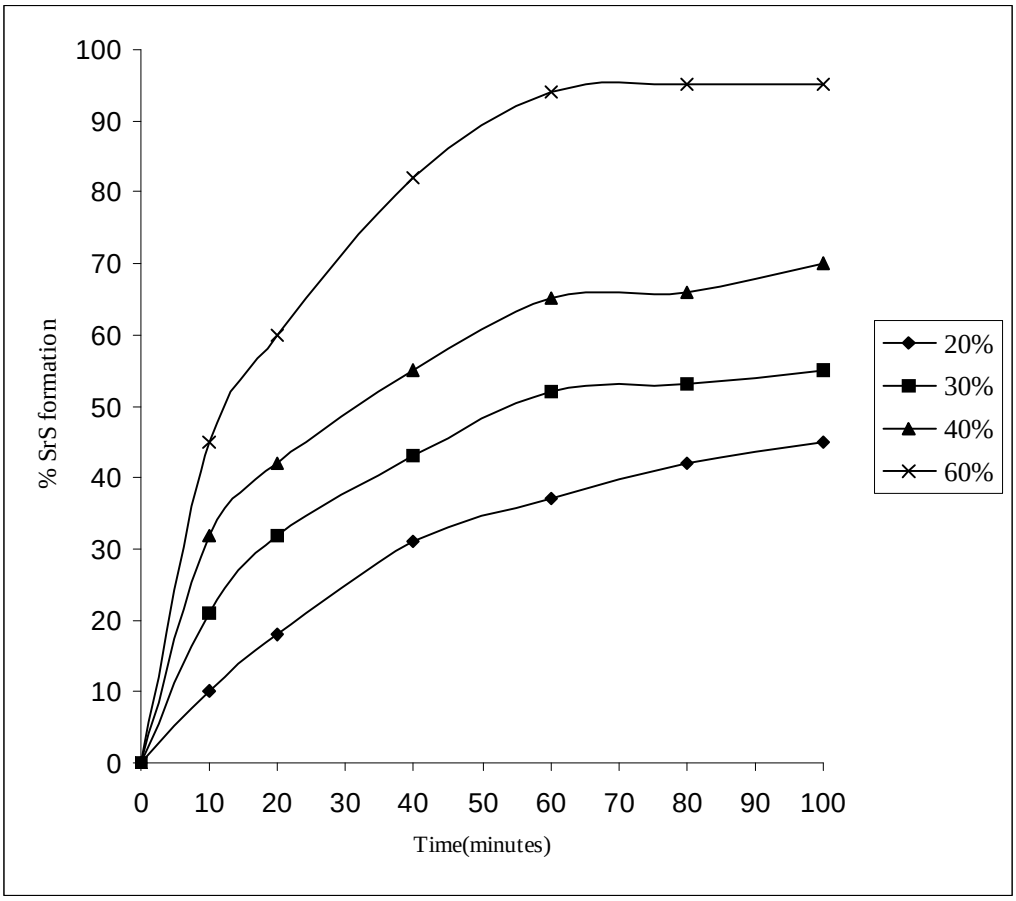

Fig. 2.3 Effect of reducing time and excess of activated charcoal on % yield of SrS at 1000^0C.

From the figure 2.3 it can be observed that up to a time period of one hour conversion increases considerably with each coal percentage mass. After one hour the conversion percentage rate becomes relatively slow. Similar trends were also observed for bituminous coal and coke, which are shown in fig. 2.4 and fig. 2.5 respectively with slight change in rate of conversion. Fig 2.6 shows the typical X-ray diffraction pattern of reduced celestite where peaks of SrS have been marked.

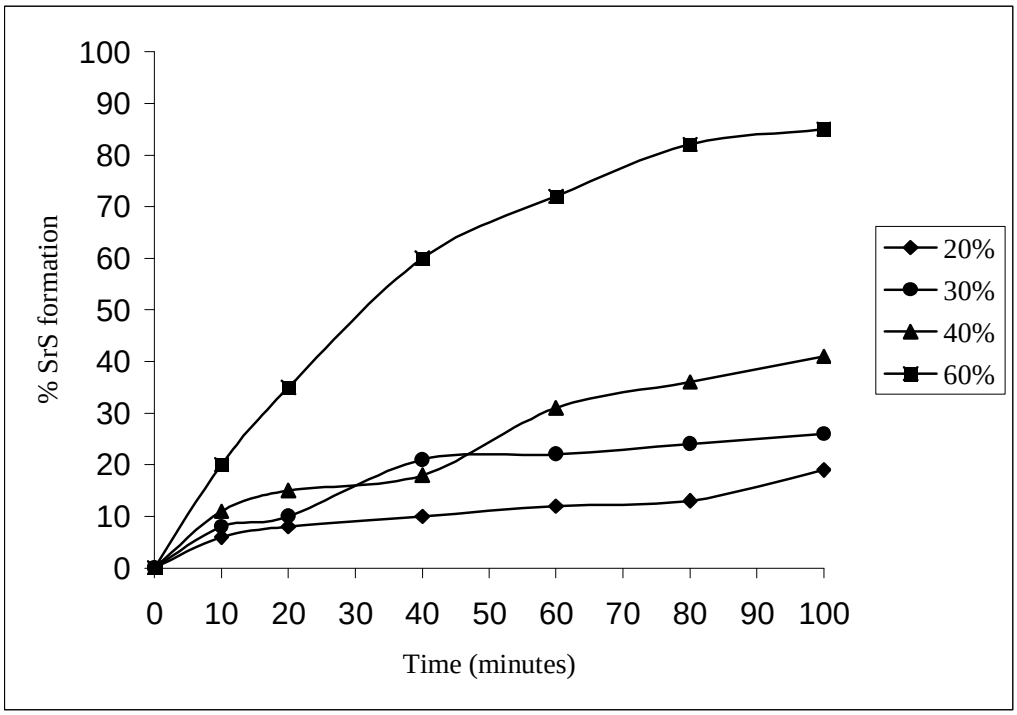

Fig 2.4 Effect of reducing time and % excess of bituminous coal on % yield of SrS at 1000^0C from celestite.

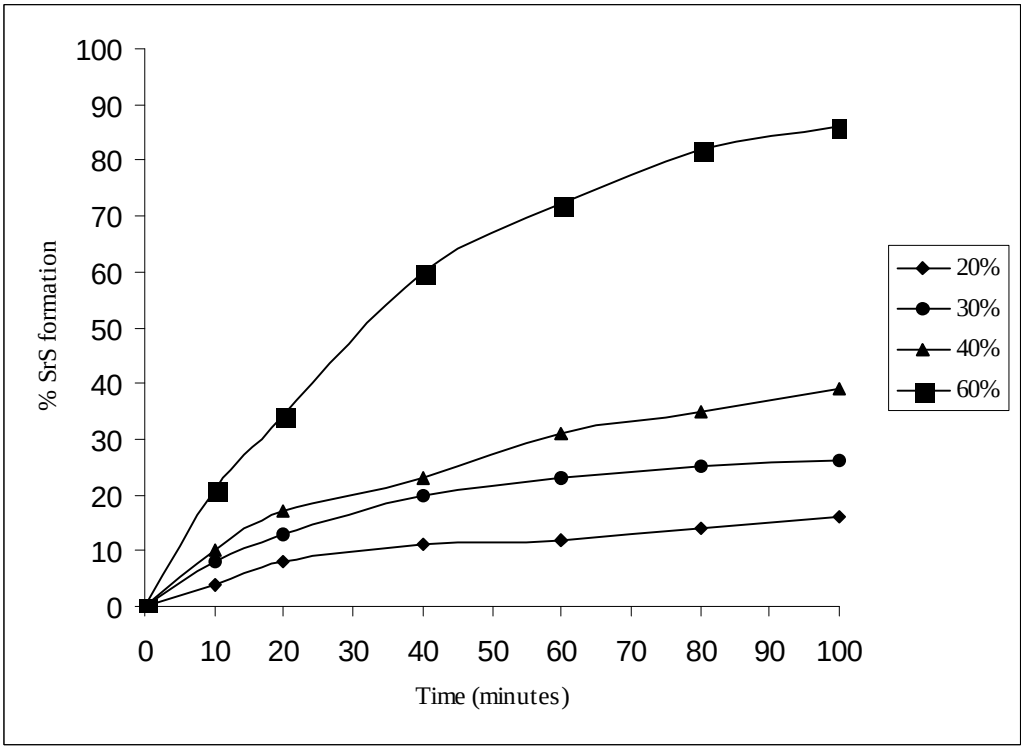

Fig. 2.5 Effect of reducing time and % excess of coke on % yield of SrS at 1000^0C.

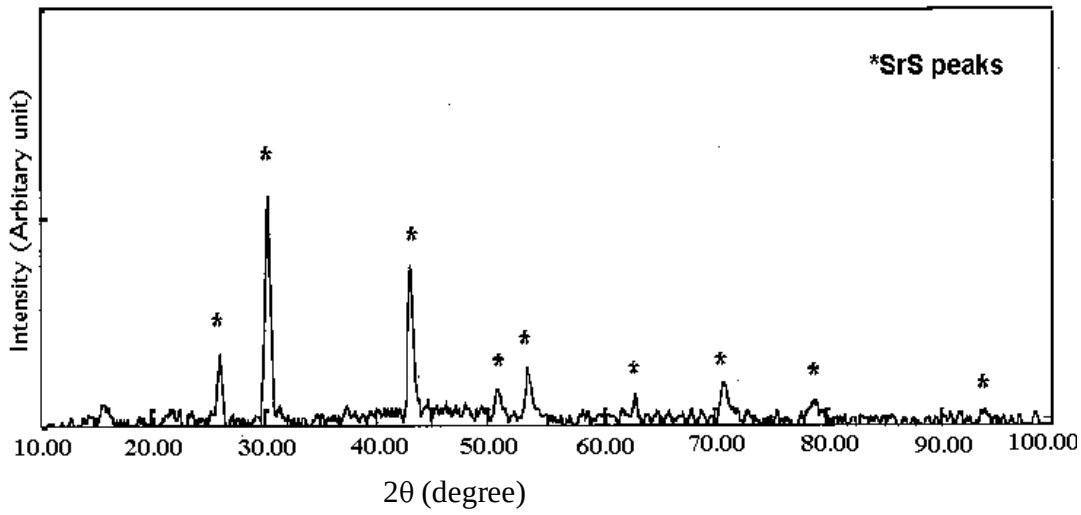

Fig. 2.6 Typical X-ray diffractogram showing the peaks of SrS obtained from black ash process.

The work by Wen Chan [5] for the reduction of Chinese celestite with different carbon source like brown coal, bituminous and coke indicates that the reducing effect with 40% excess charcoal with mass ratio of celestite is minimum and with 60% of mass ratio percentage conversion of celestite to SrS is maximum. The impurities associated with celestite such as Ba, Fe, Ca and Al has been separated in a sequence using chemical routes. However, the Chinese (Lamping) celestite contains around 4.0-8.0 % silica as impurity. It is mentioned that silica will react with the Sr present in the celestite and form a complex oxide $SrSiO_3$ that is acid soluble salt for it constant pH has to be maintained for longer duration. Moreover, the purity of the product is limited to 92%. Therefore it may be possible that some residual amount of silica may remain as contaminated phase with final product. Since the silica content in the present study is very low the possibility of silica contamination is very rare. The study of Sonawane *et al.* [6] shows that at a mole ratio of 2.5 (activated charcoal to celestite) the reduction of celestite into strontium sulphide increases with increase in temperature and time. The kinetics of the reduction reaction has been studied using different catalyst like potassium carbonate, sodium carbonate etc. The reduction temperature has reduced substantially. His study was confined to see the effect of catalyst on reduction temperature. The removal of catalyst from the final product is not specified in this work, which is around 2%. Gitis *et al.* [14], Lapsing *et al.* [15] and Erdemaglu *et al.* [4] have also suggested the similar type of reduction behavior at higher temperature with different time period. The disadvantage of these experiments is that this reaction is conducted at very high temperature 1200-1300^{0}C consuming lot of electrical energy. Recently Abdullah Obut [16] has

reported an experiment for the conversion of celestite to strontium sulphide by microwave heating. The conversion ratio in this experiment is observed to be 98%. But the temperature of conversion was 1200^0C.

In our study the results obtained with activated charcoal is better as compared to other grades of coal. The reducing time is also less as compared to other reported work [5].
SrS obtained after reducing experiments was leached in acidic solution. The reaction involving in the leaching process of strontium sulphide can be written as:

$$\mathbf{2\ SrS(s) + 2H_2O \rightarrow Sr\ (HS)_2 + Sr(OH)_2\ .....(V)}$$

$$\mathbf{Sr(HS)_2 + 2H_2O \rightarrow Sr\ (OH)_2 + 2\ H_2S.....(VI)}$$

$$\mathbf{SrO(s) + H_2O \rightarrow Sr\ (OH)_2\ .....(VII)}$$

$$\mathbf{Sr(HS)_2 + 2HCl \rightarrow SrCl_2 + 2H_2S\ .....(VIII)}$$

H_2SO_4 added to solution will precipitate Ba as $BaSO_4$. About 70-75 percent Ba^{++} gets precipitated where Sr^{++} as strontium sulphate loss percentage is 0.98%. To remove Ba^{++}, Ca^{++} up to 95% the pH of the solution was increased to 12 [5]. The Ca^{+2}, Mg^{+2}, Fe^{+2} ions hydrolyze at pH 12. So up to 95% of these impurities are eliminated at pH 12 due to hydrolysis.

2.3.2 Direct conversion method

Fig 2.7 shows the effect of temperature and time on percentage yield of $SrCO_3$ (% $SrSO_4$ conversion) for mole ratio 1.5 (Na_2CO_3/ $SrSO_4$). The experiment carried out at 25^0C exhibits the lower percentage of celestite conversion. As reaction temperature increases from 25 to 75^0C the celestite conversion to strontium carbonate increases rapidly.

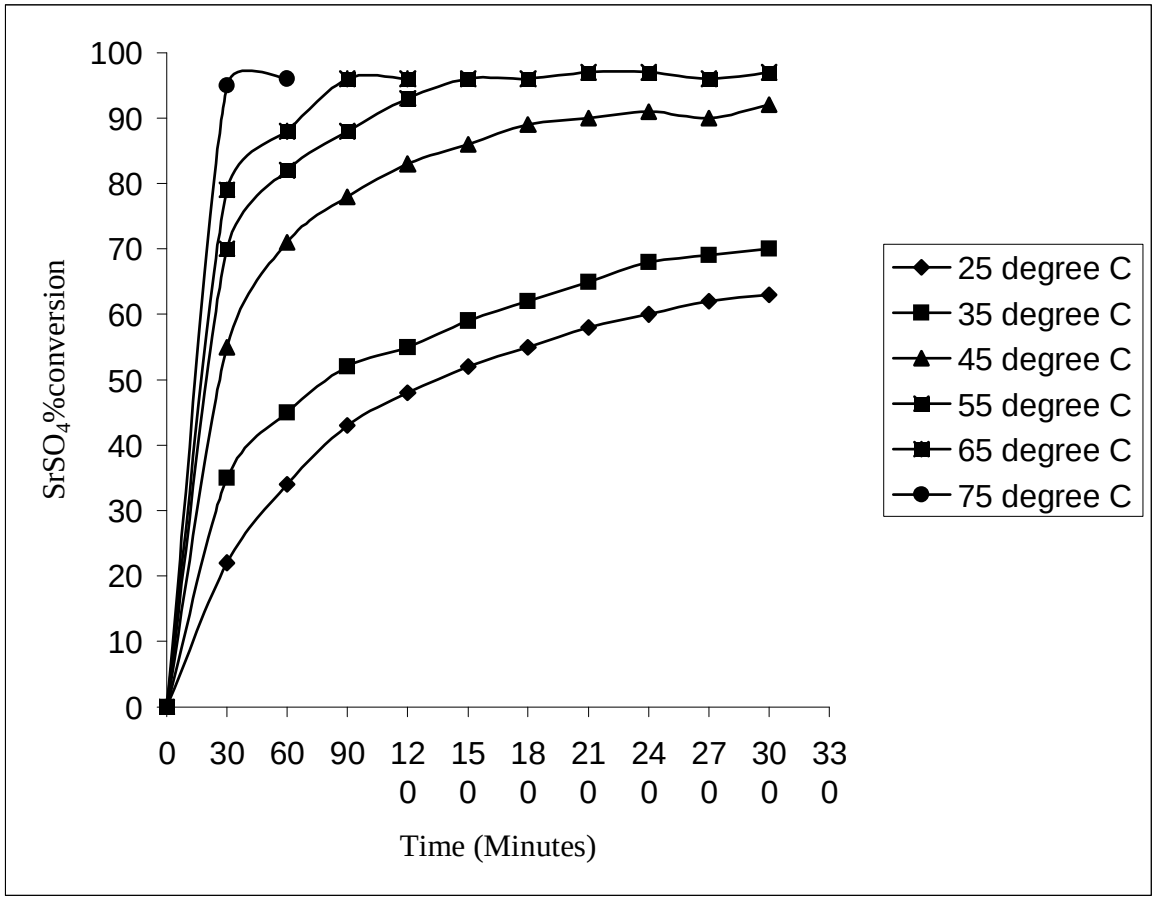

Fig.2.7 Effect of temperature and time on % yield of $SrCO_3$ for mole ratio 1.5 ($Na_2CO_3/SrSO_4$)

The effect of time and mole ratio (Na_2CO_3 / $SrSO_4$) on percentage yield of $SrCO_3$ ($SrSO_4$ conversion) from celestite at 60^0C has been shown in fig 2.8. For molar ratio of 1.0 in the present study, the percent conversion is quite low. The conversion rate of celestite increases with increase in molar ratio. For molar ratio 1.5 the conversion rate is maximum. Castillejos et al [9] performed experiments with different mole ratio (Na_2CO_3 / $SrSO_4$) 1.0 to 1.5 at 45^0C for a time period of 350 minutes. He reported the sustained increase in the rate of reaction with an increase in sodium carbonate concentration.

The chemical composition of celestite as given in Table 2.1 shows the presence of large amount of Fe (4.01%) which after acid leaching reduced to 0.60% as shown in the table 2.1. The percentage of Al_2O_3 content also reduced from 0.2 to 0.15%. In this acid leaching of celestite powder impurities like Fe, Al and Ca etc. has been reduced to great extent. Leaching also helps

in removing other soluble impurities. The celestite leaching experiment employed by Hacer Dogan et al [7] led to the reduction of impurities up to 0.005%Fe, 0.11%Ca 0.6%Ba, 0.86%Pb and 0.2% others. The level of impurity reduction in this experiment seems to be in good agreement with value reported by Hacer Dogen *et al.* [7]. The reduction of celestite with different coal shows that the best result was obtained with the activated charcoal in terms of percentage yield of SrS with respect to time as shown in fig. (2.3, 2.4 & 2.5). The reducing property decreases considerably as the excess carbon decreases from 60% to 40% of sample mass of celestite. The conversion percentage increases as time increases with each of the coal sample. The SrS conversion conducted by Wen Chen [5] using various source of coal indicated that brown coal gives maximum efficiency for the conversion from celestite to SrS. However, the present study shows the activated charcoal is most efficient coal source, which can be used in reduction of celestite to strontium sulphide. The difference in the result is due to the fact that Wen Chan [5] has not employed the activated charcoal, which is rich in fix carbon containing lower value of ash. Whereas, the study made by Sonawane *et al.*[6] for the reduction of celestite into SrS reports that the activated charcoal is most effective reducing substance for celestite reduction. In present study similar trend was also found. The effect of different molar ratio 1.0, 1.1, 1.2, 1.5 of (Na_2CO_3 /$SrSO_4$) on conversion of $SrCO_3$ with respect to time (ranging from 30-330 min. at 45^0C has been shown in fig. 2.8.

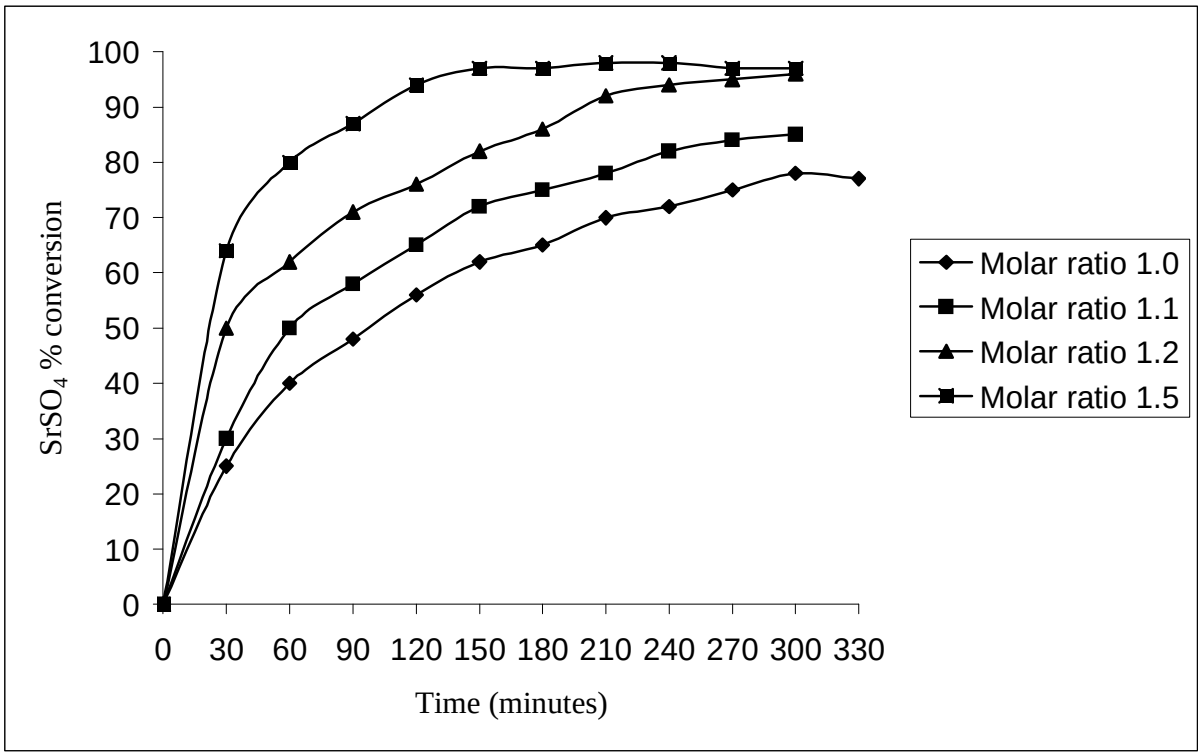

Fig. 2.8 Effect of time and mole ratio ($Na_2CO_3/SrSO_4$) on % yield of $SrCO_3$ from celestite at 60^0C.

The rate of percentage conversion of $SrSO_4$ is found to be maximum with 1.5 molar ratios of (Na_2CO_3 / $SrSO_4$). The decrease in the molar ratio exhibits the lower percentage of $SrSO_4$ with respect to time. Castillejos *et al.* [9] have reported that at a mole ratio (Na_2CO_3/ $SrSO_4$) of 1.5 maximum conversion rate of celestite to strontium carbonate was observed which matches with the result of the present study. Purification process to get strontium carbonate of desired level of purity by black ash and direct decomposition process after removing impurities is upto 97 and 98 % respectively.

Fig 2.9 shows the SEM micrograph of $SrCO_3$ where powders of different shape and size can be seen. The variation in particle size is from 2 μm to 10 μm. These particles get agglomerated during precipitation. A careful examination indicated that smaller size powders are spherical in shape where as bigger one is faceted type. The X-ray diffraction pattern of these powders shows the presence of single phase $SrCO_3$ compound (Fig.2.10).

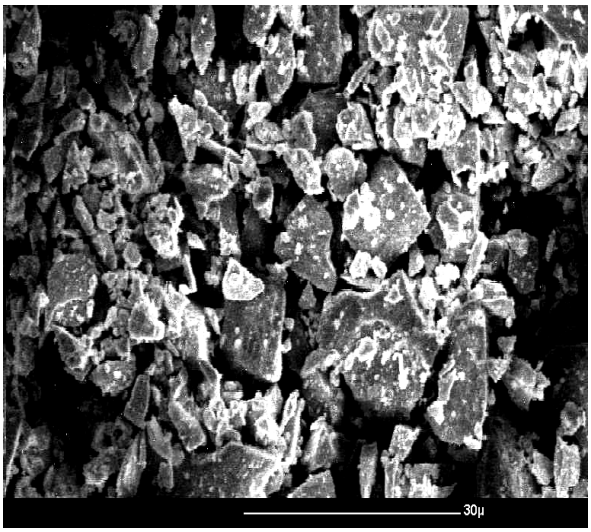

Fig. 2.9 SEM micrograph of strontium carbonate

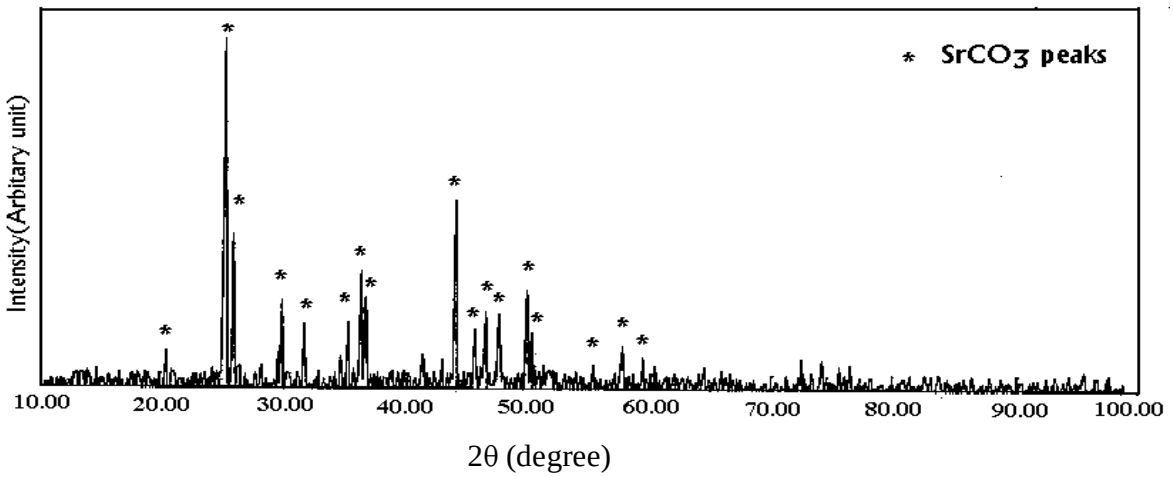

Fig. 2.10 X-ray diffractogram showing the peaks of strontium carbonate obtained from black ash method.

2.3.3 Comparison of black ash and direct conversion method

Table 2.4 shows the chemical composition obtained from both processes. The yield percentage is greater in direct conversion method (98%) as compared to black ash method (97%). Kirk-Othemar, (Encyclopedia) [1] has reported a yield of 95% strontium carbonate from black ash process. According to a Patent [17] it has been mentioned that it is possible to produce 95% pure strontium carbonate by using black ash method. However, this requires the celestite containing 85% strontium sulphate whereas by using direct conversion method strontium carbonate over 95% can be achieved. It was also claimed that pure strontium carbonate (99%+pure) can be obtained even with low-grade celestite by double decomposition method [17]. The purity of strontium carbonate obtained in present study seems to be within the range of the values reported by other workers [4, 5 & 6]. On comparing of both processes it seems that direct decomposition process is more economical as compared to black ash process as no extra equipment like furnace is required. Only the chemicals are required. Moreover, the by-product obtained can also be utilized where as it is not possible in black ash process.

Table 2.4 Comparison of the process in terms of % yield and residual impurities

Process	$SrCO_3$	$BaCO_3$	$(Ca^{+2} + Mg^{+2})$	Fe	Si
Direct decomposition method	98.01	< 0.01	0.01	0.008	0.1
Black ash method	97.85	<0.01	0.015	0.01	0.02

References

1. Krik-othmer, (1993) “Encyclopedia of chemical technology”, fourth edition 10, pp 393-405, John Willey & Sons.
2 Joyce A. Ober. (2007) Strontium USGS Report.
3. J Pual, Mac Millan, (1994) “Strontium and Strontium compound”, Ullmann’s Encyclopedia of Industrial Chemistry, A-25.
4. M.Erdmoghu, M.Canbazughu, H.Yalcin, (1998) “Carbothermic reduction of high-grade celestite ore to manufacture strontium carbonate”. Transaction of the Institution of Mining of Metallurgy, See-C, Mineral Processing and Extractive Metallurgy, vol. 107, pp.65-68.
5. W.Chen, Y.Zhu,(2000) “Preparation of strontium carbonate from celestite” Mineral Processing and Extractive Metallurgy IMM Transaction C, vol. 109, pp. 1-5.
6. R.S. Sonawane, B.B.Kale, S.K.Apte and M.K. Dongare, (2000) “Effect of catalyst on the kinetics of reduction of celestite ($SrSO_4$) by active charcoal”, Metallurgical and Materials Transaction B, Vol-31B, pp 35-41
7. Hacer Dogan, Murat Koral, Sidika Kocakusak, (2004), “Acid leaching of Turkish celestite concentrates”, Hydrometallurgy vol.71, PP 379-383.
8. Bronislaw Janczuk, Emil Chibowski, Tomasz Biajopiotrowicz and F.Gonzalez-Caballero, (1989) “Surface free energy of celestite and its floating activity”, Collides and Surfaces, vol-35, issue -1, pp 41-48.
9. A.H. Castillejos E, F.P. de la Cruzdel B, A. Urbis S.(1996), “The direct conversion of celestite to strontium carbonate in sodium carbonates aqueous media”, Hydrometallurgy ,vol. 40 pp 207-222.
10. Massone, J.,(1983), “Technology and uses of barium and strontium carbonate.” In: B.M.Coope and G.M. Charke (editors) 5th industrial Minerals int.Cengr. (Madrid, Spain, 1982) Metal Bulletin, London, pp 115-119.
11. Sutarno, R.H Lake and W.S Bowman,(1970), “The extraction of strontium from the mineral Mines and Resource’s Ottawa”, Res. Rep.(R-223), pp. 1-20.
12. M. Iwai. and J.M.Toguri, (1989), “The leaching of celestite in sodium carbonate, Hydrometallurgy”, vol. 22, pp. 87-100.

13. E. Pedak, M. Allsalu and M. Kanter Zh. (1972), “Prikl Khim, (Leningrad)”, vol. 45(12), pp. 2619-23 (In Russian)
14. E.B.Gitis, P.I.Strigunov, S.K.Solyanik, L.F.Vasileva, F.D. Pushkarnov, Y.N. Zinchenko and V.I. Krasnyakove:(1985), “Otkritiya Izobret”, vol.-46, pg. 91.
15. V. A. Lepsin, L.E. Kruglove, G.R. Bulgakove and V.I. Krashyakov:(1988), “Otkrytiya Izobret’, vol. 10, p. 89 (In Russian)
16. Abdullah Obut,(2007), “Direct conversion of celestine to SrS by microwave heating,” Minerals Engineering”, (Article in press)
17. De Buda,(1988), United States Patent No- 4,666,688, pp 1-8
18. www.tidco.com/image%5cstrontium%20carbonate.doc

Chapter 3

Upgradation of Blue dust

Overview

This chapter deals with beneficiation of blue dust to reduce the gangue materials such as silica and alumina by physical and chemical process. In the present work two types of physical beneficiation processes to carry out upgradation of blue dust have been employed. These are Magnetic separation and Froth flotation processes. The magnetic separation leads to separation of magnetic particles by applying low intensity magnetic force. The froth flotation process consists of removal of gangue material by making it to float on the upper surface. Apart from this iron oxide of high purity was also prepared from blue dust by chemical precipitation method.

3.1 Introduction

Iron has its occurrence in earth as Magnetite (Fe_3O_4) and Hematite (Fe_2O_3). The important ore of iron is Hematite due to its wide availability and it accounts for primary source of iron for the world's iron and steel industries. Iron ore is mined in about 50 countries worldwide. In India it is mined in Jharkhand, Chatishgarh, Orrisa, Karnataka, Goa and other states.

The fine particles associated with the ore mines is known as Blue dust and is present with almost all hematitic deposits in India as mentioned in chapter-1. The blue dust contains more than 95% iron oxide. It also contains alumina and silica in the range of 1-2 weight percent [1].

The beneficiation or upgradation of iron ore is defined as the process for the separation of gangue material from the ferrous materials. It also includes the separation of more-magnetic particles from less magnetic particles. Focus has been made to physical and chemical upgradation method for the beneficiation of blue dust.

Karmazin *et al.* [2] have done experiments for the beneficiation of iron ore. In this study qualitative and quantitative evaluation of liberation of economic minerals and the level of contamination of the process product by waste components were carried out for the purpose of analysis of energy utilized in the process. It was described that separator with pulsed magnetic field efficiently allows the realization of more concentration of large amount of unliberated magnetic particles as compared to conventional separators. The energy consumption at different stage of upgradation has been analyzed for the savings of energy. However, this study was based upon beneficiation of magnetite ore.

Roman et al [3] have done iron ore beneficiation using roll-type high-intensity electric field separators. They demonstrated that high-intensity electric fields can be employed for the separation of artificial magnetite processed from an iron mineral containing siderite $FeCO_3$ and ankerite $(FeCaMg)CO_3$ by using roll type separator.

According to an US Patent [4] iron ore was upgraded using separation steps based entirely on size for a mineral composition without the use of separation steps. It was claimed that relatively coarse grind of iron ore can also be beneficiated using this technique.

The present study deals with upgradation of blue dust through physical and chemical processes and compares the processes in terms of economy, process effectiveness and process easiness.

3.2 Experimental procedure

Blue dust used for this experiment was collected from Bailadila mines of Chattisgarh state. The fraction containing less than 45 micron was taken for the purpose of physical upgradation. The flow diagram describing the physical upgradation process is shown in figure 3.1.

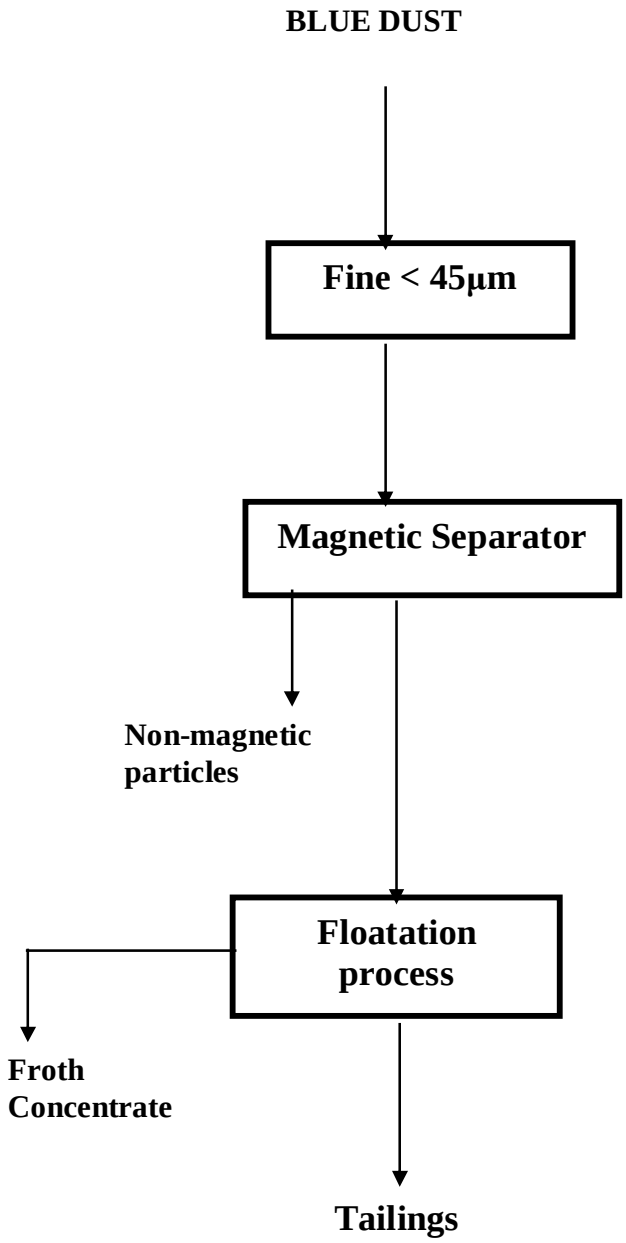

Fig. 3.1 Schematic process flow diagram for physical upgradation of blue dust

3.2.1 Magnetic Separation Method

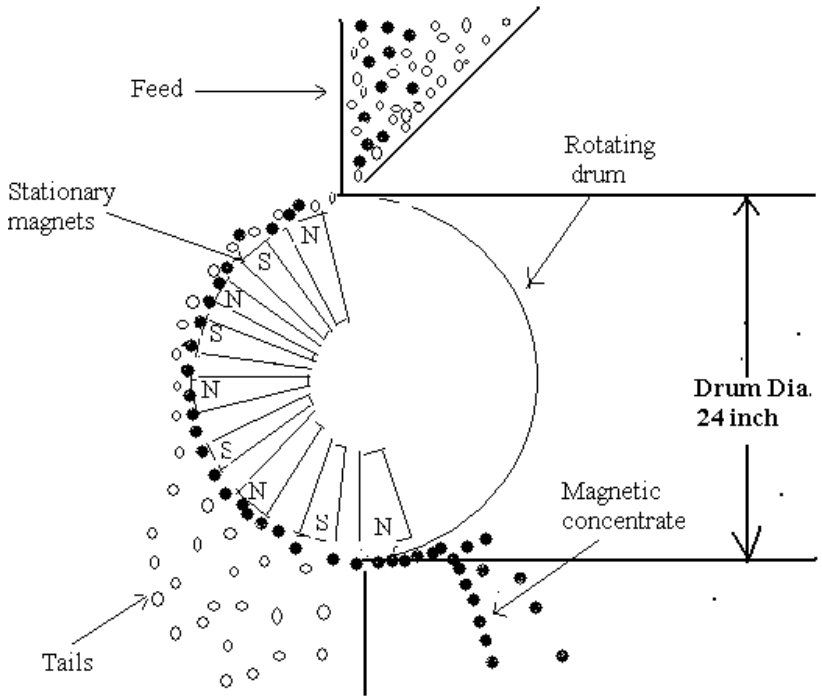

Fig.3.2 Conventional drum- type magnetic separator

For the separation of magnetic rich blue dust the conventional drum type magnetic separator was used which was indigenously designed and fabricated. First of all the drum was made to rotate which is electrically driven at low rpm. The drum rotates over stationary magnet setup as shown in figure 3.2. The magnetic field applied was 0.2 Tesla. The iron ore less than 45μm was introduced as feed through the hopper. The feed splits into two portions. The non magnetic material separates as tails whereas the magnetic materials separate out is called magnetic

concentrate. This process is used for the seperation of magnetic materials like Fe, Fe_3O_4 from the blue dust (Fe_2O_3) which is very effective for the separation of these ingredients from the iron ore.

3.2.2 Froth floatation process

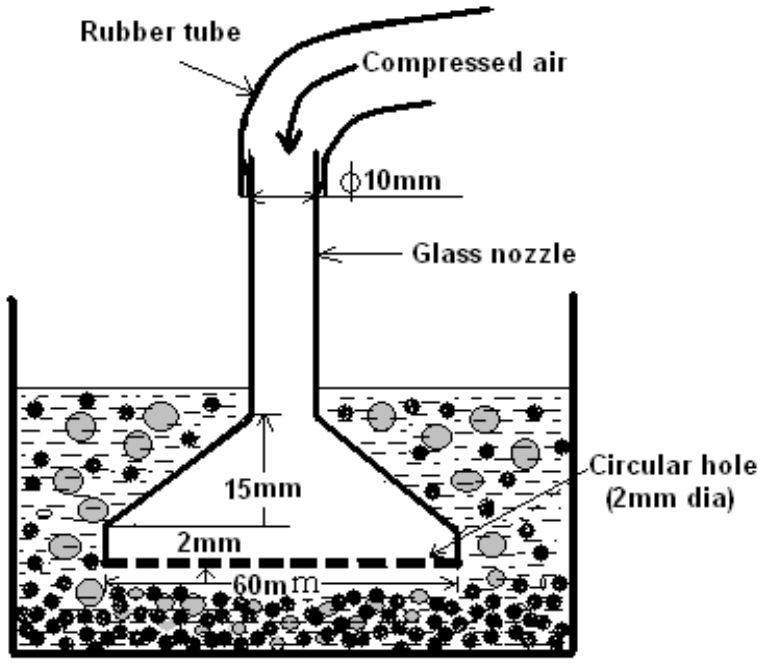

Fig 3.3 Froth floatation set up for the separation of gangue materials from blue dust

The particle size <45 μm was collected for the upgradation purpose. For it 100 gm of blue dust was taken in a 5 liter beaker. Beaker containing blue dust was heated on a hot plate at 70^0C and compressed air was passed in it through indigenously designed glass nozzle.

This leads to continuous stirring of blue dust particles. After half an hour heating and blowing process the water was discarded. This process was repeated five times to ensure complete removal of water soluble impurities. The separation of gangue materials like silica and alumina take place according to the liberation mechanism [5, 6]. After final washing the mass was filtered

and dried in an oven at 110^0C for 1hour. The schematic view of the froth floatation setup for the upgradation of blue dust fine particles is shown in fig.3.3. The black particles represent the blue dust fines and grey circles the air bubbles.

3.2.3 Chemical upgradation method

In the chemical upgradation process pure iron oxide powder was synthesized using blue dust. A batch of 50 gram blue dust (<45 μm) was taken in 2 liter borosilicate glass beaker. 100 ml of HCl (1:1) was added slowly through spout of the beaker. After that the beaker containing blue dust and acid was heated at low temperature (40-50^0C) on a hot plate to start the reaction under constant stirring. The reaction was allowed to take place for one hour. To dissolve the iron oxide completely 20-30 ml of conc. HNO_3 was added slowly with a precaution to avoid vigorous reaction due to oxidation of Fe^{+2} to Fe^{+3}. When reaction is completed the solution is cooled to room temperature. The solution is filtered through Whatman filter paper no-40 to remove silica and alumina from the iron solution. The filtered iron solution was transferred to a 5 lt. borosilicate glass beaker. The solution was diluted to approximately one liter in the beaker by distilled water. When the solution is completely in cold condition ammonia solution (1:1) was added very slowly under constant stirring with a precaution to avoid vigorous reaction. Addition of ammonia solution generates lot of heat and the iron solution becomes hot. Therefore iron solution is cooled before addition of another portion of ammonia. Addition of ammonia solution is continued till precipitation of iron hydroxide is completed. Iron hydroxide was allowed to settle down for one hour.

Iron hydroxide was filtered through Whatman filter paper no-41 and washed many times with water to make the residue on the filter paper ammonia free. The iron hydroxide mass is placed in alumina pot and heated in a muffle furnace at of 900^0C for one hour to convert iron hydroxide to iron oxide.

3.3 Result and Discussion

Table 3.1 Value of iron content in feed, tailing and concentrate after magnetic separation

Separator Type	Products	Weight (%)	Iron content (%)
Magnetic separator (drum type)	Feed	100	61.90
	Tailings	21.51	8.02
	Concentrate	78.80	62.23

The weight of tailing and concentrate after magnetic separation of blue dust is mentioned in table 3.1. It is obvious from the observed value that feed which is a source of blue dust contains 61.90% iron which increases after magnetic separation and reaches to 62.23% as shown in table above. Though there is not much variation even then this helps in separation of other elemental oxides.

Table 3.2 Chemical composition of blue dust before and after upgradation (floatation)

Compound	Before upgradation (wt%)	After upgradation (wt%)
Fe_2O_3	96.20	97.54
Al_2O_3	0.32	0.26
SiO_2	1.60	1.21
CaO	0.94	0.13
MnO	0.18	0.11

Table 3.3 Trace element analysis of blue dust by (AAS) before and after upgradation

Element	Before upgradation (wt%)	After upgradation (wt%)
Mg	0.40	0.29
Pb	0.027	0.023
Zn	0.01	0.01
Cu	Not detected	Not detected
Na	0.69	0.04
K	0.52	0.02

Table 3.4 Chemical composition of iron oxide prepared from the chemical upgradation of blue dust

Upgradation process	Chemical composition (wt %)				
Chemical upgradation	Fe_2O_3	Al_2O_3	SiO_2	CaO	MnO
	99.21	0.21	0.32	0.12	0.14

The chemical composition of iron oxide obtained from the blue dust after chemical upgradation is shown in the table 3.4. It is evident from analysis that iron oxide obtained from the chemical upgradation contains highest purity of Fe_2O_3 i.e. 99.21%. The gangue materials like alumina, silica etc. remains in traces after the upgradation. This is due to the fact that traces amount of impurities are always occluded with the bulk precipitation of iron oxide. However, this can be reduced by double precipitation. The high purity iron oxide powder may be prepared in small quantities. This process shows the feasibility to achieve pure grade of iron oxide from blue dust whereas other physical methods do not show such high quality of iron oxide.

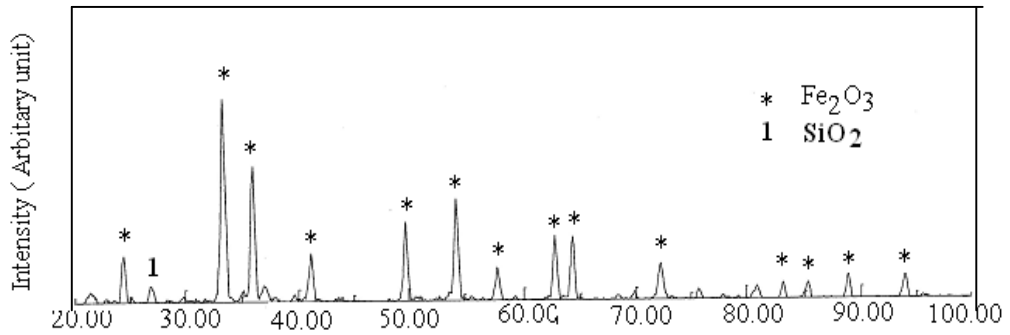

2θ (degree)

(a)

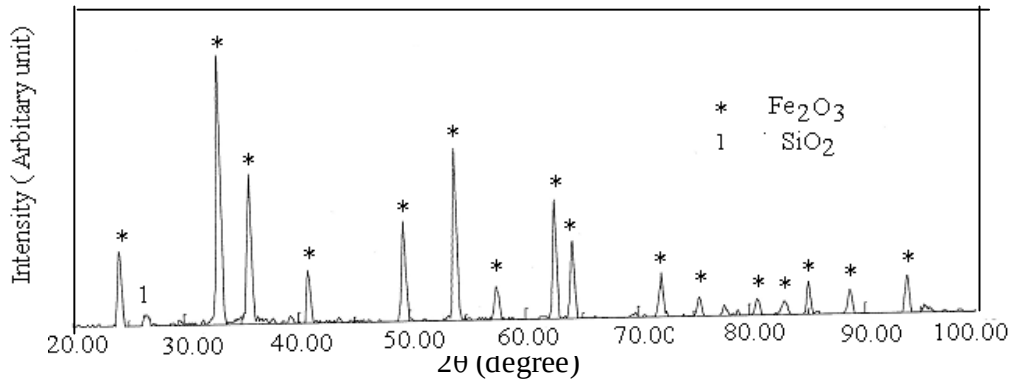

(b)

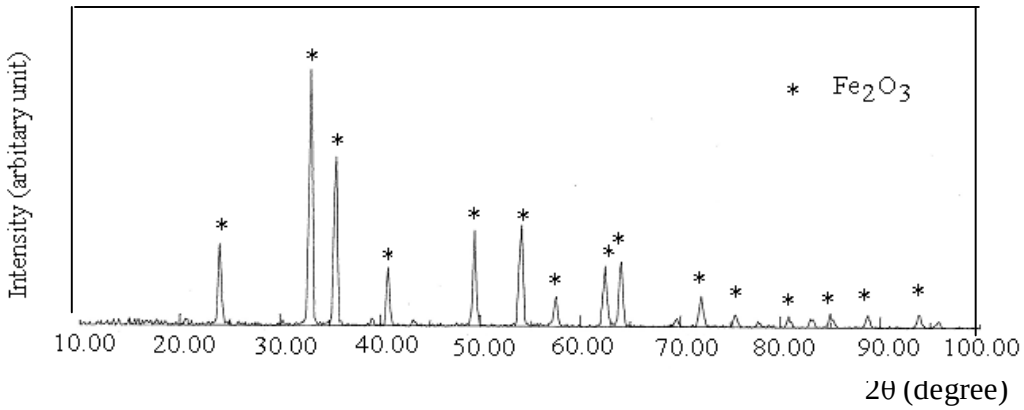

(c)

Fig. 3.4 X-ray diffractogram of blue dust (a) as received (b) after physical upgradation (c) after chemical upgradation

3.3.1 XRD phase analysis

Figure 3.4 (a), (b) and (c) shows the X-ray diffraction pattern of as received, physical upgraded and chemical upgraded blue dust respectively. The pattern shows single phase of Fe_2O_3 in each diffractogram. Presence of impurities is evident from X-ray diffraction pattern as shown in fig. 3.4 (a and b). From the X-ray diffraction pattern in fig.3.4 (a and b) it is observed that intensity of impurity (SiO_2) decreases which shows that impurity level in blue dust goes down after physical upgradation. However, X-ray pattern in figure 3.4 (c) shows that the intensity of SiO_2 peak is almost nil. This indicates that as received blue dust contains greater amount of impurities but after physical upgradation the impurities level decreases. In the case of chemical upgradation of blue dust it has lowest level of impurities. This is due to the fact that impurities level after physical upgradation reduces due to liberation mechanism. Whereas in chemical upgradation method almost all impurities are separated.

3.3.2 Microstructural studies

Figure 3.5 (a), (b) and (c) shows the SEM micrographs of as received blue dust, after physical upgradation and after chemical upgradation. The micrograph 3.5 (a) shows the shape of the particle which is faceted agglomerated type which contains large pores containing different impurities. The micrograph 3.5 (b) shows the broken particle of Fe_2O_3 generated after froth floatation. It is observed that porosity has also decreased due to continuous fracture of iron oxide. The figure 3.5 (c) represents the micrographs of pure Fe_2O_3 obtained after chemical upgradation of blue dust. In this micrograph it is observed that the particles are of uniform size. The particle size is also very small as compared to other micrographs.

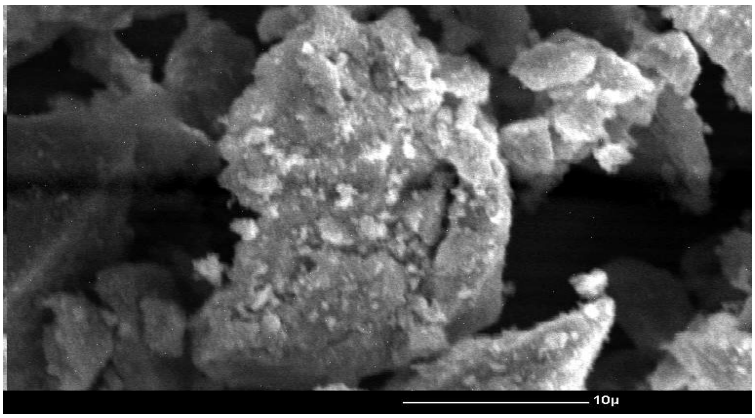

(a)

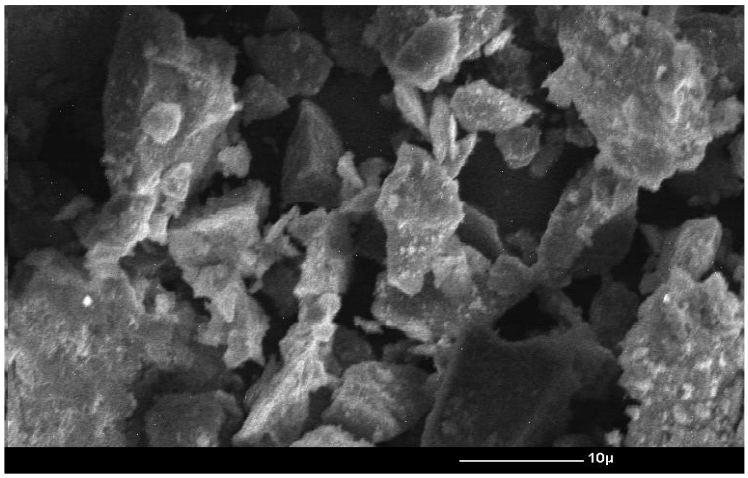

(b)

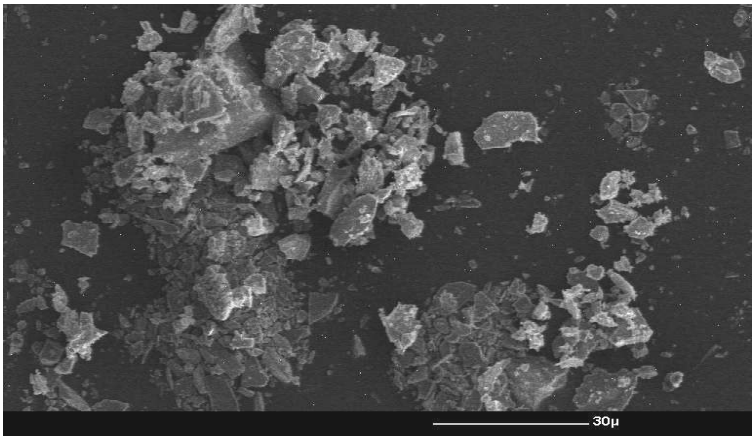

(c)

Figure 3.5 SEM micrographs of blue dust (a) as source (b) physical upgraded (c) chemical upgraded

References

1. M.P.Srivastva, S.K.Pan, N. Prasad and B.K.Mishra, “Characterization and Processing of Iron Ore Fines of Kiriburu deposit of India” International Journal of Mineral Processing, vol. 61, Issue-2, 2001, pp 93-107.
2. V.V.Karmazin, M.A. Bikbov and A.A. Bikbov, “The Energy Saving Technology of Beneficiation of Iron Ore”, Magnetic and Electrical Seperation, vol. 11(4), pp 211-224.
3. Roman Morar, Alexandru luga, Ovidiu Muntean and Lucin Dascalescu, “Iron Ore Beneficiation Using Roll-Type High-Intensity Electrical Field Seperators”, IEEE Transaction on Industry Application, vol.35(1),1999, pp 218-224.
4. James E. Forciea, “Beneficiation of Iron Ore” US Patent No- 4,206,876,1980, pp 1-2
5. D.W. Frommer, “Iron Ore Floatation” Journal of the American Oil Chemists Society, vol- 47,1969, pp 189-192.
6. Robert Ben Booth, Springdale and Earl Conrad Herkenhoff, “Froth Floatation of Iron Ores” United State Patent, No- 2461875, 1949, pp 1-8.

Chapter 4

Preparation of Strontium Hexaferrite from Celestite and Blue dust by Mechanochemical Route

Overview

The present chapter describes the process for the preparation of strontium hexaferrite from natural mineral celestite and blue dust.

The mechanical alloying process has been adopted to prepare strontium hexaferrite powder. The celestite after chemical upgradation and physically upgraded blue dust along with sodium carbonate was taken for the preparation of strontium hexaferrite in this work. The high-energy planetary ball mill with tungsten carbide jar and ball was used to prepare strontium hexaferrite powder by mechanochemical alloying. A long time of ball milling for different duration has led displacement solid-state reaction. At the end of each experiment the product was washed thoroughly, dried and sintered to prepare anisotropic magnet after annealing the ferrite powder. Phase analysis, microstructural study and magnetic properties of the sintered anisotropic magnet were carried out.

4.1 Introduction

Blue dust is iron ore fines and is found abundantly in the iron ore mines. It cannot be used directly in steel making process due to the fineness of the particle. Celestite is natural ore of strontium and is used for the preparation of strontium carbonate. Strontium hexaferrite is permanent magnet and its formula is ($MFe_{12}O_{19}$) where M stands for Sr, Ba, Pb etc. Its crystal structure is hexagonal magnetoplumbite sometimes called M-type ferrite, which is characterized by space group $P6_3/mmc$. [1]. It is most widely used permanent magnet, which accounts about 90 wt% of total production of permanent magnets market. Strontium hexaferrite finds its application in motors, loudspeakers, high frequency devices, magnetic recording media etc. [2, 3]. The details of blue dust, celestite and strontium hexaferrite is described in chapter-1.

Generally strontium hexaferrite ($SrFe_{12}O_{19}$) is prepared by the conventional method, which involves calcination of the mixture of $SrCO_3$ and Fe_2O_3 in an appropriate ratio at a temperature between 1100-1200^{0}C followed by sintering [4]. The most important factor for the production of $SrFe_{12}O_{19}$ is the cost and availability of the raw materials. Some researchers have tried to reduce the processing cost by using one of the natural raw materials directly. Mortaza Mozaffari *et al.* [5] have used celestite along with iron oxide to prepare strontium hexaferrite by mechanochemical method. However, they have taken Fe_2O_3 in pure form. Dasgupta *et al.* [6] used blue dust with pure strontium carbonate for the preparation of strontium hexaferrite by conventional calcination method.

The aim of the present work is to produce strontium hexaferrite powder directly from celestite and blue dust which are natural ore of strontium and iron by mechanochemical method with a view to make the process cost effective and to explore the possibility of commercial production of strontium hexaferrite directly from the ores. This will also help to utilize the waste and discarded fines that are causing environmental problem.

4.2 Experimental Procedure

The starting raw materials taken for this study are celestite, blue dust and sodium carbonate. The celestite ore was ground to fine powder in a mortar and pestle. The powder was sieved. The fraction less than 45 micron was collected for the experimental work. The chemical analysis of celestite and blue dust was carried out to know its chemical composition. For different trace

element analysis, atomic absorption spectrometer (Flame Type Model no. GBC-932AA, Australia) was used.

4.2.1 Chemical treatment of celestite ore

Celestite was chemically treated to remove gangue materials. For it 100 gm oven dried celestite powder (<45μm) was taken in 2 liter borosilicate glass beaker. About 500 ml of 1:1 HCl, 20 ml conc. HNO_3 and small amount of NH_4 F was added in this fine powder mass to remover gang material. The details of the process is mentioned in chapter 2.

4.2.2 Upgradation of Blue dust

The upgradation of blue dust was done by physical upgradation method. The details of the process has been described in chapter 3. The upgraded blue dust was used for the preparation of strontium hexaferrite sintered magnets.

4.2.3 Preparation of Strontium hexaferrite powder

The appropriate quantity of treated celestite, upgraded blue dust (mole ratio SrO/Fe_2O_3 =5.5) and sodium carbonate with 30% excess amount to stoichiometic ratio was taken [5]. A batch of 50 gm mixture was mixed using zircon ball and vessel in a high-energy planetary mill (Model Mega pact, Pilamec Ltd. U.K.) in a medium of analytical grade reagent (AR) hexane. After one hour of mixing the material was taken out and put into tungsten carbide jar with tungsten carbide balls. The charge to ball ratio was fixed (1:10). Hexane was used as medium for mixing which continued up to 60 hours. At every 10 hours interval sample colour was monitored till the mixture colour turned to black. During initial experimentation hexane was added to get homogenized mass. As the milling proceeds hexane evaporates leaving fine powders. The mixture was taken out after milling. Finally after 40 to 50 hrs of ball milling the powder was washed and annealed at 900^0C for 1 hour in a muffle furnace to see the presence of phases. Once the phase of strontium hexaferrite after 50 hours of ball milling followed by annealing was confirmed then these powders were selected to prepare strontium hexaferrite sintered magnets. For it 5% PVA (polyvinyl alcohol) as a binder was added to this powder and mixed well to make slurry and was allowed to dry in the open air. The pellet of 5mm diameter and 11 mm length was prepared by applying compressive force of 500 MPa under magnetic field of 2 T to make it

anisotropic. The pellet was sintered at 1250^0C for an hour in a tubular furnace in open air. The phase analysis was carried out using X-ray diffractometer (Model Rigaku D-Max IIIC). Microstructureal analysis of sintered pellets was carried out using scanning electron microscope (Model JEOL 840 A). The magnetic properties [B_r, H_{cj}, and $(BH)_{max}$] of the sintered magnets were measured using a Pulse Magnetometer (Model TC-201).

4.3 Results and Discussion

The celestite powder was chemically treated for its upgradation. The amount of different ingredients before and after acid leaching is given in chapter 2 (table 2.1). It was observed that even after acid treatment some impurities like Fe_2O_3, $BaSO_4$, SiO_2, Al_2O_3 etc. remain in small quantity (Table 2.2). The presence of these compounds is not favorable for the magnetic properties of strontium hexaferrite produced there of. The chemical analysis and trace analysis of source and upgraded blue dust is given in chapter 3 (table 3.2 & 3.3).

The reaction involved in milling can be written as:

$$\mathbf{SrSO_4 + Na_2CO_3 + 5.5\ Fe_2O_3 \longrightarrow SrFe_{12}O_{19} + Na_2SO_4 + 3O_2}$$

The characteristic feature of solid-state reaction through mechanical alloying is that it involves the formation of product phases at the interfaces of the reactants. The growth of the product phases occur by diffusion of atoms of the reactant phases through the product phases, which creates a layer preventing further reaction. Intensive milling increases the area of contact between the reactants powder particles due to reduction in particle size which allows fresh surfaces to come into contact. This allows the reaction to proceed without the necessity for diffusion through the product layer due to which solid state reaction that require high temperatures will take place at lower temperature during mechanochemical synthesis without any heat treatment. It is well known that conventional process for the preparation of $SrFe_{12}O_{19}$ is through solid-state reaction at high temperature. This requires lot of chemicals of high purity. Apart from this the requirement for calcination, milling, and high sintering temperature makes the process costly. The advantage of mechanical milling, process over other conventional method is that it does not require any external heating source for solid-state reaction to occur [7-12]. However in certain cases low temperature treatment is required to facilitate the reaction.

Table 4.1 Phases present after different ball milling duration

Ball milling time (hours)	Phases present	Heat treatment
1	Fe_2O_3, Na_2CO_3, $SrSO_4$	Not annealed
30	Fe_2O_3, Na_2CO_4, $SrFe_{12}O_{19}$	Not annealed
40	Fe_2O_3, $SrFe_{12}O_{19}$	Annealed 900^0C/1 hr
50	$SrFe_{12}O_{19}$	Annealed 900^0C/1 hr
60	$SrFe_{12}O_{19}$	Annealed 900^0C/1 hr

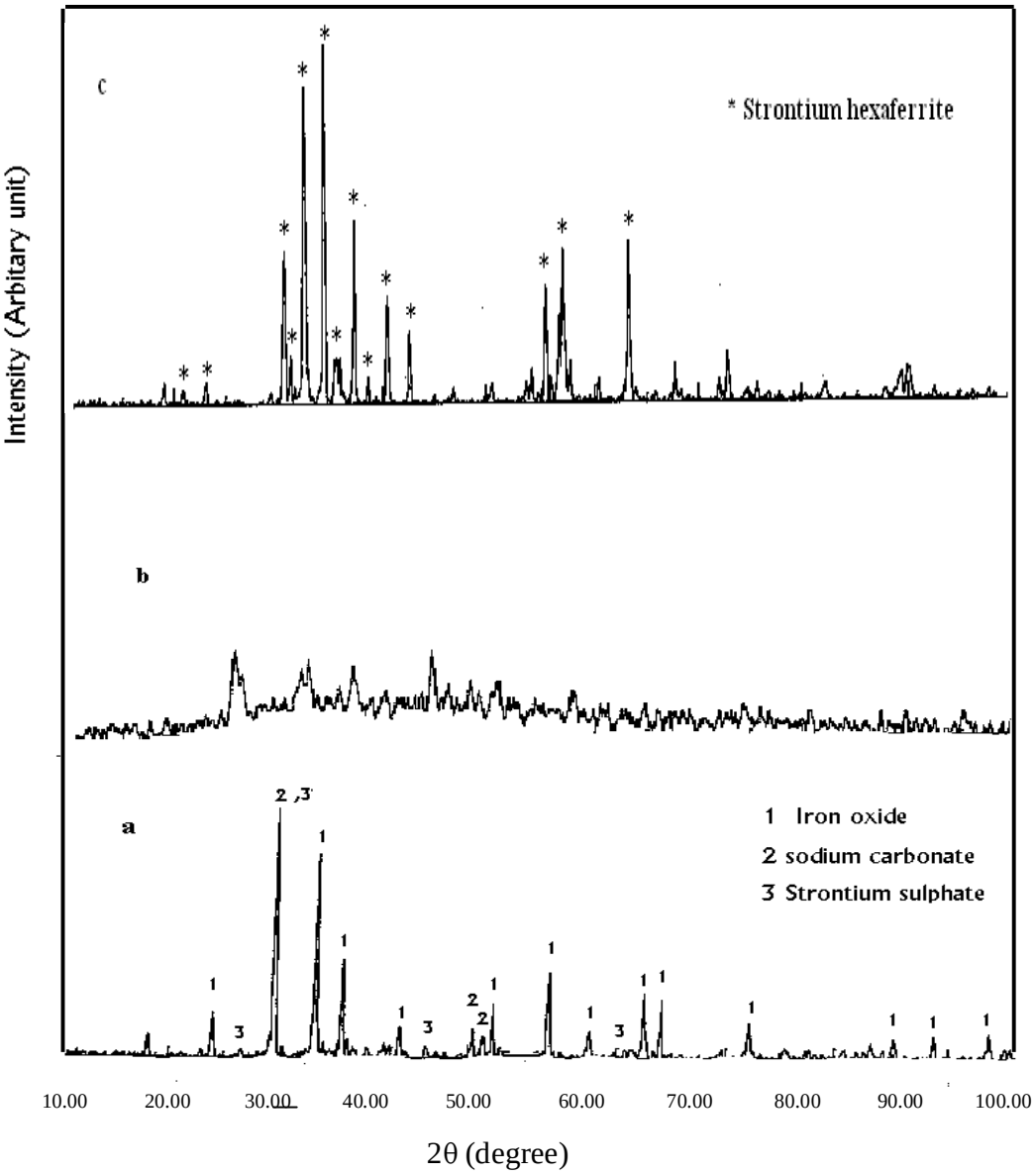

Fig. 4.1 X-ray diffraction pattern of the powders mechanically alloyed for various times (a) after 1 hr. milling (b) after 30 hrs. of milling (c) after 50 hrs. of milling followed by annealing.

4.3.1 Phase analysis

The X-ray study for the formation of strontium hexaferrite ($SrFe_{12}O_{19}$) phase is presented in fig.4.1 (a-c). The XRD pattern after 1 hour of ball milling of the mixture of celestite, sodium carbonate and iron oxide show the presence of all constituent phases which is shown in fig.4.1 (a). The fig.4.1 (b) represents the X-ray diffraction pattern of initial mixture after 30 hrs. of mechanical milling. It indicates the formation of strontium hexaferrite phase. However, presence of ingredient phases also exists. The much weak and broaden peaks of Fe_2O_3 and $SrSO_4$ are visible with formation of small amount of amorphous $SrFe_{12}O_{19}$ phase [13-15]. The peak broadening of initial oxides indicates that shorter time of mechanical activation is not sufficient to obtain crystalline phase of $SrFe_{12}O_{19}$. However, similar pattern was also observed even for higher mechanical milling time indicating that reaction is not completed. The fig.4.1 (c) shows the typical XRD pattern after 50 hrs. of mechanical milling followed by annealing at 900^0C for 1 hour. Here we can find that there is decrease in amorphization nature. More sharp peaks of $SrFe_{12}O_{19}$ are visible in this pattern showing the increased volume of ferrite phase which has formed after 50 hrs of milling followed by annealing. The X-ray pattern shows the formation of single-phase strontium hexaferrite phase. The phases present after different ball milling duration are mentioned in table 4.1. The particle size of $SrFe_{12}0_{19}$ powder after annealing was measured by applying advance Scherer equation. The calculated value of ferrite particle is 1.71μm.

The lattice parameter was calculated using following formula.

$$(1/d)^2 = 4/3\ [\ (h^2+hk+k^2)/a^2\ ]\ +\ l^2/c^2$$

Where d = inter planner spacing

hkl = Miller indices

c, a = lattice parameter.

The theoretical values of c and a are 23.037 and 5.886 Å whereas calculated values from X-ray diffractogram of these are 23.289 and 5.6613 Å respectively. The observed lattice parameters are close to the theoretical values.

4.3.2 Magnetic properties

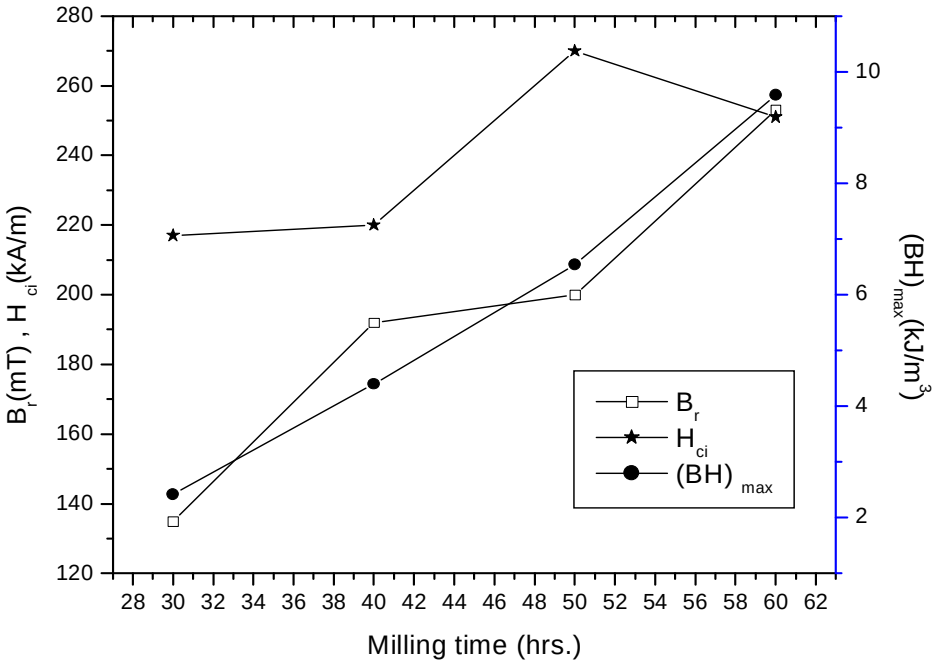

Fig. 4.2 Variation of B_r, H_{ci} with different milling time after annealing and sintering.

Magnetic properties of ferrite powder produced after different milling time followed by annealing is shown in figure 4.2. By increasing the milling time magnetic properties are observed to increase due to increasing volume of strontium hexaferrite phase. Increase in magnetic properties may be attributed due to fact that annealing releases the mechanical stresses existing in powders due to impact load [16]. The typical B-H loop of the sintered anisotropic strontium hexaferrite is shown in fig 4.3.

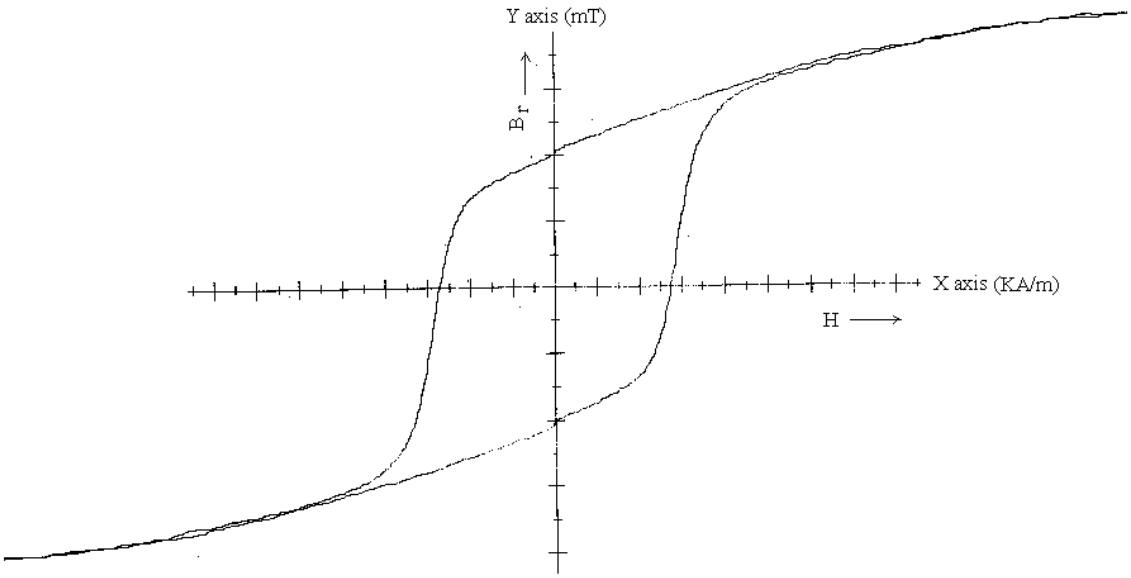

Fig. 4.3 Typical B-H loop of anisotropic sintered magnet.

Table 4.2 Comparision of magnetic properties of strontium hexaferrite by mechanochemical alloying

Sr.No.	Ingredients	Magnetic properties			References
		B_r (Gs)	H_{ci}(Oe)	BH_{max} (MGOe)	
1	Celestite, sodium carbonate iron oxide (pure)	2305	5230	1.2	Mortaza Mozaffari et al.[5]
2	Strontium carbonate (pure), iron oxide (pure)	2100	4600	1.85	C. Miclea *et al.*[13]
3	Strontium hexaferrite, iron sulphide	-	5700	-	J.Sort *et al.*[14]
4	Strontium hexaferrite	2400	4200	1.20	S.V.Ketov *et a*l [15]
5	Celestite, sodium carbonate blue dust	2533	3160	1.19	Present investigation

Mortaza Mozaffari *et al.* [5] have reported the direct utilization of celestite for the preparation of strontium hexaferrite powder using high purity iron oxide after longer time of milling (24 hours). They have employed milling process to achieve intimate mixture of celestite, sodium carbonate and iron oxide. The milled powder was calcined at 1000^0C for 10 hours. In their process no mechanochemical reaction has taken place. The product phase (strontium hexaferrite) was obtained after calcination. The magnetic properties of these sintered samples are shown in table 4.2.

Miclea *et al.* [13] have produced strontium hexaferrite powder by mechanical alloying method. However, they have used strontium carbonate and iron oxide of high purity. Severe stresses and structural deformation was reported in their work. These stresses were relieved by annealing process. Strontium hexaferrite prepared with high purities raw materials exhibit good magnetic properties (table 4.2). The coercivity is the extrinsic property, which depends mainly on particle size, annealing temperature and packing factor of the material. The single domain size of strontium hexaferrite is about 1μm [10]. Due to mechanical alloying particles size has reduced to nano size.

Sort *et al.* [14] in their experiment tried to improve the coercivity of the strontium hexaferrite by ball milling of pure $SrFe_{12}O_{19}$ and FeS. The coercivity enhancement observed is due to the formation of α-Fe_2O_3 phase which has formed after ball milling (table 4.2).
S.V.Ketov *et al.* [15] have made the nanocrystalline $SrFe_{12}O_{19}$ powder using high energy milling process from pure strontium hexaferrite powder. This process covers only improvement in magnetic properties by high energy milling and annealing (table 4.2).

The present study involves the solid-state reaction by mechanochemical reaction using celestite and blue dust. After the reaction the powder was annealed. The magnetic properties show the moderate value of remanence and energy product and the coecivity as shown in table 4.2.

The chemically upgraded celestite and modified blue dust has been used in the present experiment. Some siliceous impurities are always occluded with iron ore, which in all proportion does not favour the magnetic properties. The celestite even after chemical upgradation is not free from impurities. The lower value of magnetic properties may be attributed due to presence of

retained impurities as discussed above. Apart from this the value of sintered density of the magnet obtained in this experiment is 4.9 gm/cc, which is lower than the theoretical density 5.1 gm/cc [16]. The decrease in density also causes to lower $(BH)_{max}$ value. However, the magnetic properties obtained in the present investigation are within the range of other researchers as given in table 4.2 where they have used milling process to synthesize strontium hexaferrite.

The prolonged milling led to the decrease in the value of B_r, H_{ci} and $(BH)_{max}$ due to severe mechanical stresses and by formation of soft magnetic amorphous phase. After annealing the magnetic properties increase significantly due to recrystallisation [16-21].

4.3.3 Microstructure studies

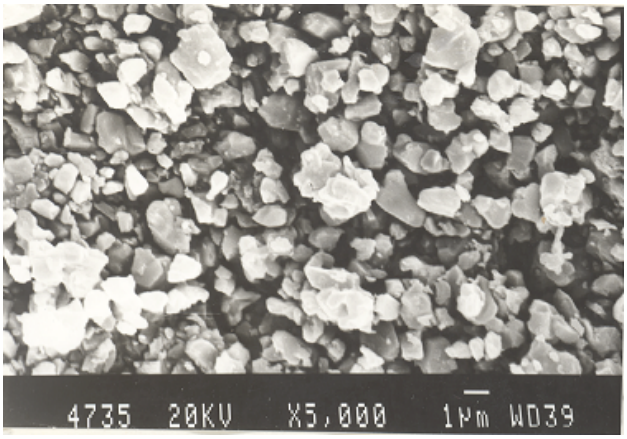

Fig.4.4 SEM micrograph of $SrFe_{12}O_{19}$ powder after annealing.

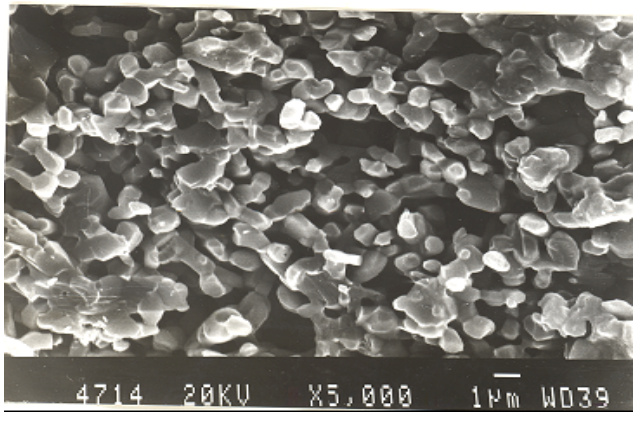

Fig.4.5 SEM micrograph of fractured surface of sintered $SrFe_{12}O_{19}$ magnet.

Fig. 4.4 shows the SEM micrograph of strontium hexaferrite annealed powder, which was obtained after gold sputtering. This shows the hexagonal grains of ferrite. Fig. 4.5 shows SEM

micrograph of the fractured surface of the ferrite magnet. The major portion of particles is in range of 1 μm. The grains are elongated, showing orientation of ferrite particles. During the process of annealing and sintering small particles of strontium hexaferrite have grown to single domain ≤1 μm.

References

1. Krik-othmer, "Encyclopedia of chemical technology" fourth edition, John Willey & Sons, 1993, pp 393- 405.
2. Joyce A. Ober, Strontium USGS Report, 2007, pp 1-7.
3. J Pual, Mac Millan, "Strontium and Strontium compound" Ullmann's Encyclopedia of Industrial Chemistry, vol. A-25., 1994.
4. Puneet Sharma, Amitabh Verma, R.K.Sidhu, O.P.Pandey, "Process parameter selection for strontium ferrite sintered magnets using Taguchi L9 orthogonal design" Journal of Material Processing Tecnology vol. 168, 2005, pp 147-151.
5 Mortaza Mozaffari, Jamshid Amighian "Direct use of celestite to prepare presintered $SrFe_{12}O_{19}$ powders" Physica B, vol. 321, 2002, pp 45-47.
6. R. Dasgupta, S.K. Bose, S.P.Narayan,), "Hard ferritess from blue dust of Bailadila mines of Madhya Pradesh" Research and Industries, vol. 40, 1995, pp 236-239.
7. G.R. Karagegedov, N.Z. Lyakhov, "Mechanochemical grinding of inorganic oxides" KONA, vol. 21, 2003, pp 76-87.
8. V. V., Boldrev, "Mechanochemistry and mechanical activation" Matter Science Forum, vol. 227, 1996, pp 511-520.
9. E. Gaffet, D. Michael, L. Muzerolles and P. Berther, (1997), "Effect of high- energy ball milling on ceramic oxide" Matter Science Forum, vol. 235-238(1), pp 511- 520.
10. C. Suryanarayna, "Nanocrystalline Materials" International Materials Reviews, vol.40 (2), 1995, pp 41-115.
11. E. Gaffet, F. Bernard, J.C. Niepce, F. Charlot, C.Gra, G. Caer, "Some recent developments in mechanical activation and mechanosynthesis" J. Material Chemistry, vol. 9, 1999, pp 305-314.
12. E. Gaffet, D. Michael, L. Muzerolles and P. Berther, "Effect of high-energy ball milling on ceramic oxide" Matter Science Forum, vol. 235-238(1), (1997), pp 511- 520.

13. C. Miclea, C. Tanasoiu, C.F. Miclea, I. Spanulescu, A. Gheorghiu and M. Cioangher, "Structure and magnetic properties of strontium hexaferrite nanopowders prepared by mechanochemical synthesis" Advance in science and technology, 2006, pp 321-326.
14. J. Sort, J. Noguess, S. Surifiach, J.S. Munoz, M.D. Baro, "Coercivity enhancement in ball-milled and heat treated Sr-ferrite with iron sulphide" Journal of Metastable and Nanocrystalline Materials, vol. 15-16, 2003, pp 599 606.
15. S.V.Ketov, Yu. D. Yagodkin, A.L.Lebed, Yu. V.Chernopyatova, K. Kholpkov,"Structure and magnetic properties of nanocrystalline $SrFe_{12}O_{19}$ alloy produced by high-energy ball milling and annealing" Journal of Magnetism and Magnetic Materials, vol. 300, 2006, pp e479-e481.
16. B.D.Cullity, "Introduction to magnetic materials" Addition Wasley, Reading, MA, (1972).
17. W. A. Kaczmarek, S.J.Campebell, E.Wu. B.Idrikowski, K.H.Miller,"Structural and Magnetic Phases in Ball Milled Strontium Ferrite" Material Forum, vol. 269-272, 1998, pp 465-460.
18. Spomenka Besenicar, Miha Drofenic,"High coercivity Sr Hexaferrites" Journal of Magnetism and Magnetic Materials, vol. 101, 1991, pp 307-309.
19. P. I. Paulin Filno, R.R.Correa, "Chatecterisation of strontium ferrite powders obtained by high energy milling" Material Science Forum, vol. 498, 2005 pp 311-315.
20. S. P. Gubin, Yu A Kokasharow, G.B. Khomutov, "Magnetic Nanoparticles, Preparation, Structure and Properties" vol. 74(6), 2005, pp 489-520.
21. H.Taguchi, F. Hirata, T. Takeishi, United State Patent: 6,132,635, 2000, pp.1-24.

Chapter 5

PREPARATION OF STRONTIUM HEXAFERRITE FROM PROCESSED ORE AND PURE CHEMICALS

Overview

This chapter describes the process for the preparation of strontium hexaferrite ($SrFe_{12}O_{19}$) from celestite (natural mineral of strontium) and blue dust (after converting celestite to strontium carbonate and physical upgradation of blue dust). The influence of various important process parameters such as Fe_2O_3/SrO mole ratio, calcination temperature and sintering temperature on the magnetic properties of strontium hexaferrite sintered magnets are discussed. In order to compare the isotropic and anisotropic magnetic properties, magnets under similar processing conditions were also prepared from pure chemicals. The magnetic properties with respect to its structural morphology e.g. particle size, shape, orientation, lattice parameters and phase formation were studied for both categories of magnets. The effect of different phases on magnetic properties is discussed in this chapter.

The phase analysis at different molar composition was carried out using XRD. The microstructural features were studied by SEM. The magnetic properties of each batch were measured using magnetometer.

5.1 Introduction

Many researchers have worked on strontium ferrite since its discovery in late 50, to improve its magnetic properties and reduce its production cost by adopting different processing routes. In order to prepare strontium hexaferrite directly from minerals/ores to reduce its production cost, some attempts has been made. Dasgupta et al. [1] have prepared strontium barium ferrite $(Ba_{0.8}S_{0.2})_{0.6}Fe_2O_3$ by using blue dust with barium carbonate and strontium carbonate of pure grade. However, they used low melting point glassy phase material ($16NaO43.2PbO40.8SiO_2$) to promote liquid phase sintering. In another experiment celestite was used with high purity iron oxide to make presintered strontium hexaferrite [2]. The celestite was changed to strontium carbonate by mechanoalloying method and then calcined it to prepare strontium hexaferrite [3]. U.S. Patent (No-4766284) has reported that strontium hexaferrite magnets can be prepared by using celestite and iron oxide with the help of welding torch which gives higher temperature but process can not be utilized at commercial scale for the bulk production [4]. The aim of the present study is to prepare strontium hexaferrite using celestite and blue dust with a view to reduce its processing cost as well as to explore the huge deposit of Indian celestite and blue dust. For it celestite was converted to strontium carbonate and blue dust was physically upgraded to remove soluble impurities. In another set of experiment strontium hexaferrite was prepared from pure chemicals. The detail of the process adopted is described in subsequent sections.

5.2 Experimental Procedure

5.2.1 Conversion of celestite into strontium carbonate

Before going for conversion of celestite into strontium carbonate it was chemically treated. The chemical treatment of celestite was carried out using HCl, HNO_3 and NH_4F. The detail of the process is mentioned in chapter 2 [5].

5.2.2 Upgradation of Blue dust

Blue dust was collected from Bailadela mines (Chattishgarh state, India). The particle size <45 μm was collected for the upgradation purpose. Blue dust powder was first physically upgraded with the help of magnetic separator. After that 100 gm of magnetic blue dust was taken in a 5 liter beaker. Beaker containing blue dust was heated on a hot plate at 70^0C and compressed air

was passed in it through indigenously designated glass nozzle. The details of the process is mentioned in chapter 3.

5.3 Preparation of strontium hexaferrite

5.3.1 Preparation of strontium hexaferrite from processed ores

Anisotropic strontium hexaferrite magnets were prepared using strontium carbonate which was obtained from celestite and upgraded blue dust. The mole ratio of (Fe_2O_3/SrO) has been taken as 5.0, 5.3, 5.6 and 5.9 for each set of experiment. The appropriate quantity of powder was weighed and mixed in hexane medium using a planetary ball mill for 3.0 hours. After milling the powder mixture was dried. The dried powder was pressed under hydraulic pressure of 500 MPa pressure using 15 cm diameter die. The pallets were calcined in a tubular furnace at 1150^0C for 3 hours. The calcined pallets were pulverized in tungsten carbide mortar and then milled in a planetary ball mill in hexane medium for 1 hour. The ball to charge ratio in this milling was 5:1. After drying 5% aqueous solution of poly vinyl alcohol (PVA) was added in the dried powder and mixed thoroughly. This mixture was allowed to dry for 12 hours. The dried powder was again ball milled in a planetary mill to make the powder free flowing for its further processing. For anisotropic magnet powder was compacted at 500 MPa pressure under magnetic field of 2 T along the pressure direction to obtain 5 mm diameter and 12mm height pellets. The pellets were sintered in an electric resistance tubular furnace at 1200^0C for 1 hour at controlled heating rate of 5^0/minute. For isotropic sample compaction was carried out in absence of magnetic field.

5.3.2 Preparation of strontium hexaferrite from pure chemicals

Analytical grade $SrCO_3$ and Fe_2O_3 prepared from the chemical upgradation of blue dust (chapter 3) were used in present study. The chemical composition of Fe_2O_3 obtained from the blue dust is mentioned in table 5.1 and chemical composition of pure $SrCO_3$ is given in table 5.2. The mole ratio of (Fe_2O_3/SrO) has been taken as 5.0, 5.3, 5.6 and 5.9 for each set of experiments. The appropriate quantity of powder was weighed and mixed in hexane medium for 3.0 hours using planetary ball mill. After milling the powder mixture was dried. The samples were prepared in the similar manner as mentioned in section 5.3.1.

The strontium hexaferrite phase was analysed with X-ray diffracometer (Model Rigaku D-Max IIIC). Microstructural analysis of sintered magnets was carried out using scanning electron microscope (Model JEOL 840 A). The magnetic properties of the sintered magnets were measured with pulse magnetometer (Model TC-201).

Table 5.1 Chemical composition of Fe_2O_3 obtained from chemical precipitation of blue dust

Compound	**Wt. %**
Fe_2O_3 (synthesized from blue dust)	99.21
SiO_2	0.32
CaO	0.12
MgO	0.14
Al_2O_3	0.21

Table 5.2 Chemical composition of pure $SrCO_3$ (Loba Chemicals Ltd., Pune, India)

Compound	**Wt. %**
$SrCO_3$ (AR Grade)	98.5
$BaCO_3$	1.75
Na_2O	0.02
CaO	0.13
Al_2O_3	0.04
Fe_2O_3	0.008

5.4 Results and Discussion

5.4.1 X-Ray Diffraction analysis

5.4.1.1 Strontium hexaferrite (Processed ore)

Fig.5.1 (a, b, c, d) shows X-ray diffractogram of strontium hexaferrite powder for mole ratio (Fe_2O_3/SrO) 5.0 calcined for 3 hours at 1100^0C, 1125^0C, 1150^0C and 1175^0C respectively. The diffraction pattern shows the formation of single phase strontium hexaferrite. However, diffracted peak of Fe_2O_3 is also seen in this diffractogram. The presence of iron oxide peak may be due to uncombined iron oxide. Fig. 5.2 (a, b, c, d) shows the X-ray diffraction pattern of strontium hexaferrite prepared at mole ratio (Fe_2O_3/SrO) 5.3 at calcination temperatures 1100^0C,

1125^0C, 1150^0C and 1175^0C respectively. Fig. 5.3(a, b .c, d) represents the X-ray diffraction pattern of strontium hexaferrite at mole ratio 5.6 and calcined at 1100^0C, 1125^0C, 1150^0C and 1175^0C respectively for three hours.

Fig. 5.4 (a, b, c, d) represents the X-ray diffraction pattern of strontium hexaferrite prepared at mole ratio 5.9 and calcined at 1100^0C, 1125^0C, 1150^0C and 1175^0C for 3 hours respectively. It is clear from figure that at mole ratio 5.0 and 5.3 the highest X-ray diffraction intensity peak is observed at 1150^0C calcination temperature. However, at Fe_2O_3/SrO mole ratio 5.6 and 5.9 the higher peak intensity was observed at 1175^0C. This shows that strontium ferrite with higher mole ratio requires higher calcination temperature. This is due to the presence of more Fe_2O_3 in the higher mole ratio compound. It is also evident from the X-ray pattern that with increase in the Fe_2O_3/SrO mole ratio the intensity of Fe_2O_3 increases. Similar behavior was also reported for the strontium hexaferrite powders prepared using pure chemicals [6].

5.4.1.2 Strontium hexaferrite (Pure chemicals)

X-ray diffraction pattern of calcined strontium hexaferrite powder at different mole ratio (Fe_2O_3/SrO) using pure chemicals is shown in fig.5.5. The diffraction peaks obtained with mole ratio 5.0 has been shown in fig. 5.5(a). The phase analysis shows that single phase strontium hexaferrite has formed. Fig. 5.5(b), 5.5(c) and 5.5(d) shows X-ray pattern of mole ratio 5.3, 5.6 and 5.9 respectively. It is observed that relative diffraction intensity of $SrFe_{12}O_{19}$ peaks are increasing as mole ratio is increased from 5.0 to 5.6. There is relatively slight decrease in peak intensity for mole ratio 5.9. The intensity of peaks represents the volume of ferrite phase formed. On comparing fig.5.1-5.4 it is found that at for each mole ratio (5.0-5.9) volume fraction of strontium hexaferrite increases with increase in temperature.

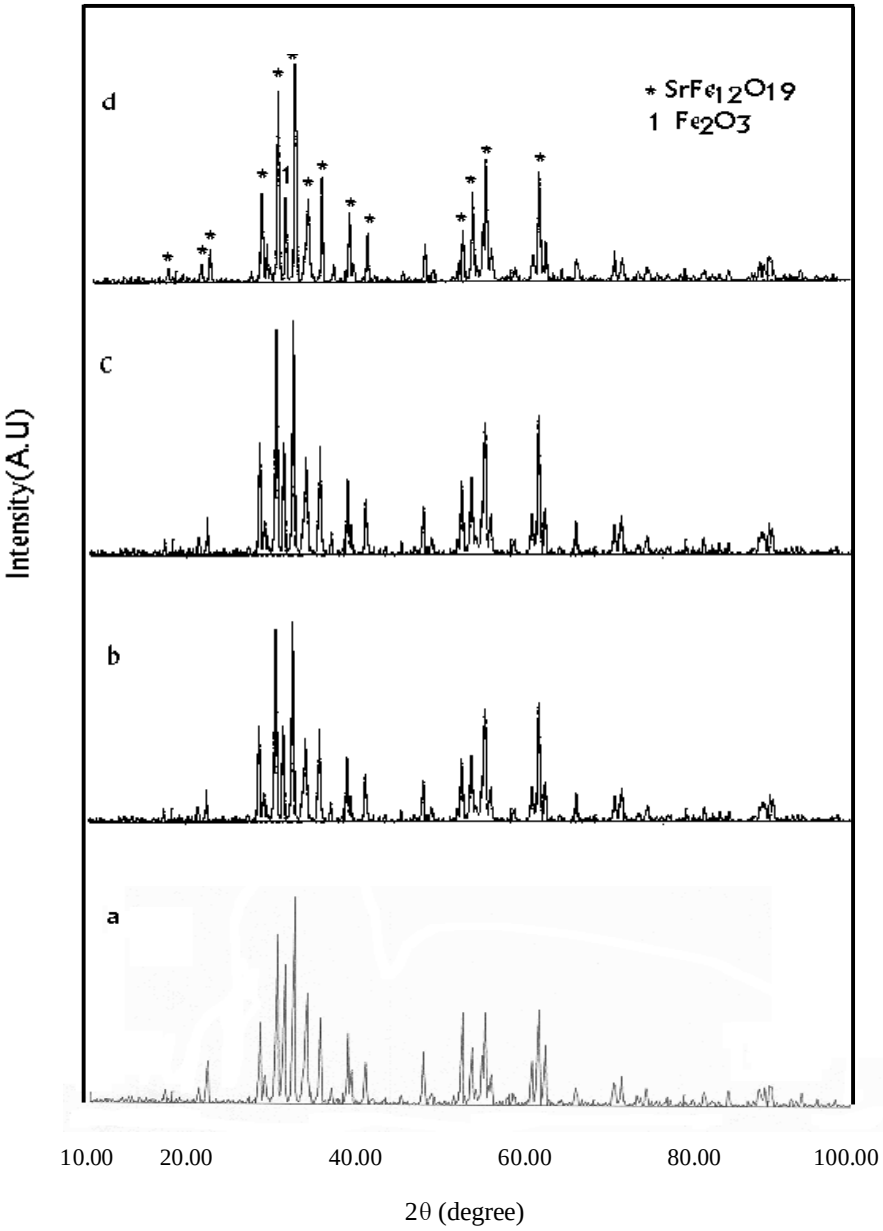

Fig. 5.1 X-ray diffraction pattern of strontium hexaferrite powder for mole ratio (Fe_2O_3/SrO) 5.0 calcined at (a) 1100^{0}C (b) 1125^{0}C (c) 1150^{0}C (d) 1175^{0}C respectively.

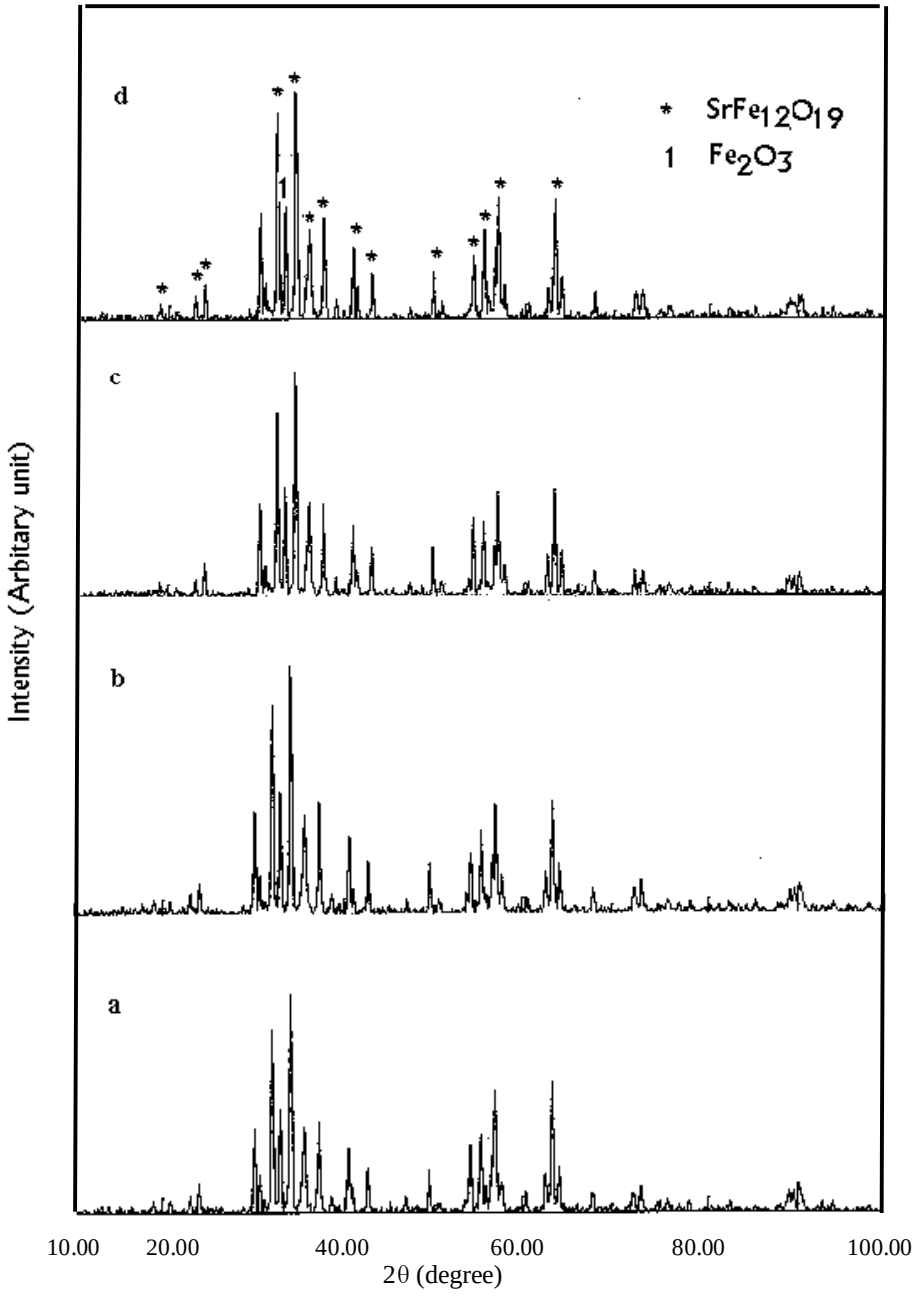

Fig.5.2 X-ray diffraction pattern of strontium hexaferrite powder for mole ratio (Fe_2O_3/SrO) 5.3 calcined at at (a) 1100^{0}C (b) 1125^{0}C (c) 1150^{0}C (d) 1175^{0}C respectively.

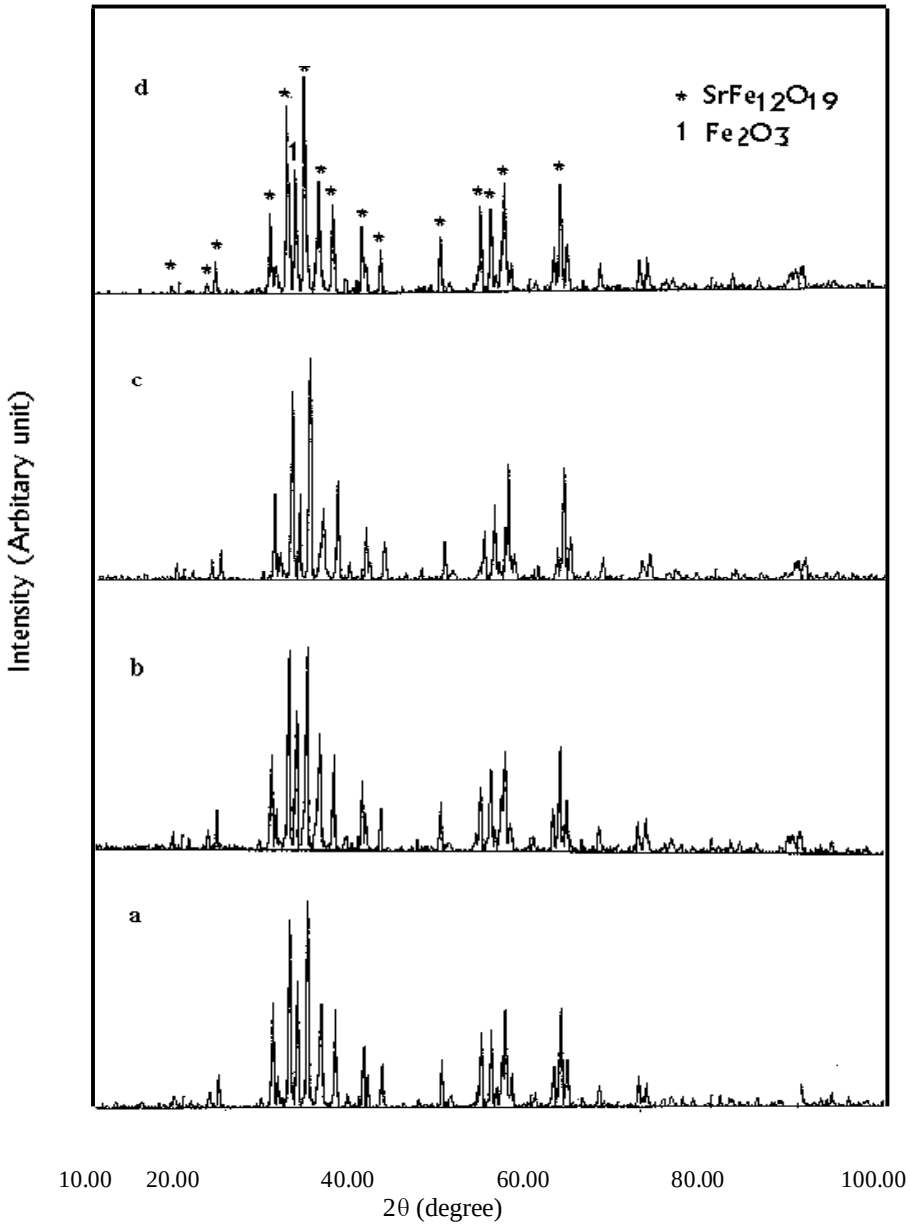

Fig. 5.3 X-ray diffraction pattern of strontium hexaferrite powder for mole ratio (Fe_2O_3/SrO) 5.6 calcined at (a) 1100^{0}C (b) 1125^{0}C (c) 1150^{0}C (d) 1175^{0}C respectively.

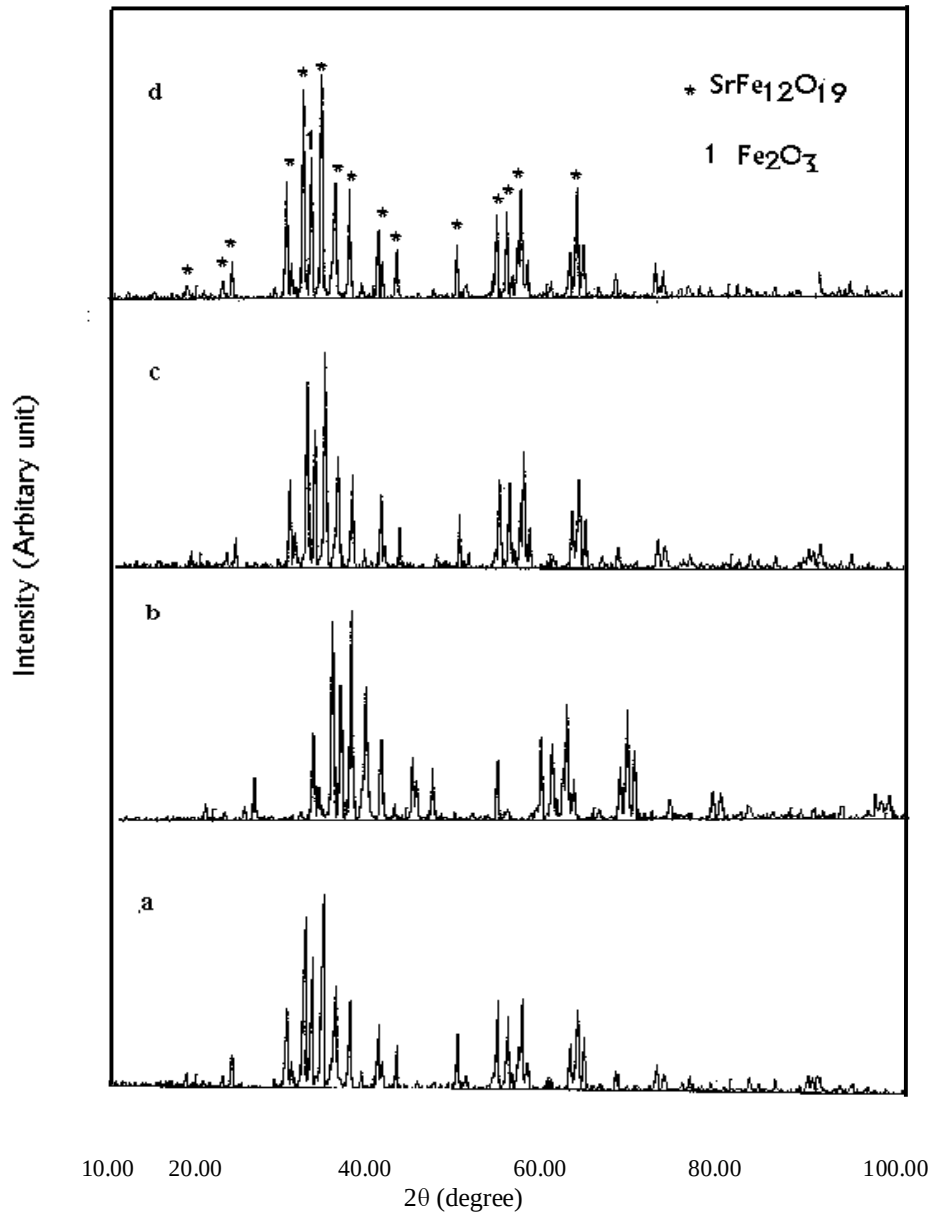

Fig. 5.4 X-ray diffraction pattern of strontium hexaferrite powder for mole ratio (Fe_2O_3/SrO) 5.9 calcined at (a) 1100^0C (b) 1125^0C (c) 1150^0C (d) 1175^0C respectively.

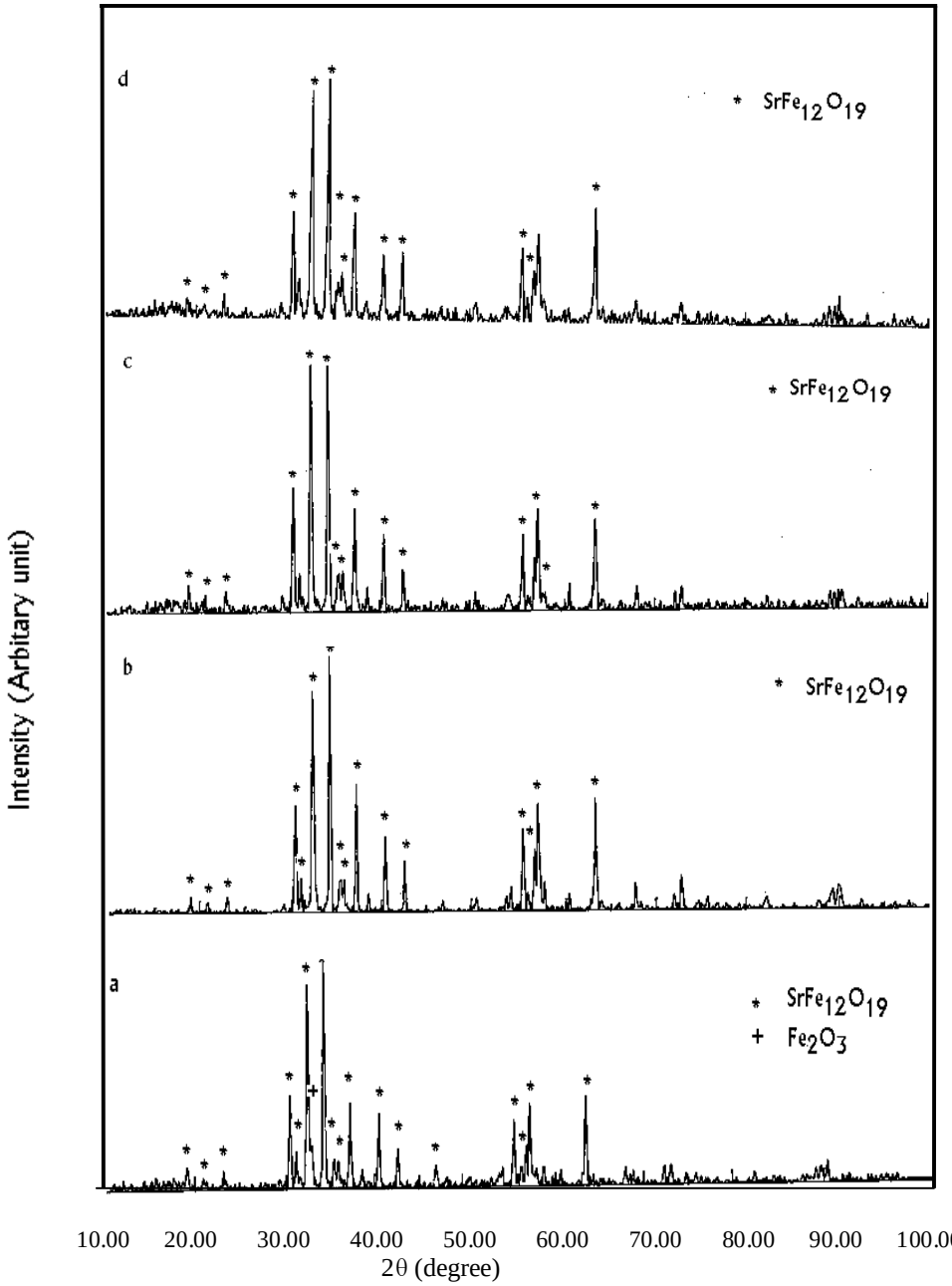

Fig. 5.5 X-ray diffraction pattern of $SrFe_{12}O_{19}$ at different mole ratio (Fe_2O_3 /SrO) (a) 5.0, (b) 5.3, (c) 5.6 and (d) 5.9 calcined at 1150^0C for 3hr prepared from pure chemicals

Table 5.3 Magnetic properties, density, shrinkage of sintered $SrFe_{12}O_{19}$ (processed ore) at mole ratio 5.0 with different calcination and sintering temperatures

Mole ratio	Calcination temperature (^{0}C)	Sintering temperature (^{0}C)	B_r (mT)	H_{ci} (KA/m)	$(BH)_{max}$ (Kj/m^3)	Radial shrinkage %	Longitudinal srinkage %	Sintered density g/cc
5.0	1100	1200	142	305	2.87	4.39	7.29	3.50
		1220	139	299	2.74	4.90	7.98	3.56
		1240	140	306	2.96	5.34	8.34	3.53
		1260	143	303	3.04	5.92	9.43	3.50
	1125	1200	143	278	2.69	3.23	7.90	3.39
		1220	147	295	3.32	3.89	7.98	3.43
		1240	139	296	3.24	3.78	8.34	3.46
		1260	149	303	3.58	3. 42	9.43	3.53
	1150	1200	144	295	3.56	3.30	8.90	3.74
		1220	148	298	3.73	3.59	8.98	3.54
		1240	145	303	3.66	5.62	8.94	3.65
		1260	150	286	3.56	6. 31	10.34	3.76
	1175	1200	139	290	2.71	3.20	7.60	3.49
		1220	131	31**2**	2.22	5.56	7.98	3.53
		1240	145	296	3.35	6.30	9.34	3.61
		1260	131	291	1.65	6. 29	9.30	3.52

Table 5.4 Magnetic properties, density, shrinkage of sintered $SrFe_{12}O_{19}$ (processed ore) at mole ratio 5.3 with different calcination and sintering temperatures

Mole ratio	Calcination temperature (^{0}C)	Sintering temperature (^{0}C)	B_r (mT)	H_{ci} (KA/m)	BH_{max} (Kj/m^3)	Radial shrinkage %	Longitudinal shrinkage %	Sintered density g/cc
5.3	1100	1200	134	316	2.35	4.39	7.36	3.49
		1220	135	310	3.39	4.90	8.01	3.52
		1240	142	306	3.27	5.34	8.42	3.50
		1260	139	313	2.57	5.92	9.53	3.61
	1125	1200	133	307	3.01	3.23	7.83	3.54
		1220	137	322	2.40	3.89	7.95	3.62
		1240	135	307	2.50	3.78	8.43	3.58
		1260	134	322	1.86	3. 42	9.51	3.59
	1150	1200	138	291	2.83	3.30	7.58	3.50
		1220	138	321	2.79	3.59	7.89	3.51
		1240	140	306	2.79	5.62	8.82	3.53
		1260	140	297	2.48	6. 31	9.54	3.65
	1175	1200	135	310	2.44	4.20	7.62	2.69
		1220	140	316	3.17	5.56	7.93	3.55
		1240	138	317	2.23	6.30	9.42	3.60
		1260	139	315	3.06	6. 29	9.29	3.62

Table 5.5 Magnetic properties, density, shrinkage of sintered $SrFe_{12}O_{19}$ (processed ore) at mole ratio 5.6 with different calcination and sintering temperatures

Mole ratio	Calcination temperature (^{0}C)	Sintering temperature (^{0}C)	B_r (mT)	H_{ci} (KA/m)	BH_{max} (Kj/m^3)	Radial shrinkage %	Longitudinal shrinkage %	Sintered density g/cc
5.6	1100	1200	126	321	2.46	3.65	3.98	3.46
		1220	129	306	2.92	3.70	4.76	3.52
		1240	130	305	2.99	3.69	3.54	3.50
		1260	127	328	2.42	3.52	3.76	3.42
	1125	1200	125	300	2.02	3.59	3.42	3.35
		1220	133	290	2.21	3.68	3.76	3.30
		1240	121	306	2.11	3.52	3.54	3.28
		1260	132	313	2.76	3.48	3.76	3.51
	1150	1200	129	308	1.74	3.39	3.39	3.24
		1220	130	314	2.28	3.53	3.92	3.20
		1240	129	318	2.86	3.53	3.32	3.41
		1260	131	287	2.39	3.48	4.70	3.51
	1175	1200	128	297	1.91	3.32	3.91	3.25
		1220	122	297	3.04	3.67	4.76	3.50
		1240	130	317	2.62	3.50	3.51	3.48
		1260	142	291	3.34	3.58	4.72	3.41

Table 5.6 Magnetic properties, density, shrinkage of sintered $SrFe_{12}O_{19}$ (processed ore) at mole ratio 5.9 with different calcination and sintering temperatures

Mole ratio	Calcination temperature (^{0}C)	Sintering temperature (^{0}C)	B_r (mT)	H_{ci} (KA/m)	BH_{max} (Kj/m^3)	Radial shrinkage %	Longitudinal shrinkage %	Sintered density g/cc
5.9	1100	1200	123	329	1.49	3.24	4.98	3.36
		1220	128	307	1.74	3.39	3.76	3.43
		1240	124	322	1.61	3.69	3.54	3.54
		1260	121	223	2.00	3.52	5.76	3.39
	1125	1200	114	312	1.17	3.17	3.93	3.23
		1220	119	317	2.37	3.41	3.76	3.40
		1240	116	309	1.41	3.25	3.54	3.34
		1260	120	328	2.39	3.49	3.96	3.41
	1150	1200	123	325	2.40	3.15	3.92	3.23
		1220	119	326	1.12	3.20	3.64	3.29
		1240	121	324	2.12	3.31	3.84	3.32
		1260	120	302	1.56	3.12	4.56	3.27
	1175	1200	124	307	2.02	3.15	3.85	3.32
		1220	120	325	1.50	3.20	5.62	3.53
		1240	123	323	1.56	3.21	4.84	3.22
		1260	120	323	1.53	3.20	3.96	3.20

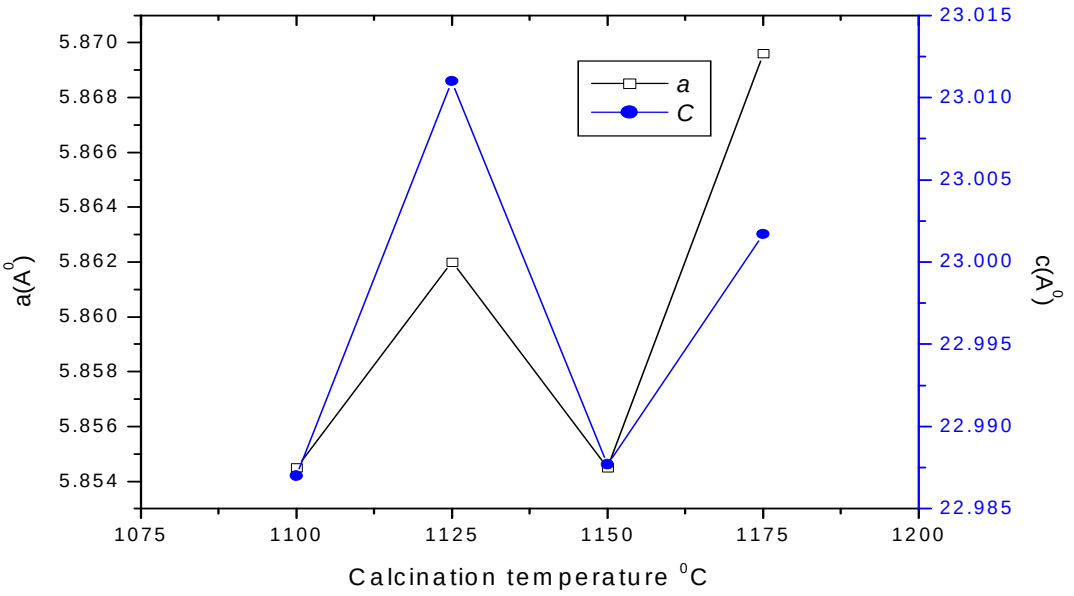

(a) Mole ratio 5.0

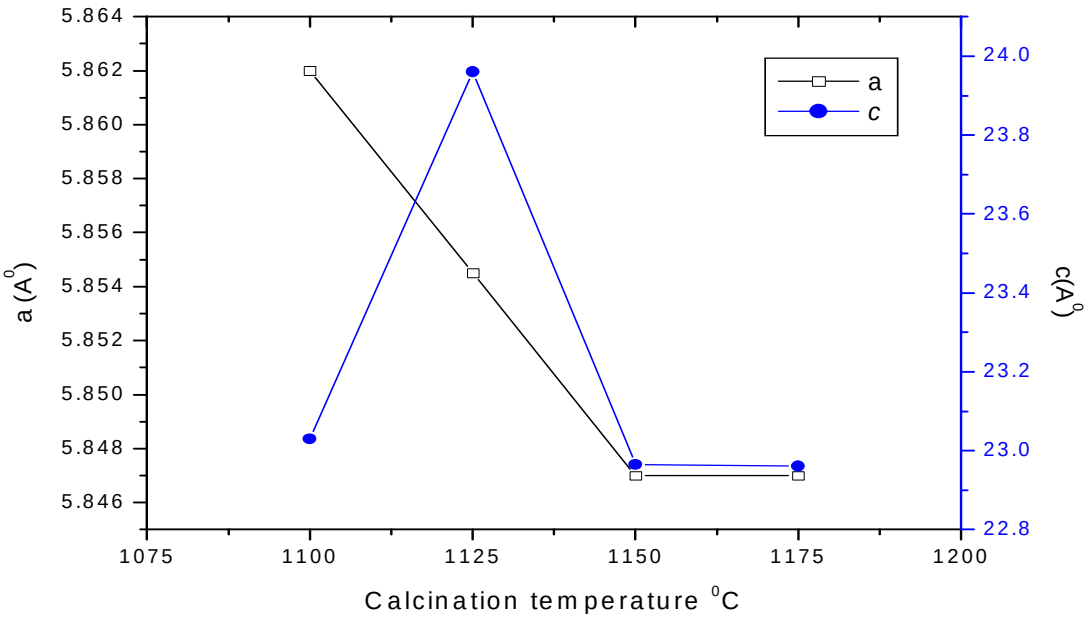

(b) Mole ratio 5.3

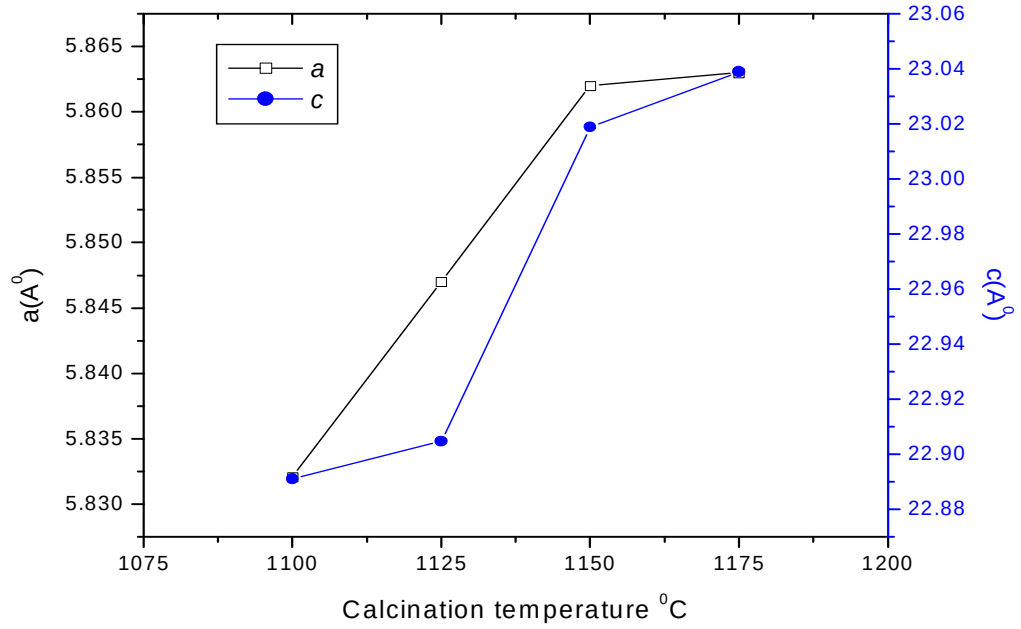

(c) Mole ratio 5.6

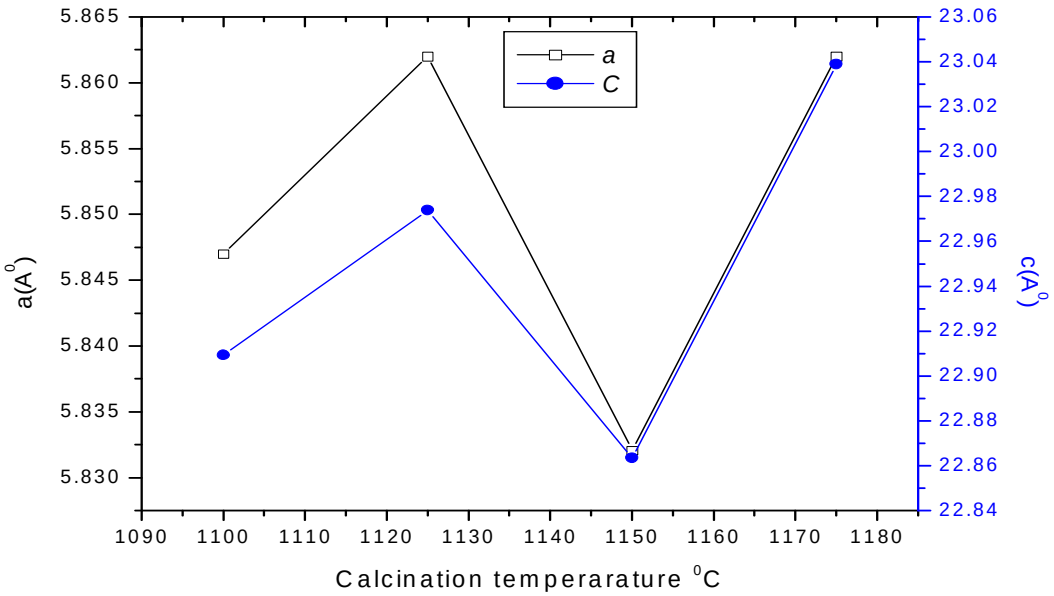

(d) Mole ratio 5.9

Fig. 5.6 Variation of *c*, *a* of $SrFe_{12}O_{19}$ with mole ratio at different calcination temperatures (a) mole ratio 5.0 (b) mole ratio 5.3 (c) mole ratio 5.6 (d) mole ratio 5.9

The variation in the value of lattice constant *a* and *c* of strontium hexaferrite (processed ore) with respect to calcination temperature at different mole ratio is shown in figure 5.6. The lattice constant both *a* and *c* decreases with increasing calcination temperature for (Fe_2O_3/SrO) mole ratio 5.0 to 5.6. However, for mole ratio 5.9 both *a* and *c* increase when calcination temperature increases.

This is due to fact that strontium ferrite with lower ferrite content have more vacant sites of Fe ions in the crystal which leads to the lower *a* and *c* of the hexagonal unit cell. For higher mole ratio there will be no vacant site, which lead to increase the *a* and *c*.

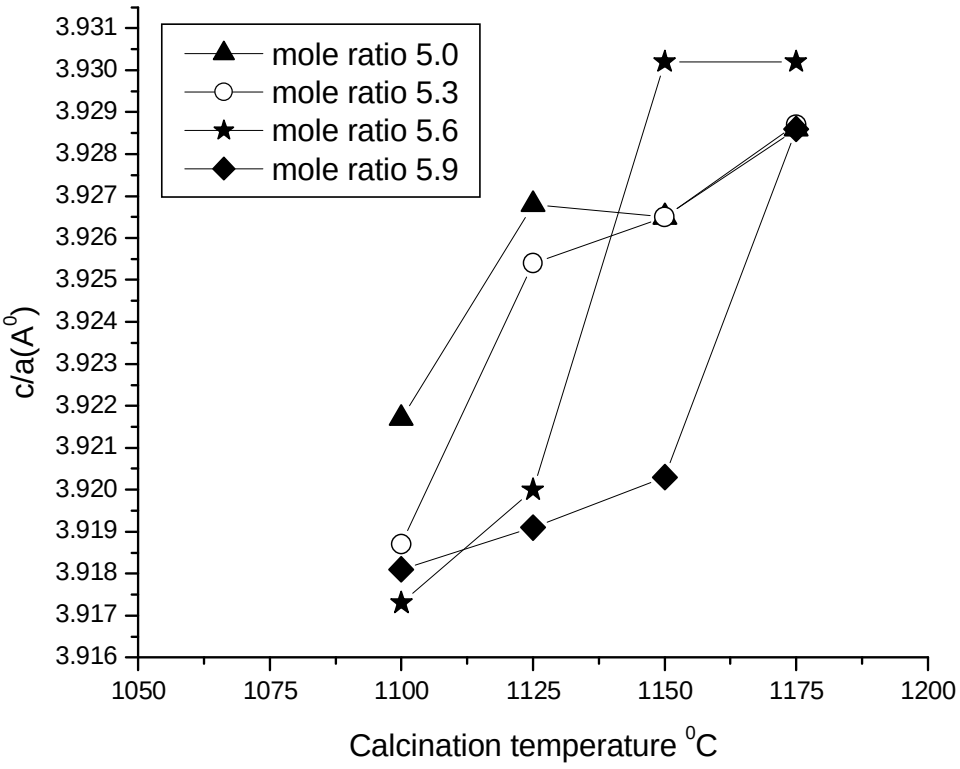

Fig.5.7 Variation of *c*/*a* of strontium hexaferrite (processed ore) with different mole ratio and calcination temperatures

Fig 5.7 shows the ratio of lattice parameters *c/a* of strontium hexaferrite powder produced from processed ore at different mole ratios and calcination temperature. As the mole ratio was varied from 5.0 to 5.9, *c/a* ratio was observed to increase with increase in calcination temperature.
This may be attributed to the fact strontium ferrite with lower ferrite content have more vacant sites of Fe ions in the crystals. For higher mole ratio there will be no vacant sites. This variation in *c/a* was also reported by Wen-Yu Zhao [7].

The value of % radial shrinkage, longitudinal shrinkage and sintered density for different mole ratio, calcination temperature and the sintering temperature is shown in table 5.3 to 5.6. A typical graph for this variation for the sample calcined at 1150^0C and sintered at 1260^0C is shown in figure 5.8. The sintered density was observed to decrease with increasing mole ratio. This was supported by continuous decrease in percentage shrinkage with increasing mole ratio. However, the shrinkage was observed to be more in axial direction than in radial direction.

It is clear from the figure 5.8 that influence of Fe_2O_3/SrO mole ratio on sintered density, axial shrinkage and radial shrinkage is very strong. This is due to the fact that when mole ratio increases iron oxide content increases. The decrease in sintered density, shrinkage is because of the fact that iron occupying the interstitial sites gets saturated during sintering in the beginning itself. During final sintering no further grain growth takes place for the samples as they are already calcined at higher temperature. This also reduces the sintering density. Higher calcination temperature also causes low driving force for final sintering, which reduces the sintering density. However, further increase makes the system to have free iron oxide which causes a lower shrinkage and decrease in density. This is also supported by an increase in value of lattice parameter *a* and *c* which shows increase in the unit cell corresponding to the same number of atoms. This result matches with the result obtained by other researchers [7, 8, 9].

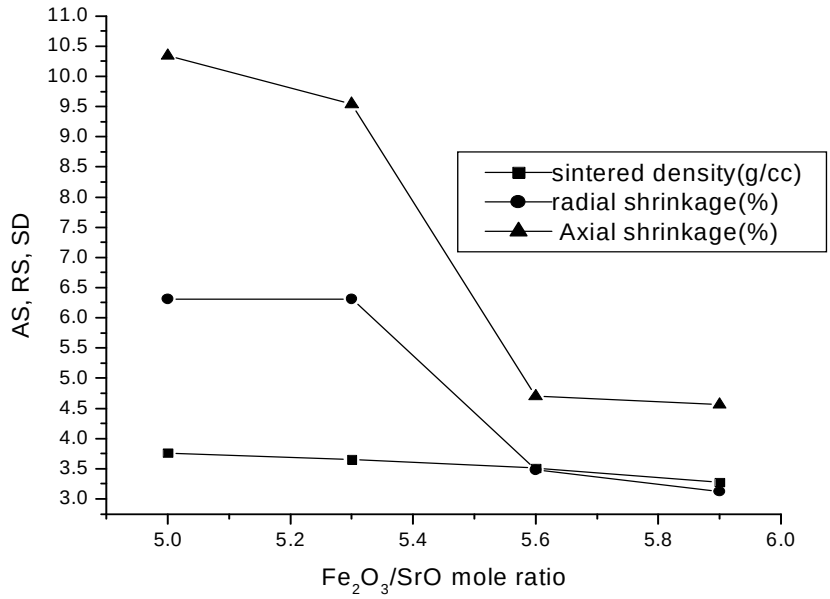

Fig. 5.8 Effect of mole ratio on sintered density, radial shrinkage and axial shrinkage of strontium hexaferrite (processed ore) calcined at 1150^0C and sintered at 1260^0C.

Fig. 5.9 and Fig. 5.10 show the value of lattice parameters *a* and *c* in (Å) with variation of mole ratio of strontium hexaferrite obtained from pure chemicals and from processed ores respectively. On comparing the lattice parameters values of ferrite prepared from pure chemicals and from processed ore we find that in both cases strontium hexaferrite phase has nearly constant value of *a* for different mole ratios. However, the ore based hexaferrite has lower value (5.8321 Å) than pure chemicals (5.8848 Å). On the other hand value of lattice parameter *c* of ferrite prepared from pure chemicals is maximum at mole ratio 5.6 whereas the ore based strontium hexaferrite has maximum *c* value at mole ratio 5.0. The ore based strontium hexaferrite has relatively lower value of *c* than that of pure chemical based ferrite. This may be due to the fact that lattice constant *c* governs the magnetic properties.

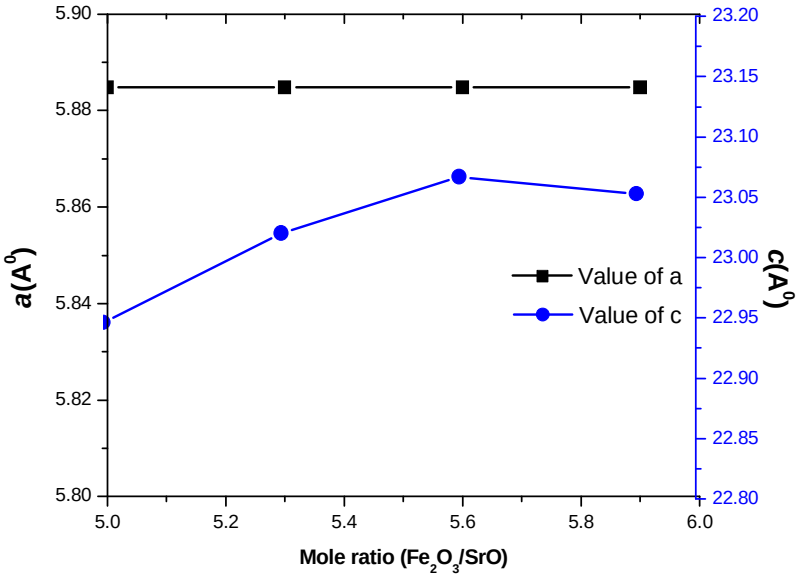

Fig 5.9 Variation of lattice parameter *a*, *c* of strontium hexaferrite (pure chemicals) calcined at 1150^{0}C for different mole ratio

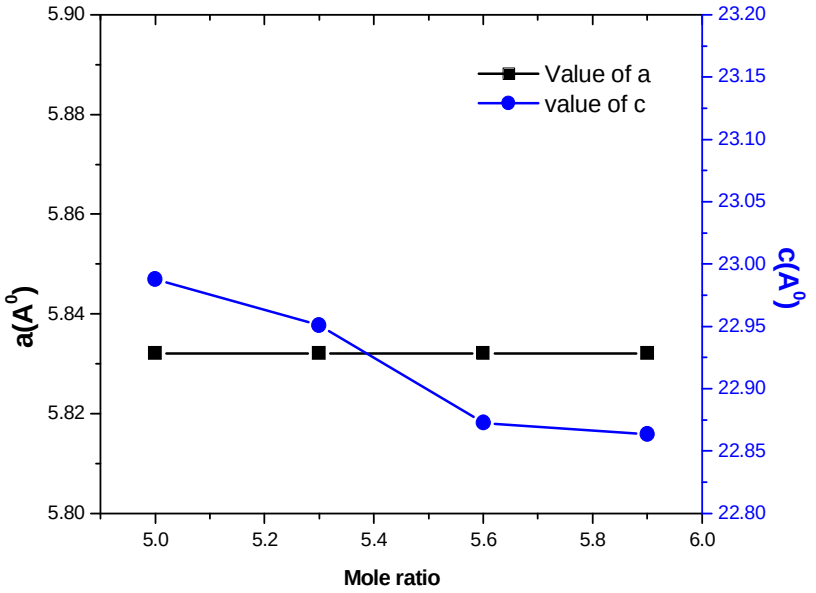

Fig 5.10 Values of calculated lattice parameters (*a* and *c*) of strontium hexaferrite calcined at 1150^{0}C obtained from celestite ore and blue dust.

5.4.2 Magnetic Properties

5.4.2.1 Magnets from processed ores

Table 5.8 and 5.10 shows the magnetic and physical properties of strontium hexaferrite sintered magnets prepared at mole ratio (Fe_2O_3/SrO) of 5.0 to 5.9. The calcination temperature was varied between 1100 to 1175^0C at an increment of 25^0C and the calcined powder was sintered at 1250^0C/1 hr. It is clear from the table 5.3-5.6 that the value of $(BH)_{max}$ and B_r is constant from mole ratio 5.0 to 5.3. As mole ratio was increased the value of remanence and energy product decreases. Remanence is extrinsic property of the magnetic material which depends upon the degree of the grain alignment as stated earlier the density decreases with increasing mole ratio. The decrease in density could be reason for the lower *Br* and $(BH)_{max}$ at higher mole ratio.

5.4.2.2 Magnets from pure chemicals

Table 5.7 shows the relationship between the magnetic properties of anisotropic strontium ferrite magnets prepared from pure chemicals with different mole ratio (Fe_2O_3/SrO). A slight increase in residual magnetic flux density appears when the mole ratio increases from 5.0 to 5.3. A further increase in the flux density is observed at the mole ratio of 5.6. When the mole ratio value increases to 5.9 a slight decrease in residual magnetic flux value is observed. This is also obvious from the fig 5.11 where mole ratio verses *Br* graph shows the increasing trend of *Br* at mole ratio 5.6. The increased value of flux density may be due to high degree of crystal grain orientation and high sintered density. The decrease in flux density value may be due to lower degree of grain orientation. The value of energy product at mole ratio 5.6 is maximum as shown in table 5.3. Similar variation in magnetic properties as a function of mole ratios (Fe_2O_3/SrO) was also reported by S. Ebrahimi [8]. Fig. 5.11 shows graphical representation of energy product value at different mole ratio. The value of energy product is directly proportional to magnetic flux density. Increase in *Br* corresponds to higher value of energy product. The value of intrinsic coercivity (H_{ci}) has a lower value at mole ratio 5.6 as shown in table 5.7. This value increases for mole ratio 5.0 and 5.9 as shown in the graphical representation in fig.5.11.

This is probably due to fact that for ferrite magnets it is very difficult to improve *Br* value and H_{ci} value at same time. It is necessary to obtain high degree of crystal grain orientation with higher sintered density to improve the remanence value. For this purpose a higher sintering

temperature is required. At the same time smaller grain size is required for the higher value of H_{ci}. This could be only possible when the particle orientation under magnetic field is done in the slurry form of the particle [9, 10].

The sintered density for the mole ratio 5.6 is greater as compared to mole ratio 5.0, 5.3 and 5.6 as shown in table 5.7. Because of higher sintered density at mole ratio 5.6 the remenence and energy product obtained is higher. The shrinkage along longitudinal direction (magnetization direction) is higher than the transverse direction. This is because of alignment of powder along magnetic direction. This leads to significant anisotropy character during sintering [11]. Fig. 5.15 and 5.16 show the *BH* loop of anisotropic and isotropic strontium hexaferrite sintered magnets obtained from pure chemicals respectively. Similarly fig.5.17 and 5.18 represent *BH* loop of magnets prepared using processed ore. These hysteresis loops are a representative graph for same mole ratio (5.6) for each category of magnets.

5.4.2.3 Comparison of Magnetic Properties

Table 5.7 Magnetic and physical properties of anisotropic ferrite samples made with pure strontium carbonate and pure iron oxide (calcined at 1150^{0}C for 3 hrs.).

Fe_2O_3/SrO Mole ratio	Sintering tempt. ^{0}C time 1Hr	B_r (mT)	H_{ci} (kA/m)	$(BH)_{max}$ kJ/m^3	Green density (g/cc)	Shrinkage axial (%)	Shrinkage radial (%)	Sintered density (g/cc)
5.0	1250	189	295	5.62	4.49	7.50	4.94	4.62
5.3	1250	197	262	6.43	4.51	8.85	6.25	4.61
5.6	1250	217	240	7.72	4.81	10.55	5.12	4.97
5.9	1250	183	283	5.31	4.43	6.60	5.20	4.58

Table 5.8 Magnetic and physical properties of anisotropic samples made with processed celestite and blue dust (calcined at 1150^{0}C for 3 hrs.)

Fe_2O_3/SrO Mole ratio	Sintering tempt. ^{0}C time 1Hr	B_r (mT)	H_{ci} (kA/m)	$(BH)_{max}$ kJ/m^3	Green density (g/cc)	Shrinkage axial (%)	Shrinkage radial (%)	Sintered density g/cc
5.0	1250	150	286	3.56	3.25	4.85	3.83	3.76
5.3	1250	140	297	2.48	3.23	4.87	3.76	3.65
5.6	1250	131	287	2.39	3.28	3.67	3.51	3.50
5.9	1250	121	324	2.12	3.27	4.23	3.62	3.27

Table 5.9 Magnetic and physical properties of isotropic samples made with pure chemicals (calcined at 1150^{0}C for 3 hrs.)

Fe_2O_3/SrO Mole ratio	Sintering tempt. ^{0}C time 1Hr	B_r (mT)	H_{ci} (kA/m)	$(BH)_{max}$ kJ/m^3	Green density (g/cc)	Shrinkage axial (%)	Shrinkag dadial (%)	Sintered density (g/cc)
5.0	1250	130	305	2.29	3.25	5.85	3.89	3.42
5.3	1250	143	297	3.55	3.23	4.63	4.43	3.40
5.6	1250	171	275	4.66	3.22	4.91	4.24	3.52
5.9	1250	147	357	2.50	3.27	4.85	3.92	3.27

Table 5.10 Magnetic and physical properties of isotropic samples made with processed celestite and blue dust (calcined at 1150^{0}C for 3 hrs.).

Fe_2O_3/SrO Mole ratio	Sintering tempt. ^{0}C Time 1Hr	B_r (mT)	H_{ci} (kA/m)	$(BH)_{max}$ kJ/m^3	Green density (g/cc)	Shrinkage axial (%)	Shrinkage radial (%)	Sintered density (g/cc)
5.0	1250	105	299	1.85	3.25	4.01	3.49	3.40
5.3	1250	123	320	1.59	3.23	3.89	3.36	3.41
5.6	1250	123	323	1.56	3.29	3.29	3.45	3.50
5.9	1250	119	301	1.09	3.27	2.98	3.40	3.36

Table 5.8 shows the magnetic properties of the anisotropic magnets made from processed celestite and blue dust. We find that sample of mole ratio 5.0 shows higher values of *Br* and $(BH)_{max}$. The presence of uncombined iron oxide detereoits the B_r and $(BH)_{max}$ value as it is non magnetic phase[12]. This unreacted Fe_2O_3 phase is due to saturated intestinal site occupied by Fe^{+3}[7]. Because of this the values are decreasing with increasing mole ratio. The variation in magnetic properties with different mole ratio is shown in fig.5.13. The value of sintered density is maximum with the mole ratio 5.0. The axial shrinkage is directly proportional to the sintered density. On the other hand if we compare the H_{ci} value of strontium hexaferrite magnets prepared using pure chemicals we find that there is not any major change in coercivity value. This is probably due to the presence of Fe_2O_3 phase which plays a complex role like particle isolation, exchange coupling etc. [13].

Table 5.9.shows the magnetic properties of isotropic strontium ferrite magnets prepared by pure strontium carbonate and iron oxide with different mole ratio (Fe_2O_3/SrO). It was observed that at mole ratio 5.6 the value of B_r and H_{ci} is higher as compared to other mole ratio and it is in increasing order from mole ratio 5.0 to 5.6 as shown in fig.5.12. On the other hand downwards trend is observed from mole ratio 5.6. As compared to anisotropic magnets the value of *Br*, $(BH)_{max}$ is less. This is due to the less alignment of the particle since the powder was not compacted under magnetic field. The sintered density is more for the mole ratio of 5.6. Because

of higher sintered density the values of B_r and $(BH)_{max}$ is more as compared to other mole ratios as shown in table 5.9.

Table 5.10 represents the value of magnetic properties, density and shrinkage of isotropic magnets made from processed celestite ore and blue dust. The values of B_r, $(BH)_{max}$ is lower since the particles are not aligned.

The graphical representation of the magnetic properties is shown in fig.5.14.

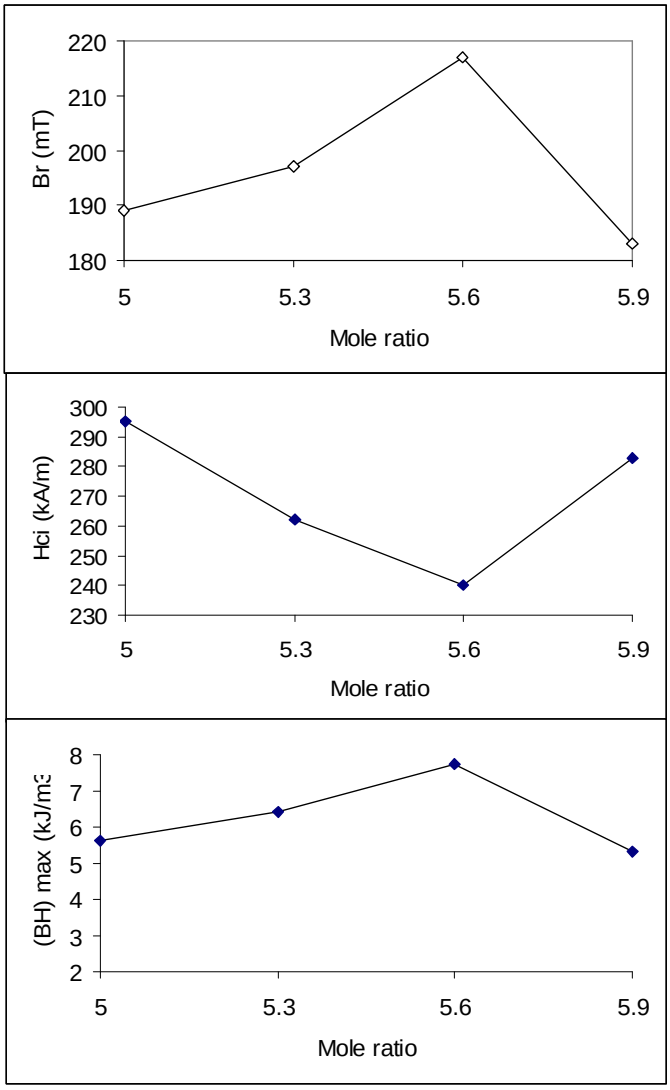

Fig 5.11 H_{ci}, $(BH)_{max}$ and B_r verses mole ratio of anisotropic $SrFe_{12}O_{19}$ (Pure chemicals) sintered at 1250^0C for 1 hr.

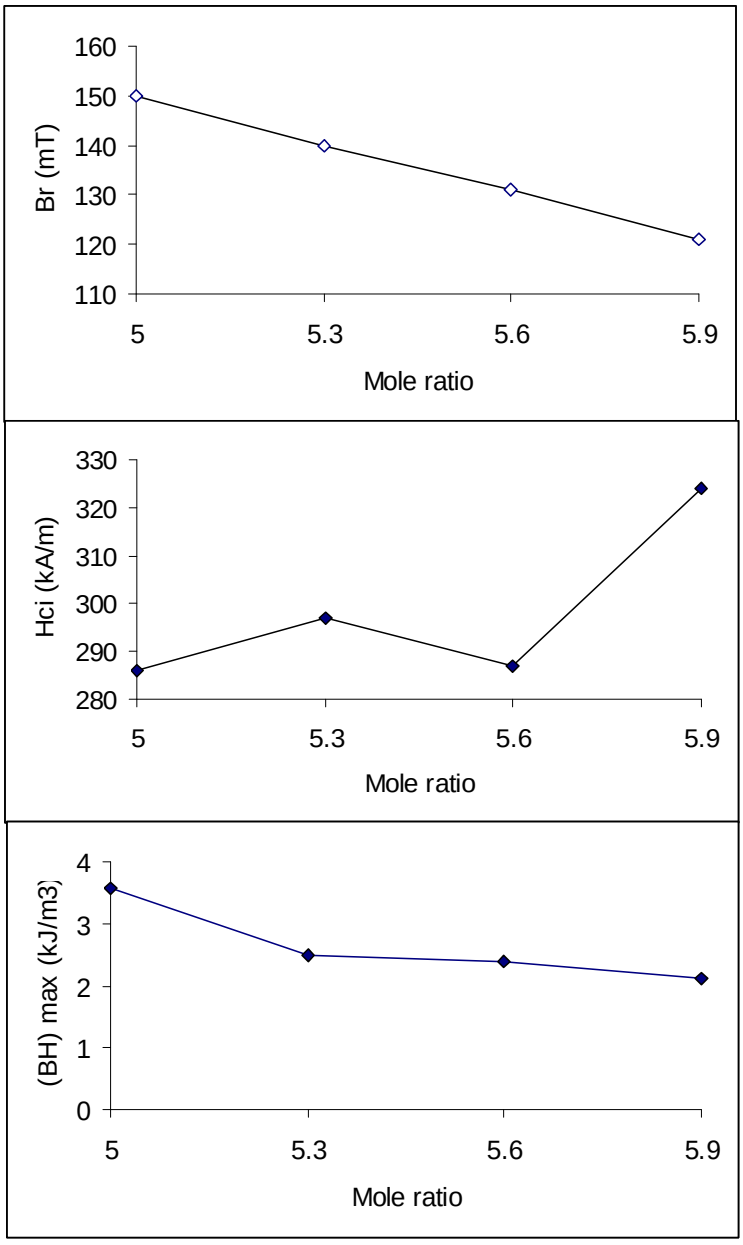

Fig 5.12 H_{ci}, $(BH)_{max}$ and B_r verses mole ratio of isotropic $SrFe_{12}O_{19}$ (Pure chemicals) sintered at 1250^0C for 1 hr.

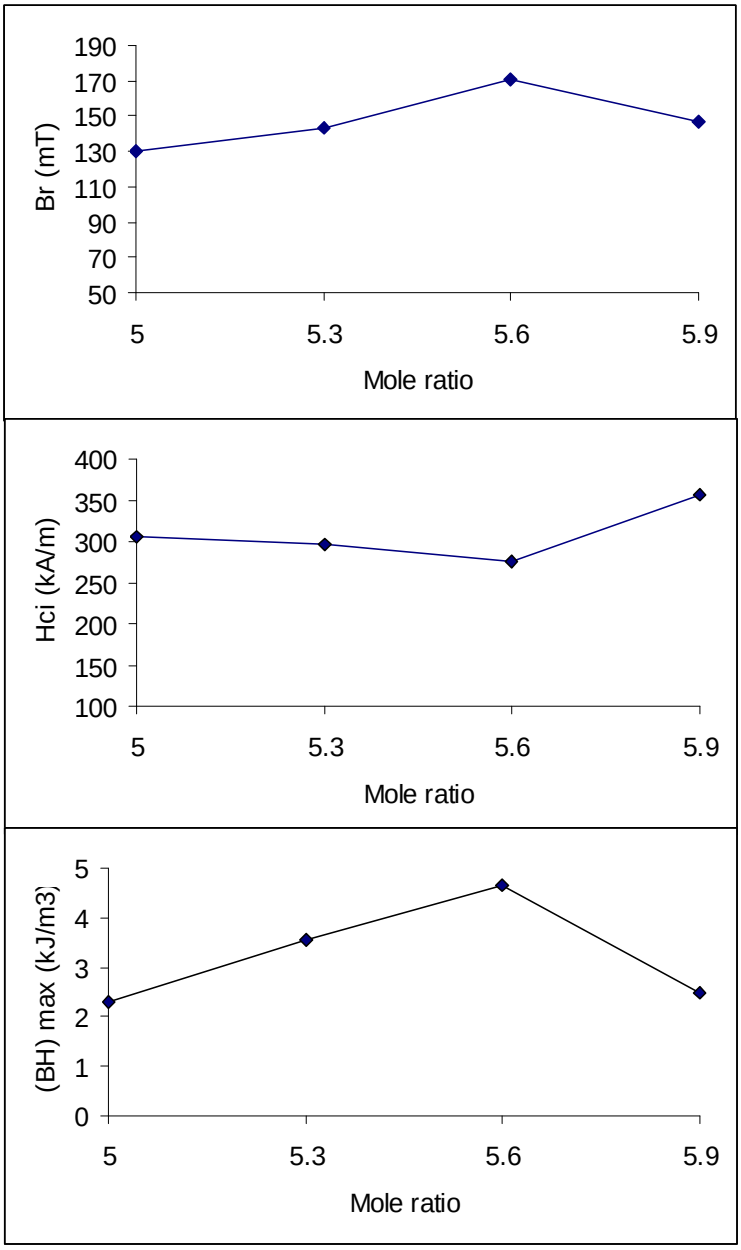

Fig. 5.13 H_{ci}, $(BH)_{max}$ and B_r verses mole ratio of anisotropic $SrFe_{12}O_{19}$ prepared using celestite and blue dust sintered at 1250^0C for 1 hr.

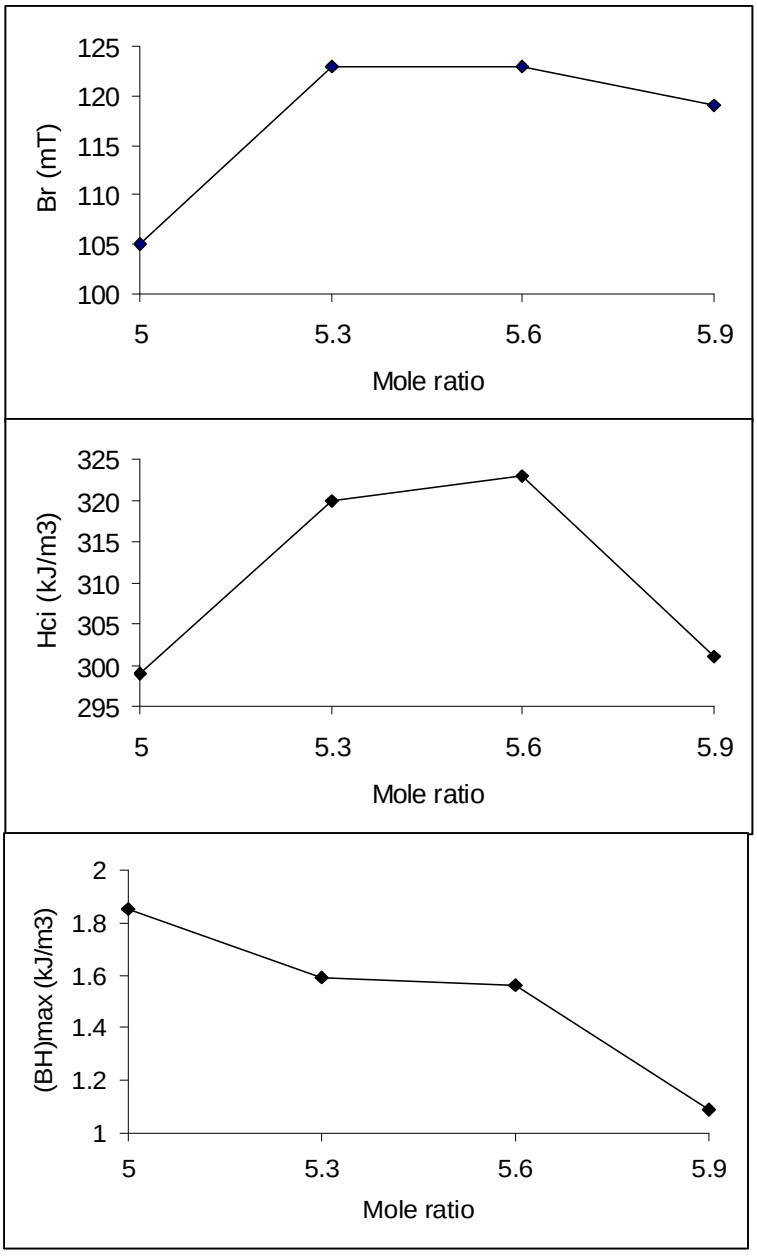

Fig 5.14 H_{ci}, $(BH)_{max}$ and B_r verses mole ratio of isotropic $SrFe_{12}O_{19}$ processed ore sintered at 1250^0C for 1 hr.

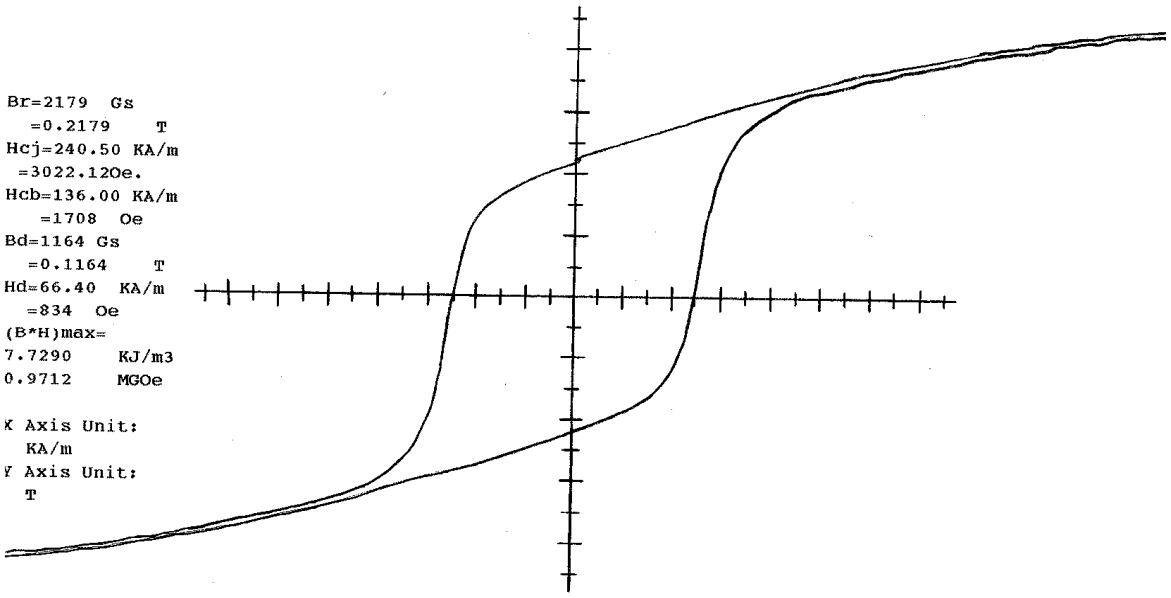

Fig 5.15 Hysteresis loop of anisotropic $SrFe_{12}O_{19}$ (pure chemicals) mole ratio 5.6

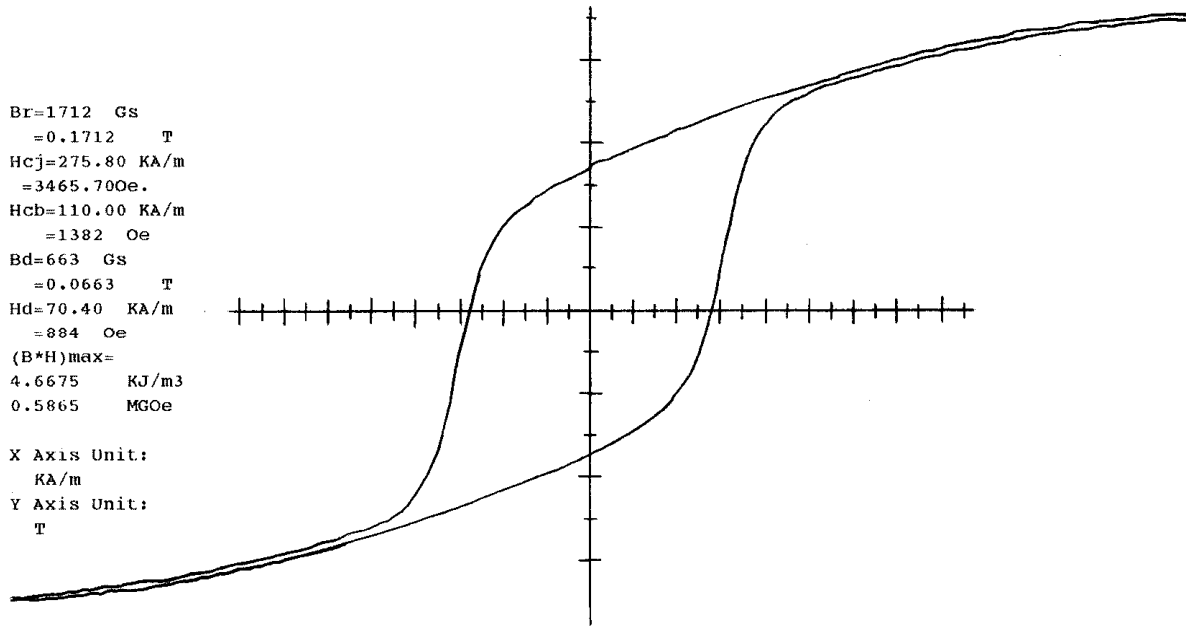

Fig 5.16 Hysteresis loop of isotropic $SrFe_{12}O_{19}$ (pure chemical) mole ratio 5.6

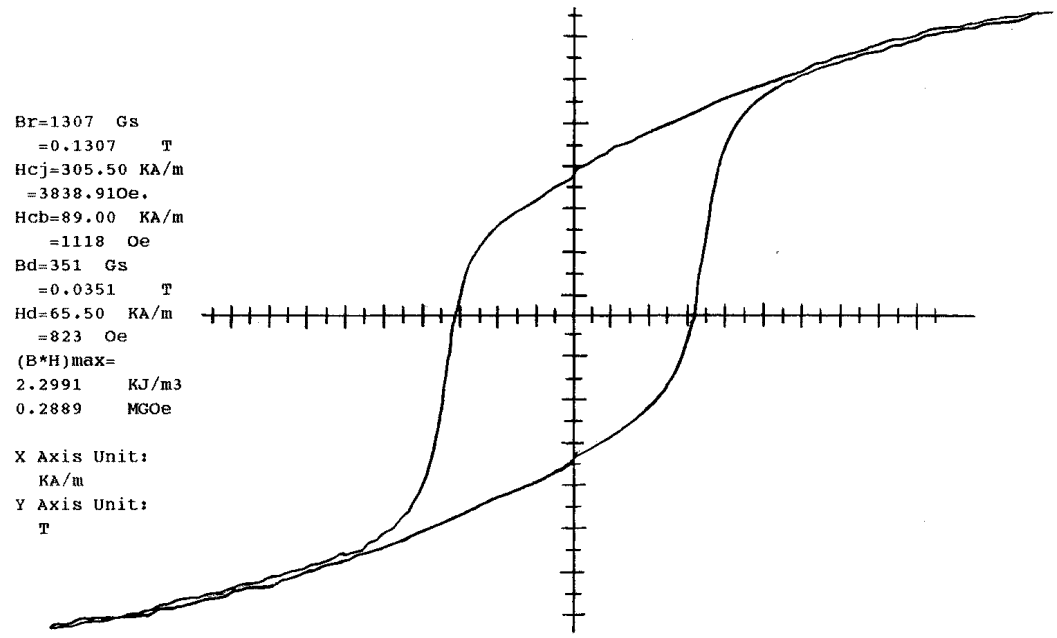

Fig 5.17 Hysteresis loop of anisotropic $SrFe_{12}O_{19}$ (processed ores) mole ratio 5.0

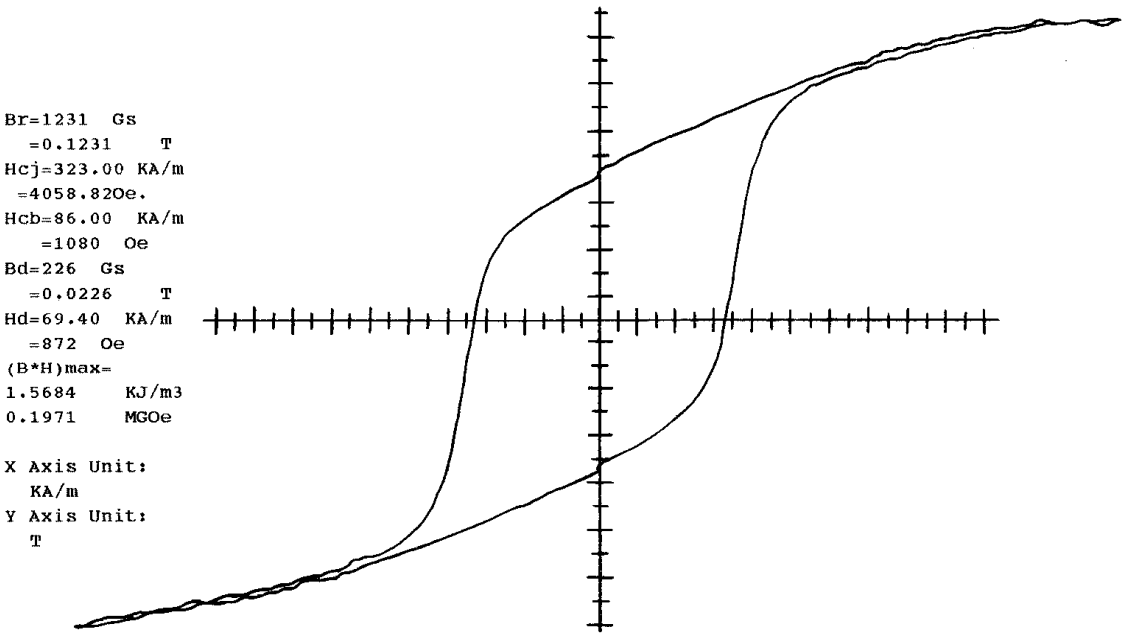

Fig 5.18 Hysteresis loop of isotropic $SrFe_{12}O_{19}$ (processed ores) mole ratio 5.0

5.4.3 Microstructures

5.4.3.1 Fractured surface of $SrFe_{12}O_{19}$ prepared from processed ore (calcined at 1150^0C)

Fig.5.19-5.24 shows the SEM micrographs of ferrite magnets at different mole ratio with variation in sintering temperature. Fig. 5.19 (a, b) shows micrographs of ferrite at mole ratio 5.0 and 5.3 sintered at temperature 1200^0C. It is seen from the micrograph that particle alignment is not proper at sintering temperature of 1200^0C but comparatively particle alignment is better in case of 5.19 (a). However, uniformity of particle size is low causing less coherency in structure and lower value of sintered density. This leads to decrease in the value of magnetic properties.

Fig.5.20 (a, b) shows SEM microstructures of ferrite sintered at 1200^0C for mole ratio 5.6 and 5.9. The micrograph shows the similar trend as discussed above. Fig.5.23 (a, b) shows the SEM micrographs of ferrite magnets sintered at 1250^0C for mole ratio 5.0 and 5.3. In this micrograph particles have become elongated to platelet type structure. This may be the concurrent decrease of crystallites along c-axis [14, 15]. Fig.5.24 (a, b) shows the micrographs of ferrite sintered at 1250^0C for mole ratio 5.6 and 5.9. In this microstructure also higher porosity was observed which led to lower sintering density. Fig. 5.21 (a,b) and fig. 5.22 (a,b) show the fracture surface of ferrite sintered at 1220^0C at mole ratio 5.0, 5.3, 5.6 and 5.9 respectively.

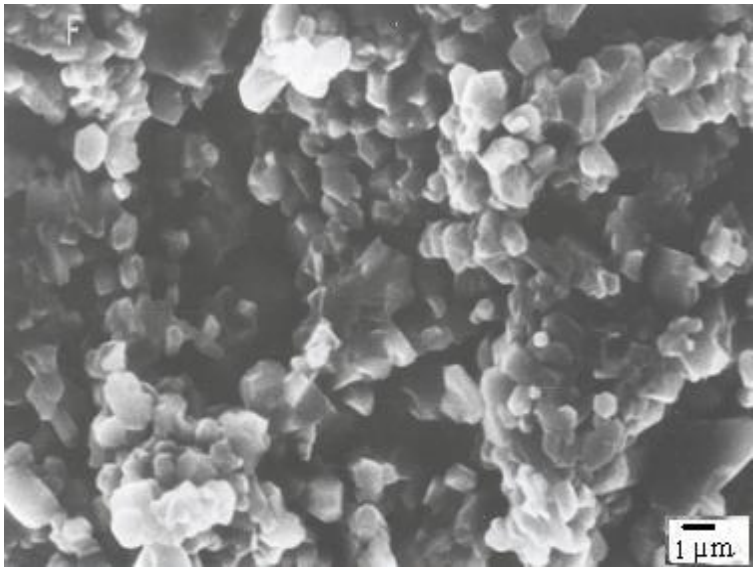

(a)

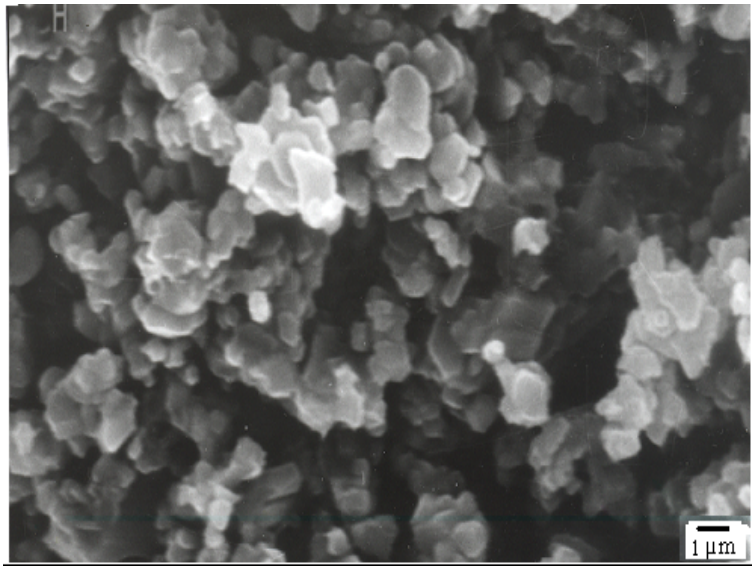

(b)

Fig. 5.19 (a, b) SEM micrograph of ferrite magnet (processed ore) for mole ratio 5.0 and 5.3 respectively and sintered at 1200^0C

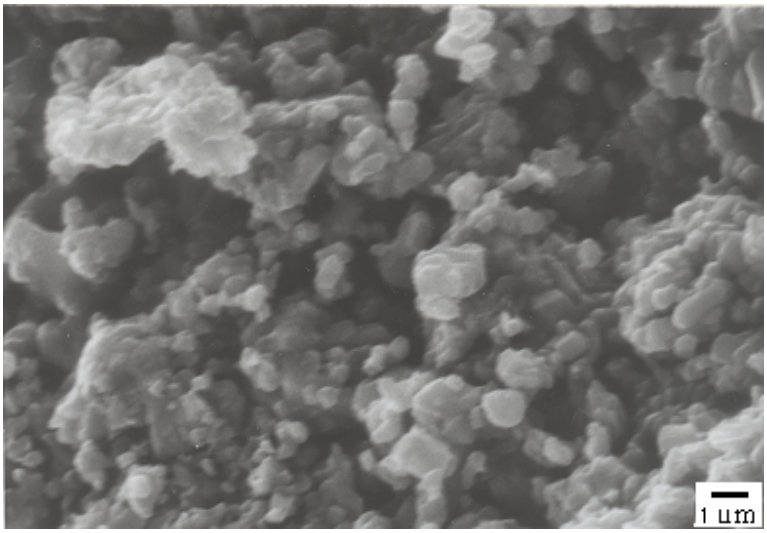

(a)

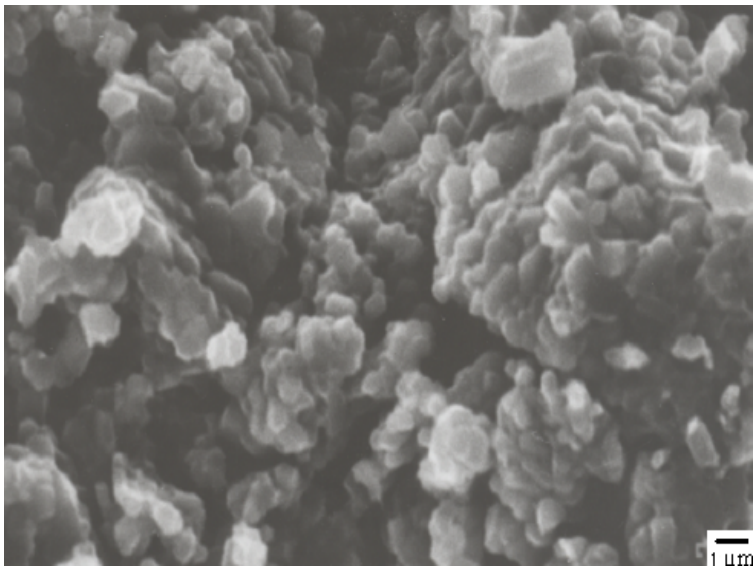

(b)

Fig.5.20 (a, b) SEM micrograph of ferrite magnet (processed ore) for mole ratio 5.6 and 5.9 respectively and sintered at 1200^0C.

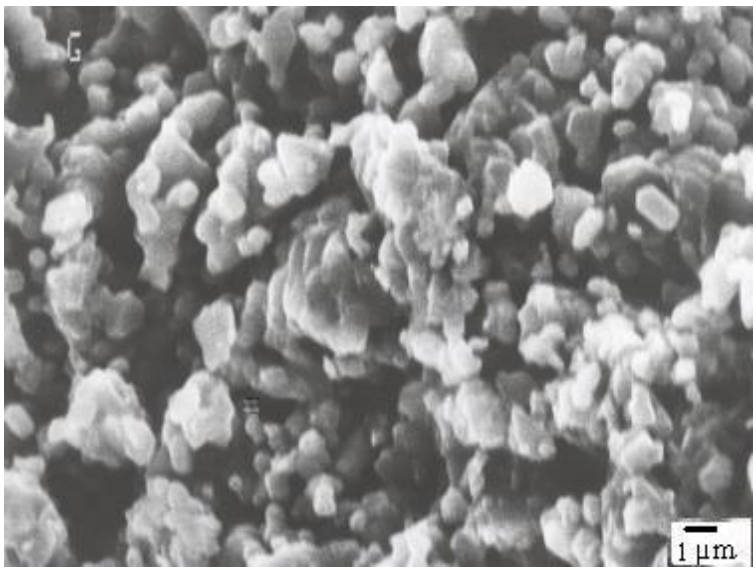

(a)

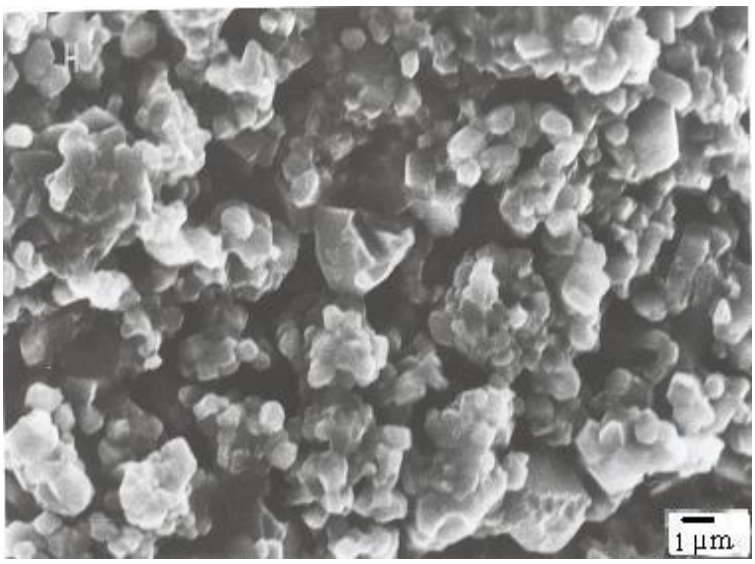

(b)

Fig.5.21 (a, b) SEM micrograph of ferrite magnet (processed ore) for mole ratio 5.0 and 5.3 respectively and sintered at 1220^{0}C

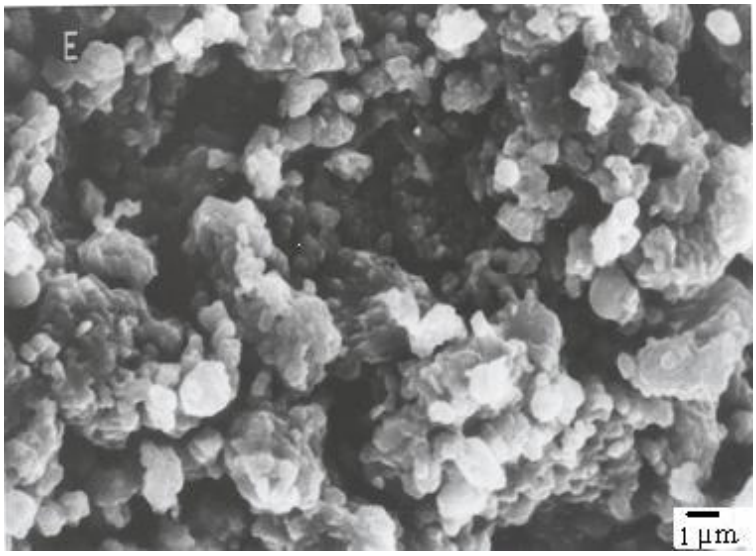

(a)

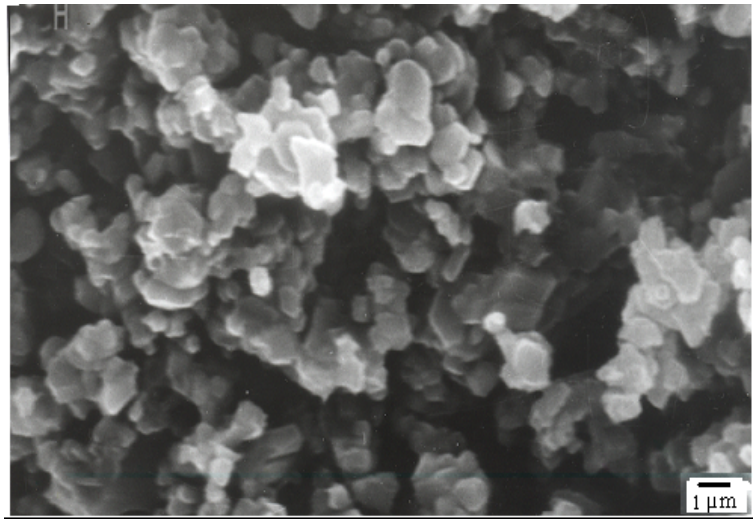

(b)

Fig.5.22 (a, b) SEM micrograph of ferrite magnet (processed ore) for mole ratio 5.6 and 5.9 sintered at 1220^0C

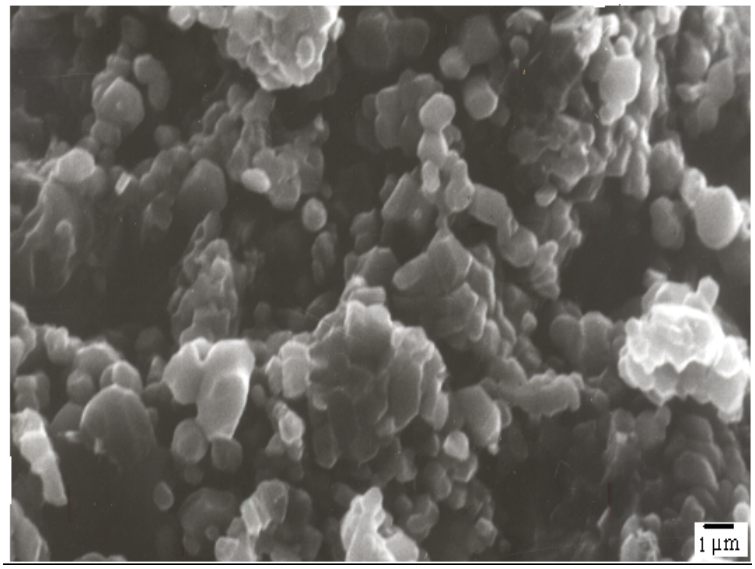

(a)

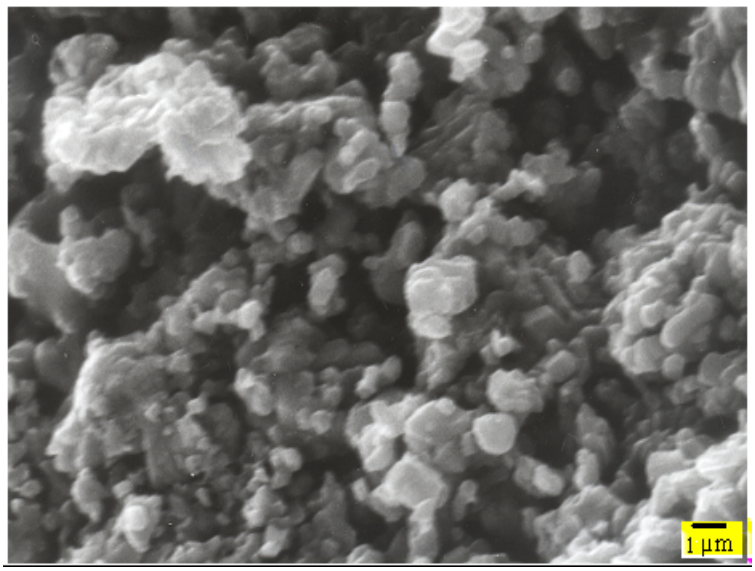

(b)

Fig 5.23 (a, b) SEM micrograph of ferrite magnet (processed ore) for mole ratio 5.0 and 5.3 respectively and sintered at 1250^{0}C

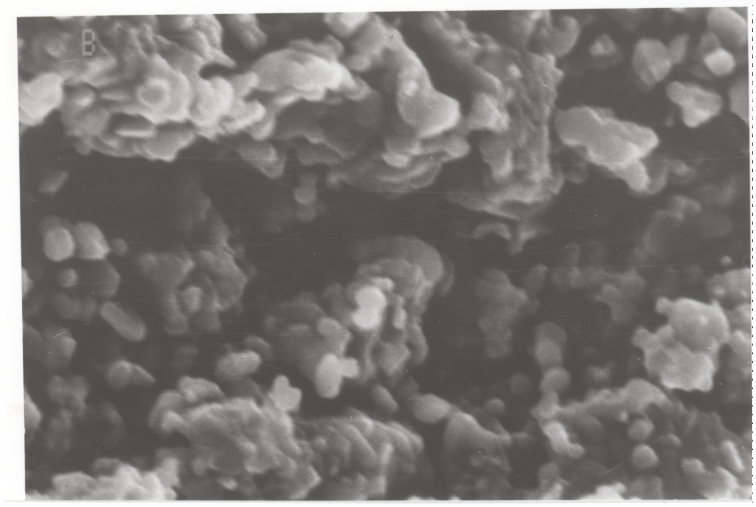

(a)

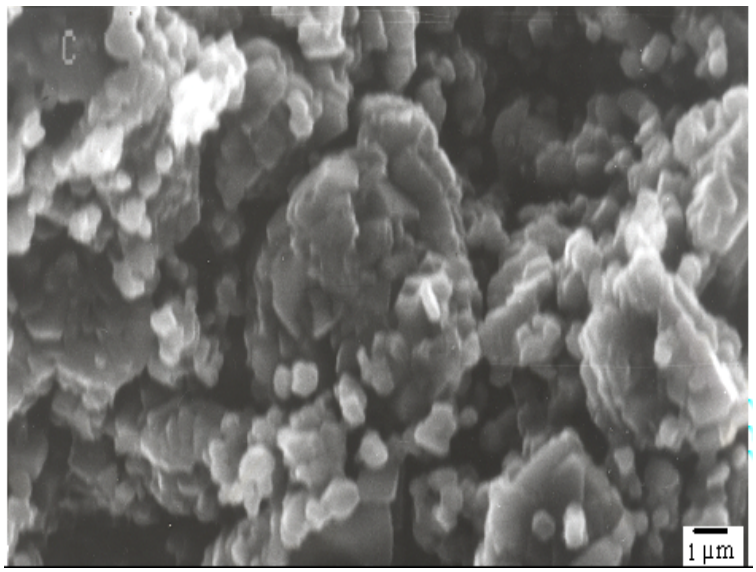

(b)

Fig.5.24 (a, b) SEM micrograph of ferrite magnet (processed ore) for mole ratio 5.6 and 5.9 respectively and sintered at 1250^{0}C

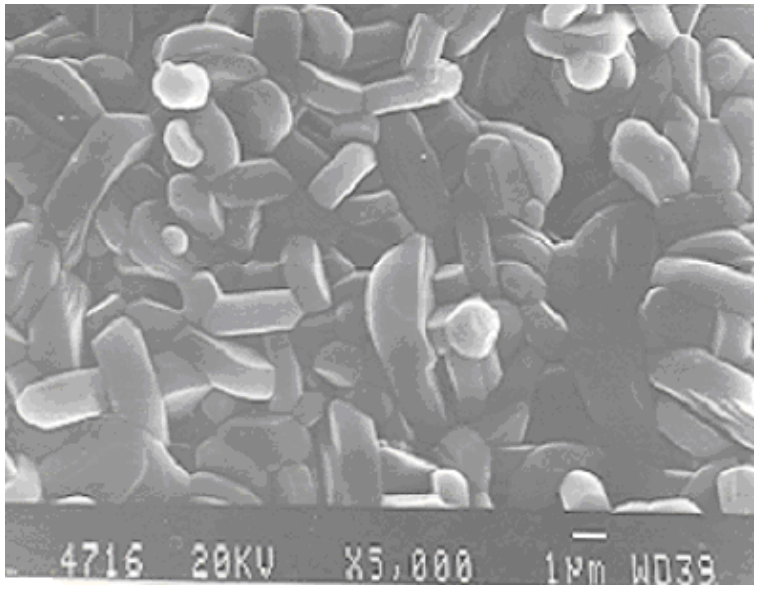

(a)

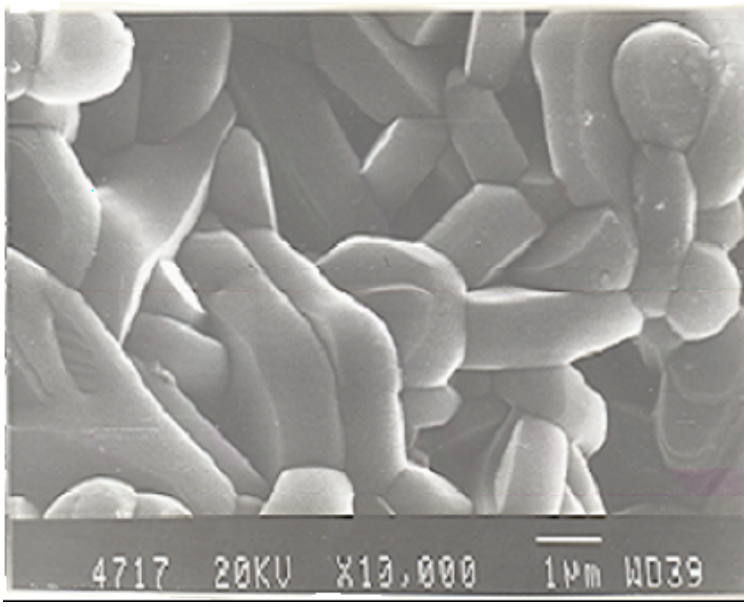

(b)

Fig. 5.25 (a), (b) SEM micrograph of fractured surface anisotropic $SrFe_{12}O_{19}$ prepared from pure chemicals (mole ratio Fe_2O_3/SrO= 5.6) at lower and higher magnifications 1250^0C.

Fig. 5.25 (a, b) shows scanning electron micrographs of fractured surface of anisotropic strontium hexaferrite at lower and higher magnification, prepared from pure chemicals. The structure shows the ferrite particle in the platelet hexagonal shape which is clearly visible in micrograph at higher magnification (fig.5.22b). The particles are well aligned along the *c*-axis giving rise to good magnetic properties [6]. The micrographs exhibit the morphological feature of hexaferrite grains. If we compare the microstructure of sintered magnets prepared from pure chemicals and processed ore (as shown in fig. 5.19 to 5.24) it is found that the hexagonal platelet shape of ferrite particles from pure chemicals is uniformly aligned along its axis whereas in the case of ferrite produced from processed ore it does not show uniform particle alignment. Moreover, ferrite produced from pure chemicals has greater coherency. The microstructure observed in ferrite produced from processed ore show porous structure due to less coherency.

References

1. www.tidco.com
2. R.Dasgupta, S.K.Bose and S.P.Narayan, "Hard ferrites from Blue dust of Bailadila Iron Ore Mines of Madhya Pradesh" Research and Industry, vol.40, 1995, pp 236-239.
3. Mortaza Mozaffari, Jamshid Amighian, "Direct Use of Celestite to Prepare Presintered $SrFe_{12}O_{19}$ Powders" Physica B, vol. 321, 2002, pp 45-47.
4. Patrick E. Cavanagh, "Production of Compounds by Reaction of Solid Materials at High Temperatures Produced by Plasma Arc Torches" United States Patent No- 4766284,1988, pp 1-9.
5. R.K.Tiwary, S.P.Narayan and O.P.Pandey, "Conversion of Indian Celestite to Strontium Carbonate" International Journal of Mining and Mineral Engineering, 2007 (Accepted).
6. Puneet Sharma, Amithabh Verma, R.K.Sidhu and O.P.Pandey, "Effect of Processing Parameter on the Magnetic Properties of Strontium Ferrite Sintered magnets using Taguchi L9 orthogonal design" Journal of Material Processing Technology, vol. 168, 2005, pp 147-151.
7. Wen-Yu Zhao, Ping Wei, Hai-Bin Cheng, Xin-Feng Tang and Qing-Jie Zhang,"FTIR Spectra, Lattice Shrinkage and Magnetic Properties of CoTi- Substituted M-Type Barium Hexaferrite Nanoparticles" Journal of Ammerican Ceramic Society, vol. 90(7), 2007, pp 2095-2103.

8. S.A. Seyyed Ebrahini, “The Control of the Reactions of Strontium Hexaferrite Formation by the Molar Ratio of Precursors” Key Engineering Materials, vols.280-283, 2005, pp. 471-472.
9. Spomenka Besenicar and Miha Drofenik, “High Coercivity Sr Hexaferrite”, Journal of Magnetism and Magnetic Materials, vol. 101, 1991, pp 307-309.
10. Yasunobu Ogata and Mikio Yamamoto, “Method of Producing Ferrite Magnet”, United States Patents No- 5538657, 1996, pp. 1-13.
11. F. Toussaint, D. Bouvard, P. Tenaud and E.D. Marcello, “Experimental and Numerical Analysis of the deformation of Ferrite Segment during Sintering”, Journals of Material Processing Technology, vol.147, 2004, pp 72-78.
12. J.F.Wang, C.B.Ponton, R.Grossinger, I.R. Harris, “A Study of La-Substituted Strontium Hexaferrite by Hydrothermal Synthesis” Journal of alloys and compound, vol. 369, 2004, pp. 170 – 177.
13. J. Sort, J. Nogues, S. Surinach, J.S. Munoz and M.D. Baro, “Coercivity Enhancement in Ball-Milled and Heat-Treated Sr-Ferrite with Iron Sulphide” Journal of Metastable and Nanocrystalline Materials, vols. 15-16, 2003,pp. 599- 606.
14. Suk- Joon G.L. Kang, “Sintering, Grain Growth and Microstructure”, Technology and Engineering, 2005, pp 3-23.
15. R.L.Coble, “Sintering Crystalline Solids, Intermediate and Final State Diffusion Models”, Journal of Applied Physics, vol. 32, pp 787-792.

Chapter 6

Conclusions

Overview

The present chapter summarizes the results of the various experiments described in the previous chapters. Effect of different experimental variables for conversion of Indian celestite to strontium carbonate and factors influencing conversion rate is outlined. The mechanochemical process for preparation of strontium hexaferrite from blue dust and celestite ore and the effect of different processing variables on the magnetic properties is mentioned. A comparison of magnetic properties of strontium hexaferrite prepared from pure chemicals and also from ores has been discussed. Further, the structural and magnetic properties of strontium hexaferrite prepared from natural mineral have been discussed. The scope for future work for preparation of strontium hexaferrite from ores is described in brief.

It is observed that chemical treatment of celestite reduces Fe_2O_3 content significantly i.e. from 4.01% to 0.60%. The other impurity such as CaO also reduces from 0.36% to 0.1% by applying this process. Before conversion of celestite by direct decomposition method it is necessary to employ celestite upgradation by acid leaching to remove the acid soluble impurities from the ore. In the black ash method reduction of celestite to strontium sulphide depends upon the different variables like nature of reducing agents and its quality, temperature and time. The activated charcoal was found most suitable agent for reducing celestite to strontium sulphide. The reducing effect of celestite to SrS decreases considerably when the activated charcoal is less than 40%. It is also found that the conversion process is completed after 60 minutes and after that it becomes virtually constant. In the direct conversion method celestite conversion is influenced by various parameters like molar ratio ($Na_2CO_3/SrSO_4$), temperature, time etc. The rate of percentage conversion of $SrSO_4$ is found to be maximum at mole ratio 1.5 ($Na_2CO_3/SrSO_4$). The maximum yield of $SrCO_3$ can be achieved by optimizing the various parameters using this method. The direct conversion method seems better process as it does not consist of big set up like reducing gaseous set up as used in black ash process. Direct reduction method has the advantage of simplicity, low consumption of acidic material and high recovery of strontium carbonate. Strontium carbonate produced from this process exhibit high purity and can be used in the production of ceramic ferrite magnets. On comparing the black ash and direct conversion methods in terms of purity of $SrCO_3$ it is found that the former gives 97% and later gives 98% pure $SrCO_3$. The direct conversion method may be suitable for high grade celestite where Ba like impurities is less. However, low grade celestite contains large amount of Ba for which black ash method can be utilized. The single decomposition method may be suitable for glass grade strontium carbonate whereas double decomposition method may be most suitable for ferrite grade strontium carbonate replacing the expensive pure $SrCO_3$. The Indian celestite contains medium amount of impurities like Fe, Ba etc. and therefore may be graded as medium grade celestite.

The physical upgradation of blue dust shows that the magnetic separation process prior to froth floatation process is necessary to get magnetic particles separated. Magnetic separation process is an easy operational process. Although there is not major change in the chemical composition of blue dust after physical upgradation process however, there is small decrease in impurities

level like CaO, SiO_2 etc. The silica content reduces to 1.21% after floatation process which was 1.60% before upgradation.

The chemical upgradation of blue dust by acid precipitation method exhibits a better purity level of iron oxide. The purity of iron oxide obtained by this process is 99.21%. The impurity content is almost negligible. This iron oxide can be utilized for the preparation of strontium hexaferrite since it has high purity level. This will also be used as a substitute for expensive high purity iron oxide. However, the preparation of iron oxide by chemical precipitation method is suitable for small amount.

Preparation of strontium hexaferrite from celestite and blue dust by mechanochemical route shows very promising method for preparation of strontium hexaferrite from the celestite and blue dust. This process has advantage that the whole preparation process is completed in a single setup using high energy ball mill. This process produces ferrite powder of nano size. During the process solid-state reaction occurs and this does not require any additional step like conversion of celestite to strontium carbonate and high temperature reaction for the preparation of strontium hexaferrite powder. Therefore it makes the process easy and economical.

The results of magnetic properties obtained in the present investigation shows that strontium hexaferrite with moderate values of remenence, coercivity and energy product can be obtained by mechanical alloying of celestite and blue dust followed by annealing.

The value of $B_{r,}$ H_{ci} and BH_{max} are 2533(Gs), 3160 (Oe) and 1.19 (MGOe) respectively. The values of magnetic properties obtained in the present investigation are in the range of results reported by other researchers. These magnets can be used in those components where moderate magnetic properties are required.

The lower cost of starting raw minerals (celestite and blue dust) will make the process more economical to produce strontium hexaferrite magnets as compared to the other conventional methods where high purity chemicals are utilized.

Magnets prepared from processed celestite and blue dust exhibits comparatively lower values of magnetic properties. However, by comparing in terms of cost per unit of magnetic energy it is found that ferrite prepared from its natural ores is economical. Moreover, the coercivity values are in moderate range. By comparing the magnetic properties of magnets prepared at different mole ratio (Fe_2O_3/SrO) we find that there is optimum condition at which magnetic properties are higher. These types of magnets are suitable in especially small scale industries like toys, electric mixers etc.

Strontium hexaferrite magnets prepared from processed ore and pure chemicals shows large difference in magnetic properties and sintered density of sintered magnets. It is clear from the study that magnetic properties of the sintered magnets prepared from processed ore is almost equal at mole ratio 5.0 to 5.3. When mole ratio is increased the value of remanence and energy product decreases. It is also observed that magnets prepared from processed ore exhibit better magnetic properties at mole ratio 5.0 to 5.3 whereas magnets prepared from pure chemicals shows better magnetic properties at mole ratio 5.5. The comparison of microstructures of the both kinds of sintered magnets reveal that the particle alignment in the case of magnets prepared from pure chemicals is better as compared to magnets prepared from processed ore.

The celestite and upgraded blue dust can be a good substitute to expensive chemicals strontium carbonate and iron oxide for the preparation of strontium hexaferrite which will reduce the production cost of ferrite magnet industries significantly.

The magnetic properties of ferrite magnets obtained from processed ore are less as compared to magnets prepared from the pure chemicals. However, by comparing processing cost per energy value of these magnets it seems to be promising magnetic materials for the application in small industries.

The commercial production of strontium hexaferrite from celestite and blue dust will significantly help to explore the huge deposits of natural minerals strontium and iron ores fines. This will also help to prevent the pollution problem caused by dumping of iron ores fines. This will also help the country to utilize the celestite ore and make them self-dependent as well as save the foreign money in turns.

Suggestion for Future Work

In the present study conversion of Indian celestite to strontium carbonate was carried out by adopting different procedures. A number of other strontium compounds can also be synthesized from celestite. Considering this fact it is suggested that efforts should be made to prepare other strontium compound like, strontium nitrate, strontium hydroxide etc.

In the present work preparation of strontium hexaferrite from celestite and blue dust and its effect on magnetic properties are studied. The other physical properties like dielectric characteristics, semiconductor properties, photoluminescence properties, resistivity, high frequency application etc. are needed to be studied in detail. So, it is suggested that study should be made to observe the variation in other physical properties mentioned above on this magnet by preparing it from celestite and blue dust.

Apart from the conventional calcination method strontium hexaferrite was prepared by mechanoalloying followed by annealing using celestite and blue dust. However, possibility for preparation of strontium hexaferrite by mechanochemical method directly (without annealing) should be studied. So, it is suggested that different process condition should be studied to explore the possibility to prepare strontium hexaferrite directly by mechanochemical method from celestite and blue dust. In addition to above areas it is suggested to prepare nano powders of strontium hexaferrite from celestite and blue dust to explore its better magnetic properties. Also effect of doping rare earth elements on magnetic properties should be studied.